Insulin Signaling & Glucose Metabolism in Glycolytic & Oxidative Muscles of High Fat Fed & Endurance Trained Rats

Arta Mohasses

GRADUATE PROGAM IN KINESIOLOGY AND HEALTH SCIENCE
YORK UNIVERSITY
TORONTO ONTARIO
NOVEMBER 2016

Abstract:

This study examines the effects of a chronic high-fat diet (HFD) and chronic endurance exercise (CEE) upon muscles of varying oxidative (Ox) and glycolytic capacities. We report that chronic HFD leads to significantly high levels of blood glucose and insulin concentrations. These high concentrations were due to the reduction in the activity of key proteins in the insulin-signaling (IS) cascade, leading to blunted rates of glycogen synthesis (GSR) and reduced glucose-6-phosphate (G6P) content in all muscles fiber types (MFTs) of HF fed rodents. Conversely, CEE increased insulin sensitivity, increased GSR and G6P content. Our work has shown that hyperlipidemia causes all MFTs to develop insulin resistance regardless of Ox capacity. However, it appears that the Ox fibers are more severely affected by insulin resistance and that the pathogenesis of insulin resistance is different between muscle fiber types.

Acknowledgements:

Narges and Mehrdad Mohasses: To my amazing parents who have done nothing but push me to do better even when I may not have believed I could. Thank you for being the most giving and encouraging parents a boy could ask for. I hope I can repay you every day and make you proud.

Dr. Rolando Ceddia: I cannot put into words how much your dedication, patience, and understanding has meant to me. You are the best teacher I have ever had in my life; I do not think I will ever stop learning from you. Thank you for sticking by me when it would have been easier to let go.

Diane Sepa-Kishi: A calm and warm influence in the lab. One of the most dedicated people I have had the pleasure of meeting and working with. Thank you for all your input and it was your notes that brought forth some great new ideas. Thank you for always being such a great role model and I am looking forward to visiting your lab one day, my friend.

Michelle Victoria Wu: You were the first person I became friends with in this endeavor and I know with your work ethic you are definitely going to be very successful in your life. I have enjoyed our conversations about life and friends, always happy to chat together. Been a lot of fun working with you and I may start a fire one day just to say hi.

Abinas Uthyakumar: Lots of inside jokes over the two years we worked together, we went through a lot of ups and downs. I do not care what Michelle says she misses us talking and joking so obnoxiously near her workspace. Numerous stories of how "well" we did our experiments, and that all-nighter. I am glad that I can call you a friend, it has always been a pleasure and I wish you all the success in the world. Thank you.

Dr. George Bikopolous: Thank you for showing me the ropes during the summer of 2013. Since then you have always been a very helpful friend and wishing yourself and the wife lots of success in the future.

Dr. Ricardo Pinho: Big Ricardo, irmão, you were always a very positive influence in the Lab. Made the transition into the lab during my first year much more fun and positive. Thank you and hope you and your family are well.

Dr. Chris Perry: Thank you for being a part of this entire process, and for chairing my committee. It meant the world to get your support to help get the defense in place. Wishing you the very best in all of your future endeavors.

Adib Razavi: You have become a very important person in the few years. Your friendship has meant the world to me; it would have been a very different experience without you. You have been and always will be a positive influence in my life. Thank you for always going above and beyond to keep me in touch with our work, in what promises to be a very exciting adventure. I am shakin with anticipation.

Alexander Arthur: Thank you for all your understanding over the last few years, being so patient and always considerate of what was needed to get this thesis done. I cannot wait to see what the future will bring the three of us. You are a great friend and a fantastic colleague. Tuck it…..Roll it.

Aryeah and Omaya Mohasses: My brother and my sister-in-law, thank you to you both for you love and support. You are both great role models for how to balance things in life. Looking forward to what life is going to bring you next.

Friends: Lots of people can be named here, thank you all for being a part of my life and supporting me along the way.
Mani my dearest friend, thank you for always being there for me. My best friend since the 3rd grade, I cannot wait to see what life will bring us. I miss you a lot but I know you will be a massive success at medical school.
Nathaniel you have been a great friend and someone I have become very close with over the last few years, thank you.
Victoria Thank you for your friendship and your support for the last 4 years.
Corinne Thank you for your feedback; I really appreciated your input.

Table of Contents:

List of Figures:

List of Abbreviations:

$O_2 \cdot^-$: Superoxide
H_2O_2: Hydrogen peroxide
11β-HSD1: 11β-hydroxysteroid dehydrogenase type 1
ADP: Adenosine diphosphate
AMPK: 5' Adenosine monophosphate-activated protein kinase
AKT: Protein kinase-B
ANG II: Angiotensin II
ATP: Adenosine 5'-triphosphate
AT^1R: Angiotensin 1 receptor
AUC: Area under the curve
DAG: Diacylglycerol
DIO: Diet-induced obesity
EDL: Extensor Digitorum Longus
Epit: Epitrochlearis
EX: Exercise
FAT: Fatty acid translocase
FFA: Free fatty-acid levels
G6P: Glucose 6 phosphate
GLUT4: Glucose transporter 4
GS: Glycogen synthase
GSK: Glycogen synthase kinase-3
HF: High fat
HK II: Hexokinase II
IGF-1: Insulin-like growth factor
IL-6: Interlukin-6
IMTG: Intramuscular triglycerides
IR: Insulin receptor
IRR: Insulin receptor-related receptor
IRS-1: Insulin receptor substrate-1
NMR: Nuclear magnetic resonance
PDK1: Phosphoinositide-dependant kinase-1
PI3K: phosphatidylinositol-3-OH kinase
PIP_3: Phosphatidylinositol (3,4,5)-trisphosphate
PP1: Protein phosphatase-1
RAAS: Renin angiotensin aldosterone system
RER: Respiratory exchange ratio
ROS: Reactive oxygen species
RTK: Receptor tyrosine kinase
SC: Standard Chow
SOD: Manganese superoxide dismutase
Sol: Soleus
SED: Sedentary
SH2: Src-homolgy-2
TA: Tibialis Anterior

T2D: Type 2 diabetes
TNF-α: Tumor-necrosis factor α
UDP-glucose: Uridine 5′-diphosphate-glucose

1. Introduction

The rise of obesity rates worldwide is alarming. By the year 2030, it is estimated that the number of obese adults will rise to 1.35 billion and overweight adults will rise to 375 million[1]. Epidemiological studies have indicated that obesity is an important risk factor for heart disease, hypertension, and diabetes[2]. Diabetes alone is projected to rise from 171 million in 2000 to 366 million by 2030[3]. Diabetes can be categorized into two etiopathogenic categories: type I and type II (T2D)[4]. Type I is developed as a result of an autoimmune pathogenesis occurring in the pancreatic islets which leads to complete loss of the β-cell's ability to secrete insulin[4]. This form of diabetes only accounts for 5-10% of all cases while T2D accounts for 90-95% of cases[4]. T2D patients are able to produce insulin, however, they show a blunted response to insulin action[4]. The reduced or impaired response to insulin observed in T2D subjects is known as 'insulin resistance'[5]. Obesity has become the most critical factor in the pathogenesis in metabolic diseases, which is one reason why obese subjects tend to develop insulin resistance[5]. The state of insulin resistance is characterized by a reduction in insulin-stimulated glucose transport and metabolism[6]. The decrease in glucose transport translates to severe reductions in the ability of peripheral tissues, more specifically the muscle, to dispose of glucose and aid glycemic control[6].

Muscle glycogen synthesis is one of the key pathways for glucose disposal, as it accounts for up to 75% of the insulin-stimulated whole-body glucose disposal[7]. This is due to the fact that the skeletal compartment makes up a significant part of total body mass (~40% and 30% of total body mass in men and women, respectively) and it can store up to 1 to 2% of its weight in glycogen[8-9]. Impairment in the ability of skeletal muscles to uptake glucose and synthesize glycogen in response to insulin can markedly reduce the clearance of glucose from the circulation and lead to hyperglycemia.

Hyperglycemia is avoided via insulin stimulated muscle glucose uptake. Insulin stimulation initiates a cascade of intracellular signaling events that lead to translocation of glucose transporter 4 (GLUT 4) to the plasma membrane of the myocyte[10]. Once located at the plasma membrane, GLUT 4 facilitates the influx of glucose[11]. This is concomitantly followed by the activation of key enzymes involved in the regulation of glycogen synthesis[12]. The ability for insulin to trigger such intracellular events in the muscle is crucial for proper regulation of glycemia. However, it is important to note that the skeletal muscle contains different fiber types, each with their own distinct metabolic characteristics.

One of the principle differences between fiber types is the amount of mitochondrial content. This is an important difference as recent research has shown that the obese state can cause changes to insulin sensitivity and disrupt the insulin-signaling cascade through a number of mechanisms that are directly or indirectly influenced by mitochondrial activity. These include increased oxidative stress[8], elevated levels of inflammatory cytokines[13], and accumulation of intramyocellular lipid intermediates[14]. Among these mechanisms, it is the accumulation of intramyocellular lipids intermediates specifically diacylglycerol (DAG) and ceramides that have received a lot of attention[14]. This theory is supported by observations that the increased DAG content in muscle cells, which are oversupplied with lipids, causes the impairment of the subsequent intracellular signaling[15]. Therefore, it is anticipated that conditions that reduce DAG content help prevent the development of insulin resistance and disturbances to glucose metabolism. In this context, it is not known how muscles that express a mitochondria rich muscle fiber type cope with diet-induced obesity, and whether a fiber type, which expresses more mitochondria, is more suited to dealing with diet-induced obesity over a fiber type that expresses less.

2. Literature Review

2.1 Muscle Fiber Type

Systemic plasma glucose concentrations are tightly regulated through a complex system of glucose uptake and delivery[16]; this careful regulation is vital in order to avoid the adverse effects of hypo- and hyperglycemia[17]. In the postprandial state, plasma glucose elevations are balanced by triggering an insulin response that stimulates cells to uptake and utilize glucose[22-23]. This regulation of insulin-stimulated glucose disposal occurs through the interaction of a number of tissues, including the liver, brain, skeletal muscle, small intestine, pancreas and adipose tissue[18]. After the brain, skeletal muscle exerts the largest influence over insulin-stimulated glucose disposal[18].

Skeletal muscle consists of varying fiber types each with distinct physiological characteristics[19]. Based on histochemical staining and enzymatic analysis, muscle fibers have been categorized into three groups: type I (slow twitch oxidative muscles), type IIa (fast twitch oxidative and glycolytic muscles) and type IIb (fast twitch glycolytic muscles)[20]. An example of a muscle rich in type I fibers is the soleus muscle[23]. This particular muscle is comprised mainly of intermediate and slow twitch motor units and its fibers are rich in mitochondria[23]. Type I fibers have greater insulin binding capacity, have increased insulin receptor kinase activity and autophosphorylation capacity in comparison to fast twitch type II glycolytic fibers[21,22]. Type I fibers are red and fatigue resistant due to an abundance of mitochondria and myoglobin. These fibers undergo oxidative metabolism which is used to provide a stable and sustainable supply of ATP[23]. Conversely, type II fibers are less oxidative due to fewer mitochondria and myoglobin content[23]. Type II fibers can be further subcategorized into type IIa and type IIb fibers. Type IIa contains both oxidative and glycolytic enzymatic properties and as a result, have a slightly

greater rate of fatigue than type I fibers[23]. Finally, type IIb fibers essentially rely on glycolytic metabolism and have the lowest amount of mitochondria[23]. Type IIb only provides a short burst of ATP making these fibers more prone to fatigue[23].

In the context of diabetes, studies have demonstrated a link between fiber type and insulin resistance[19-20]. Patients with T2D have a higher number of glycolytic fibers, particularly type IIb, a feature which has been linked to insulin resistance[26-27]. Type I fibers, on the other hand, are correlated with insulin responsiveness and maximal oxygen uptake[28]. However, under diabetic conditions, type I fibers display reduced content of insulin receptors, insulin receptor substrate-1, and glucose transporter 4 (GLUT4) proteins[28].

2.2 Mechanisms of Muscle Glucose Uptake

It has been established that improper functioning or reduced content of GLUT4 is a key factor in the pathogenesis of insulin resistance[29]. The GLUT4 is a member of a category of proteins known as glucose transporters (GLUTs)[24]. GLUT4 is present in insulin-responsive tissues such as the skeletal and cardiac muscles, and is crucial to the regulation of systemic glycemia because it facilities the diffusion of glucose from circulation into the muscle cells[30-31]. During this process, elevated glycemia stimulates the release of insulin[30]. This hormone then binds to its receptors on muscle cells and leads to a cascade of intracellular signaling events that culminate with the translocation of GLUT4-containing vesicles from the perinuclear region to the plasma membrane[12,32]. GLUT4 fuses with the plasma membrane and promotes the transport of circulating glucose into the cell (Figure 1.0). In fact, experiments using 3-O-methyl glucose have shown that insulin stimulation causes an 8.6-fold increase in glucose uptake[33]. This significant fold increase in insulin-stimulated glucose uptake is accompanied by an 8-fold increase in the presence of GLUT4 at the plasma membrane of muscle cells[33].

2.3 Intramuscular Glucose Metabolism

Once inside the muscle cell, glucose can be metabolized through various pathways[34]. However, experiments utilizing euglycemic-hyperinsulinemic clamps have shown that intramuscular glucose is primarily disposed of via glycogen synthesis[35]. Thus, glycogen synthesis is the primary pathway of glucose disposal during the postprandial state. Inside the cell, glucose is actively phosphorylated to form glucose-6-phosphate (G6P)[36]. G6P can either be catabolized through glycolysis or stored as glycogen[37]. Subjects with impaired glucose tolerance display a severe reduction in glycogen synthesis and, to a lesser extent, glycolysis[38]. Furthermore, under hyperinsulinemic and hyperglycemic condition muscle glycogen synthesis becomes the predominant means of glucose disposal[37-38]. Hyperglycemic-hyperinsulinemic clamps along with NMR analysis, have also shown that the rate of muscle glycogen synthesis decreased by 60% in diabetic subjects in comparison to controls[41]. Moreover, it was found that glycogen synthesis accounts for 90% of non-oxidative glucose disposal and 70% of whole-body glucose metabolism[41].

Since muscle glycogen synthesis is the principal means of insulin-stimulated glucose disposal researchers have attempted to define the proteins that are considered as the potential rate limiting elements of skeletal muscle glycogen synthesis. The three key proteins thought to be involved are glycogen synthase (GS), GLUT4 and hexokinase II (HKII) [42-43]. HK II is the enzyme responsible for the phosphorylation of glucose that enters the myocyte via GLUT4, whereas GS is the terminal enzyme in muscle glycogen synthesis that actively converts uridine 5′-diphosphate-glucose (UDP-Glu) into glycogen (Figure 1.0)[44]. It has been determined that the primary rate-limiting protein of muscle glycogen synthesis is GLUT4. This was based on observations that subjects who suffered from lipid-induced insulin resistance had a decrease in

both intramuscular glucose and G6P content[45]. This provided evidence that glucose transport was impaired in these subjects as less glucose was entering the cell, thus less was being actively converted into G6P[46].

2.4 Mechanism of Intramuscular Insulin Signaling

The signaling mechanisms by which insulin stimulates glucose uptake and metabolism are a complex and involve the interaction of many enzymes[47]. Insulin is a peptide hormone that is produced by the β-cells of the pancreas and functions as a potent regulator of whole body glycemia[48]. Once secreted, insulin circulates in the bloodstream and binds to its receptors present on the plasma membrane of myocytes[47].

The insulin receptor (IR) consists of two extracellular α-subunits and two transmembrane β-subunits that are linked by disulfide bonds[49]. Upon insulin binding to its receptor, the α-subunit induces tyrosine autophosphorylation of the β-subunit and vice versa[50]. This leads to phosphorylation of the insulin receptor substrates (IRS)[50]. IRS proteins are a critical node of insulin-signaling, particularly the IRS-1 and IRS-2 isoforms. In fact, it has been demonstrated that IRS-1 knockout mice presented with skeletal muscle insulin resistance, while IRS-2 knockout mice display hepatic insulin resistance[46-47]. Furthermore, a decreased expression of IRS proteins has been associated with obesity[52].

Phosphorylation of the tyrosine residues induces a conformational change in IRS proteins[53]. This conformational change generates a "docking site" that allows for proteins containing the src-homology-2 (SH2) domains to interact with and facilitate further signal transduction[53]. SH2 domains are present in p85α which is a regulatory subunit of phosphatidylinositol-3-OH kinase (PI3K)[53]. When p85α activity is upregulated via insulin stimulation, it binds with a catalytic subunit known as p110 to form active PI3K[54]. Activation of

PI3K causes the phosphorylation and intracellular accumulation of phosphatidylinositol (3,4,5)-trisphosphate (PIP_3)[55]. PIP_3 is the vital secondary messenger in the initiation of the downstream signaling enzyme phosphoinositide-dependent kinase-1 (PDK1)[56].

PDK1 then stimulates the phosphorylation of protein kinase B (Akt), a serine/threonine kinase that exists in 3 isoforms (Akt 1, 2 and 3).[52] Akt is known as a critical signaling factor in the regulation of cellular metabolism, growth, and survival[52]. Studies in humans have shown that impairment of the phosphorylation and activation of Akt as a contributing factor to skeletal muscle insulin resistance[52]. Thus, PI3K phosphorylation of threonine 308 and serine 473 residues of Akt are critical to the signal transduction, and this phosphorylation leads to the downstream phosphorylation of glycogen synthase kinase-3 (GSK-3)[57,58].

GSK-3 exists in 2 isoforms: α and β, and unlike most other kinases, it is constitutively active in cells[59]. Its activity is inhibited by extracellular factors, such as insulin or epidermal growth factor[58]. However, when active, GSK-3 indirectly regulates the activity of glycogen synthase (GS) by reducing the activity of protein phosphatase-1 (PP1)[60]. PP1 is essential in the activation of GS, as under basal conditions GS exists in its inactive phosphorylated form, P-GS. When insulin stimulation occurs, PP1 is activated as a result of GSK-3's phosphorylation, causing it to be deactivated[59]. PP1 activation will cause the dephosphorylation of sites 3a, 3b, 3c and 4 of GS on serine residues 640, 644, 648 and 652, respectively.[61] Dephosphorylation of GS will activate this enzyme and promote glycogen synthesis. Any interruption of insulin action will decrease GS activity and this is detrimental to glycogen synthesis as GS is the terminal enzyme of this pathway[60]. The activity of GS is not only regulated by covalent action via insulin stimulation, but it is also controlled through allosteric regulation by G6P[62].

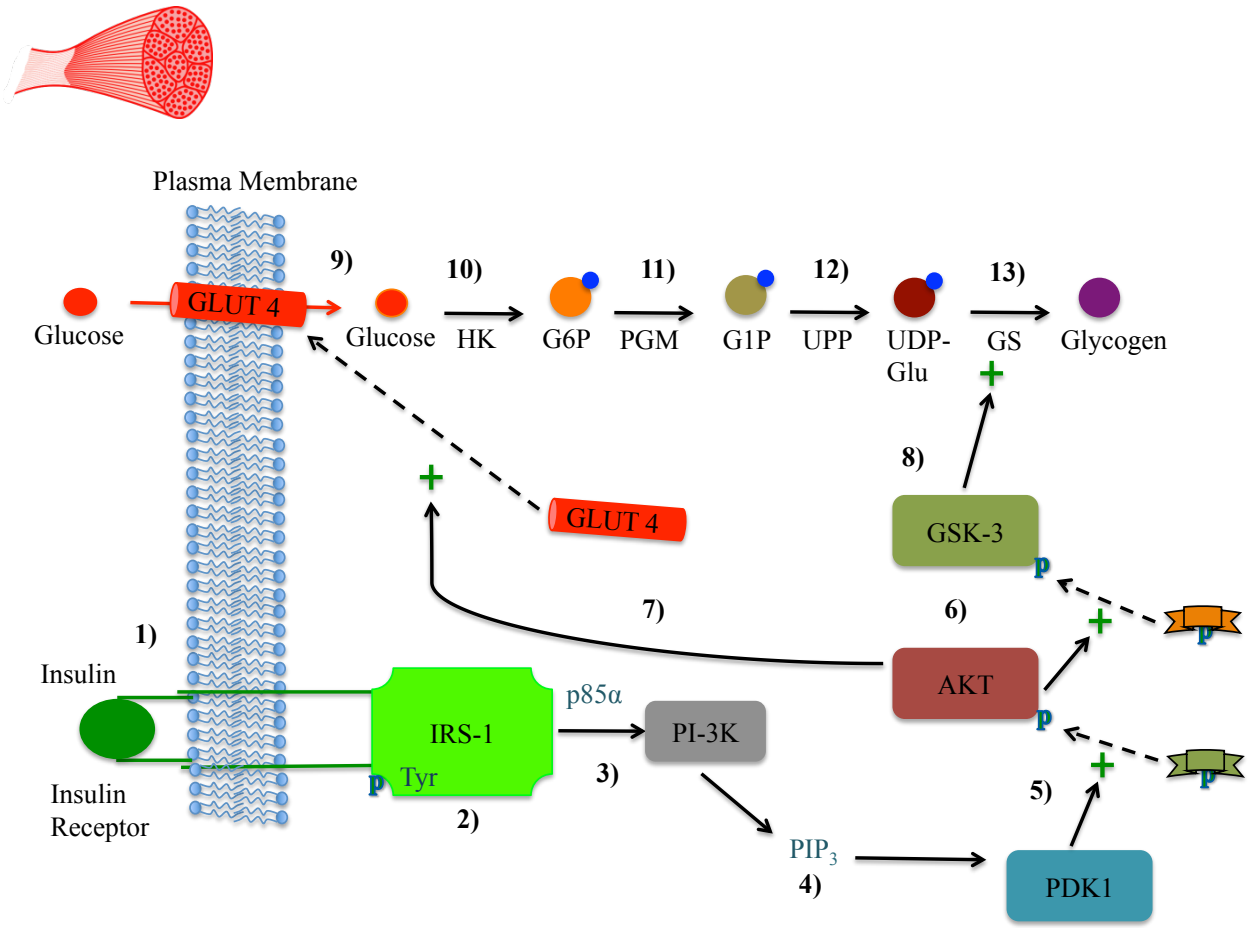

Figure 1: Schematic of glucose uptake and glycogen synthesis via insulin stimulation. Insulin binds to its receptors (1) and triggers autophosphorylation of IRS-1 protein at the tyrosine residue (2). Tyrosine phosphorylation of IRS-1 leads to the activation of PI-3K (3), which, in turn, leads to PIP3 accumulation (4) and activation of PDK1 (5). The latter promotes phosphorylation of AKT (6). Phosphorylated AKT then promotes phosphorylation/deactivation of GSK-3 (7). Additionally, AKT also aids in the signaling involved in translocation GLUT4 to the plasma membrane (8) GSK-3 phosphorylation causes GS to be dephosphorylated and hence activated. (9). Once fused to the membrane, GLUT4 facilitates the entry of glucose that is then phosphorylated by hexokinase II (HK) producing glucose 6 phosphate (G6P) (10). (11), G6P undergoes subsequent enzyme action by phosphoglucomutase (PGM) leading to the production of glucose 1-phosphate (G1P) (12). G1P subjected to action ubiquitin-proteasome pathway (UPP) leading to the production of uridine diphosphate glucose (UDP-Glu) (13). UDP-Glu is finally converted into glycogen via the active GS. Adapted from Lawrence and Roach[42].

GS has nine different amino acid residue sites and it can undergo multi-site phosphorylation[63]. The activation of this enzyme requires the phosphorylation of more than one of its amino acid residues[61,63]. It is not just a number of different sites that require

phosphorylation but phosphate groups must be added in a particular order and this is described as ordered hierarchical phosphorylation[63]. Hierarchical phosphorylation requires a number of regulatory phosphorylation sites; each unit contains a primary phosphorylation site and a secondary site (Figure 2.0)[63]. For example, the deactivation of GS via GSK-3 only occurs when GS has been previously phosphorylated by casein kinase II[44]. In this case, casein kinase II is a primary site kinase which phosphorylates site 5, while GSK-3 is the secondary site kinase which phosphorylates sites 3a, 3b, 3c and 4 leading to the deactivation of GS[44]. Hierarchical phosphorylation has been exemplified *in vivo* and this has demonstrated that the phosphorylation of sites 3a, 3b, 3c and 4 occurs to a greater extent once casein kinase II has phosphorylated of site 5[64].

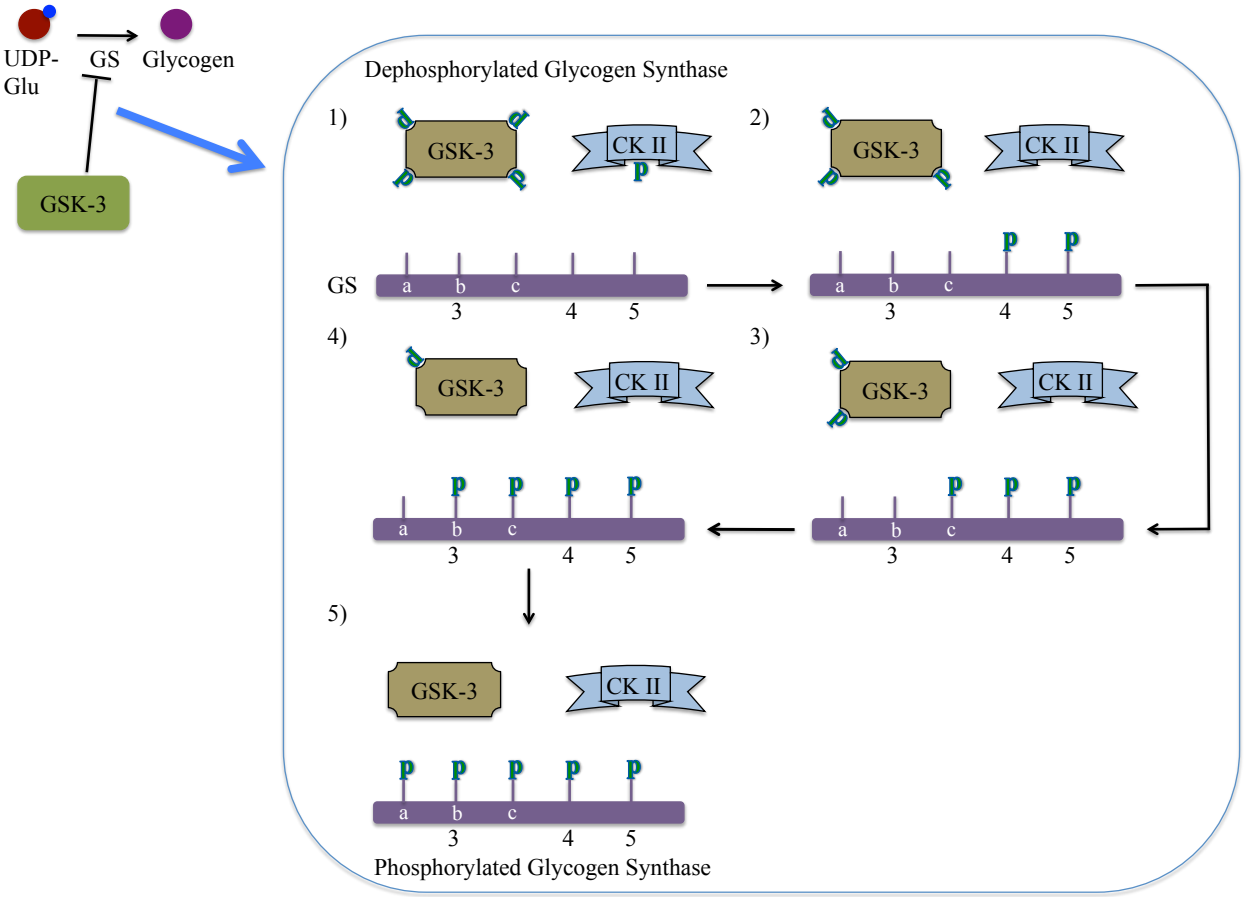

Figure 2: Schematic representation of the ordered hierarchical phosphorylation on sites 3, 4 and 5 of GS, via GSK-3 and casein kinase II (CKII), 1) Dephosphorylated sites 3, 4 and 5 of GS protein 2) After muscle glycogen synthesis is complete, inactivation of GS is initiated via CK II phosphorylation of site 5, followed by subsequent phosphorylation of site 4 by a GSK-3. 3) Proceeding site 4, site 3c is phosphorylated 4) Followed by site 3b 5). Finally, site 3a is phosphorylated completing the deactivation of GS. Adapted from Roach[63].

In addition to undergoing hierarchical phosphorylation, GS is present as two distinctive isoforms: the active (I) and inactive (D) G6P-independent forms[65]. The major structural difference between I and D isoforms is the presence of a covalently bonded phosphate group on the D isoform[64]. These isoforms are interchangeable through reversible covalent modifications, whereby the D can change to the I isoform or vice versa[66]. Leloir et al. were the first to show that G6P can activate GS and further research has established that G6P is an allosteric regulator of GS[62]. Allosteric regulation is achieved by G6P binding to an amino acid residue found on the structure of GS[44]. Upon binding to GS, G6P causes the rearrangement of specific amino acid residues, which in turn causes conformational changes of GS (Figure 3)[44]. This structural change of GS renders the enzyme more vulnerable to dephosphorylation via phosphatases 1 and 2A (Figure 3)[67].

The allosteric activation of GS is a more potent form of activation than covalent activation[65]. This was made evident by a study in mice expressing a mutant GS enzyme[65]. The mutated protein would not be activated by G6P, but would still be able to undergo dephosphorylation upon insulin stimulation of the myocyte[65]. Mice expressing the G6P-insenstive GS enzyme exhibited an approximate 80% reduction of insulin-stimulated muscle glycogen synthesis[65]. This study demonstrates allosteric activation as the primary pathway for GS activation during insulin-stimulated glycogen synthesis[65].

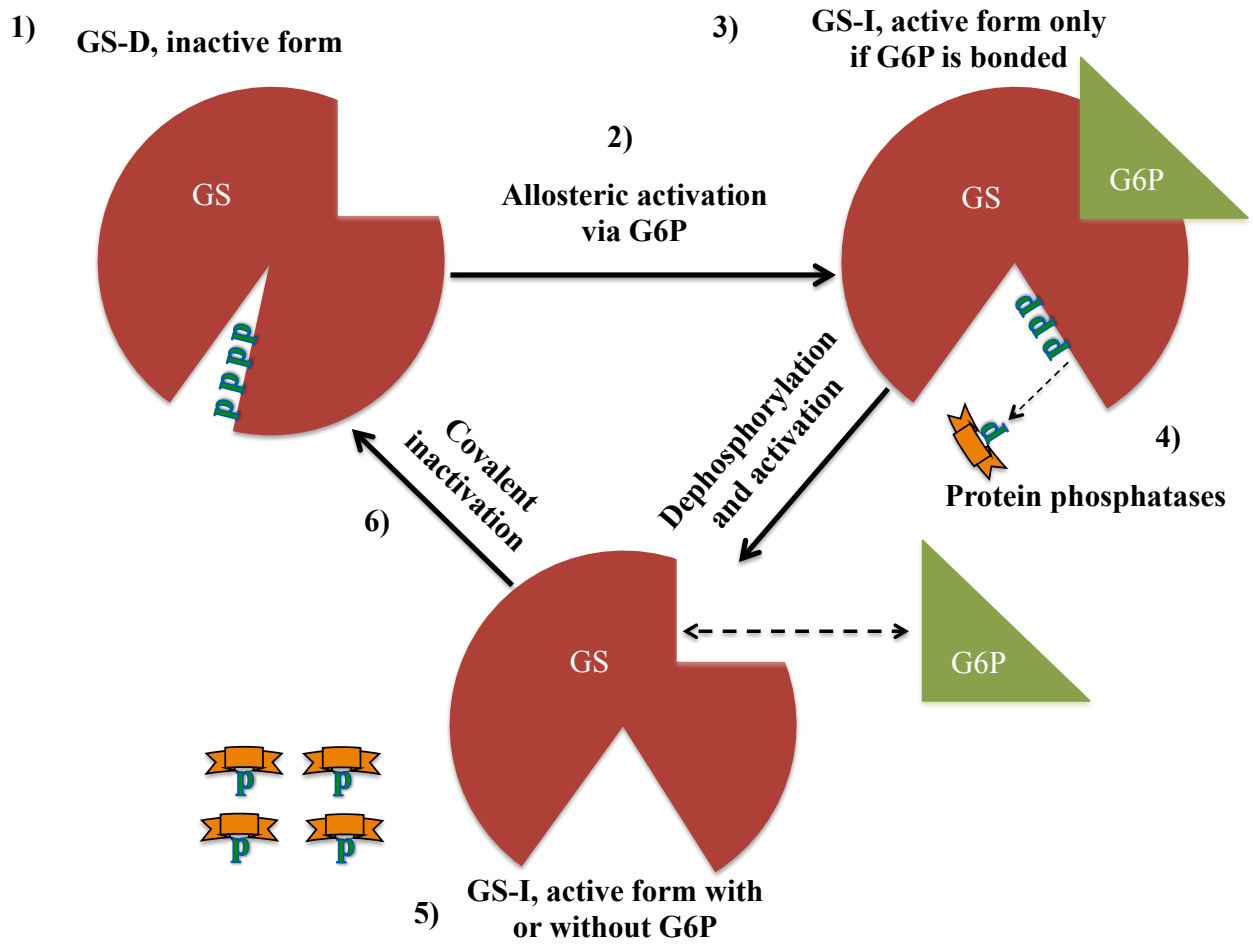

Figure 3: Schematic representation of glucose-6-phosphate allosteric and covalent regulation, that lead to the development of either I or D isoform of glycogen synthase. 1) GS present in its D, inactive, form 2) GS is allosterically activated when G6P binds to GS, and stimulates a conformational change 3) the binding of G6P over-rides the phosphate action upon GS, thus activating the enzyme. Additionally, the change in shape leaves the phosphate groups more vulnerable to protein phosphatases 4) Phosphatases remove the phosphate groups, thus activating GS 5) GS is now active with or without the G6P 6) After no further muscle glycogen synthesis is required GS is covalently inactivated by the addition of the phosphate groups via casein kinase II and GSK-3. Adapted from Villar-Palasi and Guinovart[68].

2.5 Insulin resistance and its effects on muscle

Muscle glycogen synthesis is one of the main processes affected by T2D. The fundamental concern in type 2 diabetic patients is that they often display high concentrations of insulin in the circulation since they are resistant to the action of this hormone[4]. Similarly, obese subjects tend to develop insulin resistance which suggests a link between obesity and T2D[5]. The state of insulin resistance is characterized by a reduction in insulin-stimulated glucose transport and metabolism[69]. The decrease in glucose transport leads to a subjugation in the ability of peripheral tissues, more specifically the skeletal muscle, to aid in systemic glycemic control[70]. This leads to hyperinsulinemia since the pancreas attempts to compensate for this by increasing insulin secretion[71].

Over the years varying mechanisms have been discovered that provide a greater understanding as to why insulin resistance develops in the muscle. Mechanisms involving the production of inflammatory cytokines[71], increased concentrations of glucocorticoids[72], increased reactive oxygen species (ROS) production,[8] and intramyocellular accumulation of lipid intermediates[73] have been identified as inducers of insulin resistance. The common feature shared by all of these mechanisms is that each condition can result of impairment of normal mitochondrial functioning from the excessive intake of a lipid rich diet, which is typical of obesity. Thus, it is essential to comprehend how diet-induced obesity (DIO) affects skeletal muscle glucose metabolism.

2.5.1 Inflammatory Cytokines

It is becoming increasingly understood that the adipose tissue it not just a site of storage but a metabolically active tissue, that is capable of producing biologically active substances known as adipokines[74]. With consumption of a high-fat diet, there is a significant expansion of

the adipose tissue that triggers the release of adipokines. Specific adipokines such as tumor-necrosis factor α (TNF-α) and interlukin-6 (IL-6) have been linked to the development of insulin resistance in muscle[75-76,66-67].

TNF-α is a pleiotropic cytokine with the ability to induce apoptosis, cell proliferation, and stimulate the production of inflammatory molecules[79]. TNF-α is mainly produced by macrophages, particularly those that have infiltrated inflamed, obese adipose tissue[66-67]. It can also be produced by skeletal muscle[79]. The deletion of TNF-α and its receptors in mice makes these animals less susceptible to developing insulin resistance[80]. TNF-α increases serine phosphorylation of IRS-1 via the mitogen-activated protein kinase pathway; which interrupts the insulin signaling cascade and prevents further activation of downstream targets[80].

IL-6 has proven to be quite controversial, as some studies report that IL-6 has the ability to increase insulin sensitivity and glucose transport in muscle[81], whereas others have shown that muscle-derived IL-6 can have adverse effects on glucose metabolism[82]. Acute *in vivo* treatment of mice with IL-6 reduces PI3K activity and insulin-stimulated glucose uptake[82]. This has been attributed to the promotion of serine phosphorylation of IRS proteins as opposed to tyrosine, thus impairing the ability of insulin to increase PI3K activity[82].

2.5.2 Reactive Oxygen Species (ROS)

Similar to inflammatory agents, hyperlipidemia can cause an increase in the production of ROS. The link between obesity and ROS is demonstrated by research indicating that increases in FFA concentrations causes oxidative stress as a result of mitochondrial uncoupling[83]. Oxidative stress is defined as a state where ROS concentrations overwhelm the endogenous antioxidant capacities of a system[84]. When ROS concentrations reach these heights, an inverse relationship with glycemic control is developed [85]. ROS are formed when electrons escape the

electron transport chain and react with oxygen to form a reactive molecule that contains oxygen and a charged species known as superoxide ($O_2\cdot^-$)[86]. Superoxide is converted by manganese superoxide dismutase (SOD) to hydrogen peroxide (H_2O_2)[87]. H_2O_2 can then be reduced to water when found in the mitochondria and reduced to water and oxygen when found outside the mitochondria[87]. Skeletal muscle can generate superoxides and if there is inadequate removal, then $O_2\cdot^-$ and H_2O_2 can cause a redox imbalances in the myocyte that lead to the activation of stress-sensitive intracellular signaling pathways[88]. Activation of these pathways increases the activity nuclear factor kappa-light-chain-enhancer (NF-κB) and PKC, factors that are able to cause insulin resistance[88]. NF-κB is a transcription factor that regulates the expression of a number of genes, some of these genes include the pro-inflammatory cytokines: TNF-α and IL-6[88]. PKC is a kinase that can be activated by lipid metabolites and interrupts in the insulin signaling cascade[88] (this is discussed in greater detail later in this paper). It is hypothesized that if mitochondria can be manipulated to increase the activity of SOD to reduce $O_2\cdot^-$ accumulation, then perhaps oxidative stress may be avoided[89]. Lark et al. (2015) attempted to prove this hypothesis by breeding mice that overexpress SOD with mice that have enhanced H_2O_2 scavenging[89]. They concluded that mice that solely overexpress SOD and the mice that retain the SOD overexpressing gene and the enhanced H_2O_2 scavenging gene are not protected from diet-induced insulin resistance[89]. Rather it seems that the mice who only have enhanced H_2O_2 scavenging gene can avoid diet-induced insulin resistance and thus drugs that can mitigate this pathway will benefit the treatment of insulin resistance more so than those that target $O_2\cdot^-$[89].

However, the increase of FFA uptake is not the only means by which ROS concentrations can increase. Obesity can cause increases in ROS production. The excess adipose tissue that develops in the obese state is able to produce and secrete into circulation, the peptide hormone

angiotensin II (ANG II)[90]. Transgenic rats who overexpress angiotensin II (ANG II) exhibit an increase of ROS which thus induces insulin resistance of the skeletal muscle[91-92]. Under these conditions, ROS have the capacity to affect various insulin signaling pathways such as PI3K activity[70]. Additionally, when ANG II increases ROS production in skeletal muscle, it leads to the impairment of the tyrosine phosphorylation of IRS protein, AKT activation and glucose transport[91].

2.5.3 Glucocorticoids

Glucocorticoids are a class of steroid hormones which bind to glucocorticoid receptors: and unlike other hormones (such as insulin) its receptors are found in the cytoplasm[93]. Glucocorticoids are a subcategory of corticosteroids and cortisol is a corticosteroid, which is produced by the adrenal cortex. Cortisol behaves as a glucocorticoid in that it binds to the glucocorticoid receptor, thus the term glucocorticoids is used to describe cortisol that has glucocorticoid activity[72]. One of the main functions of glucocorticoid is to maintain blood glucose levels during times of physiological stress[94]. Glucocorticoids inhibit glucose uptake by the muscle and even promote gluconeogenesis[95]. As such, there is a clear link between the excessive action of this hormone and insulin resistance[94].

It has been shown that the production of glucocorticoids is increased in the insulin resistant and obese states[96]. The detrimental effects of glucocorticoids' are likely due to their ability to alter glucose metabolism non-genomically[72]. After chronic dexamethasone (an exogenous glucocorticoid) treatment, insulin-stimulated phosphorylation of AKT was decreased[72]. The decreased phosphorylation of AKT could be attributed to a decrease of IRS-1 tyrosine phosphorylation and IRS protein expression[97]. This effect was paralleled by decreased glucose uptake and disposal in skeletal muscle[93]. Glucocorticoids do not alter GLUT4 content,

but rather the action of GLUT4 is decreased in dexamethasone-treated Sol tissue[93]. It is important to note that these effects are not solely caused by glucocorticoids that derive from the adrenal gland since they can also be produced in the muscle via 11β-hydroxysteroid dehydrogenase type 1 (11β-HSD1)[98], which is an enzyme that actively converts cortisone into glucocorticoids[98]. An elevation of 11β-HSD1 content/activity is observed in obese insulin-resistant humans even when plasma glucocorticoid concentrations are normal[94]. According to Morton et al. (2001), 11β-HSD1 knockout mice are more glucose tolerant and display an improved lipid profile when placed under stress or induced to obesity[99]. However, the exact pathways by which these improvements occur are still unclear.

2.5.4 Lipid-mediated Insulin Resistance

The notion of lipids potentiating insulin resistance is exemplified by Santomauro et al. (1999) who demonstrated that overnight reduction of free fatty acids from ~600 to ~300 μmol/l normalized insulin sensitivity in obese non-diabetic patients[100]. The insulin-sensitizing effect of lowering circulating fatty acid levels can be linked to the 'glucose-fatty acid cycle' proposed by Philip Randle[101]. This cycle describes the interplay between glucose and fatty acid fuel selection that is present in mammalian tissues[101]. Randle et al. (1964) theorized that increases in fat uptake would cause an increase in fatty acid oxidation, which would inhibit pyruvate dehydrogenase, increase cytoplasmic citrate concentrations and inhibit phosphofructokinase activity[102]. This would lead to an accumulation of G6P and inhibition of hexokinase II activity (figure 4.0, A).

However, these findings contrast more recent work by Roden et al. (1996) and Dresner et al. (1999) who found that there is a decrease of intramyocellular G6P in humans with increased plasma fatty acid concentrations[45,103]. This research concluded that fatty acids caused skeletal muscle insulin resistance as a result of inhibition of glucose transport, instead of inhibiting

pyruvate dehydrogenase activity[104] (figure 4.0, B). These findings along with more current research brought forth a different theory, one that suggests that the impairment of glucose transport occurs as a result of a accumulation of toxic lipid intermediates, such as Diacylglycerol (DAG) as opposed to the shift in substrate usage that is proposed by the Randle cycle[105,106]. This is considered the most popular hypothesis concerning the development of skeletal muscle insulin resistance[14]. (Figure 4.0, B).

DAG is a relatively simple lipid molecule comprising of a glycerol molecule linked through ester bonds to two fatty acids in positions 1 and 2[109]. Furthermore, DAG is a well-known precursor of IMTG synthesis and it makes up part of the cell membrane and is a second messenger signaling lipid[109]. In the context of skeletal muscle insulin resistance, DAG is a well-known allosteric activator of protein kinase C (PKC) specifically PKC- θ[15]. PKC has both genomic and non-genomic effects upon the myocyte. The non-genomic effects concern the phosphorylation of serine residues of IRS1/2, which prevents insulin-stimulated IRS tyrosine phosphorylation[15]. This causes impairment of the early stages of the insulin-signaling cascade[15]. The genomic effects of PKC relate to increasing the activity of NF-κB [105-106].

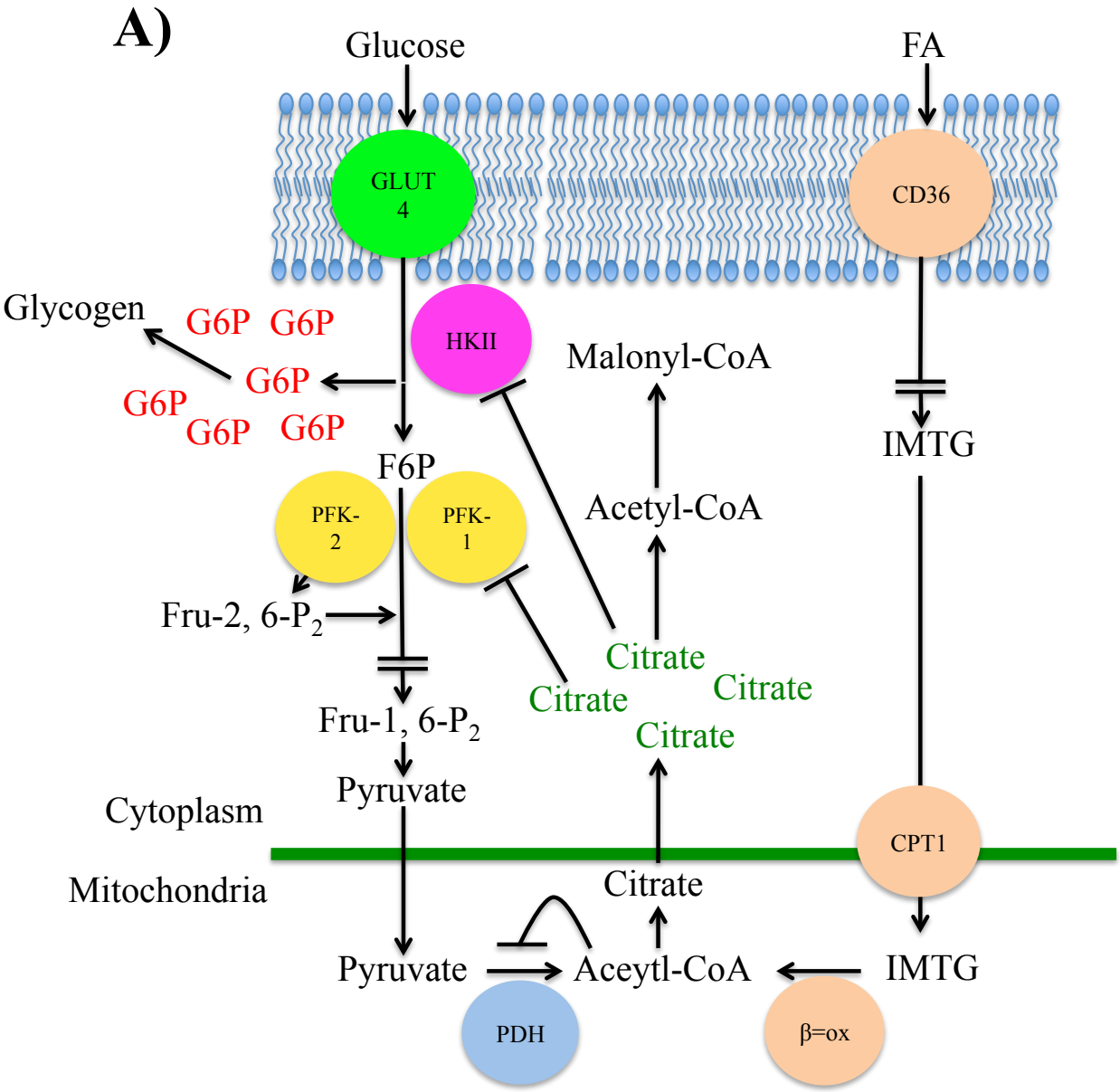
A)
Glucose
FA
GLUT 4
CD36
Glycogen
G6P
G6P
G6P
G6P
G6P
G6P
HKII
Malonyl-CoA
IMTG
F6P
PFK-2
PFK-1
Acetyl-CoA
Fru-2, 6-P2
Citrate
Citrate
Citrate
Citrate
Fru-1, 6-P2
Pyruvate
Cytoplasm
CPT1
Mitochondria
Citrate
Pyruvate
Aceytl-CoA
IMTG
PDH
β=ox

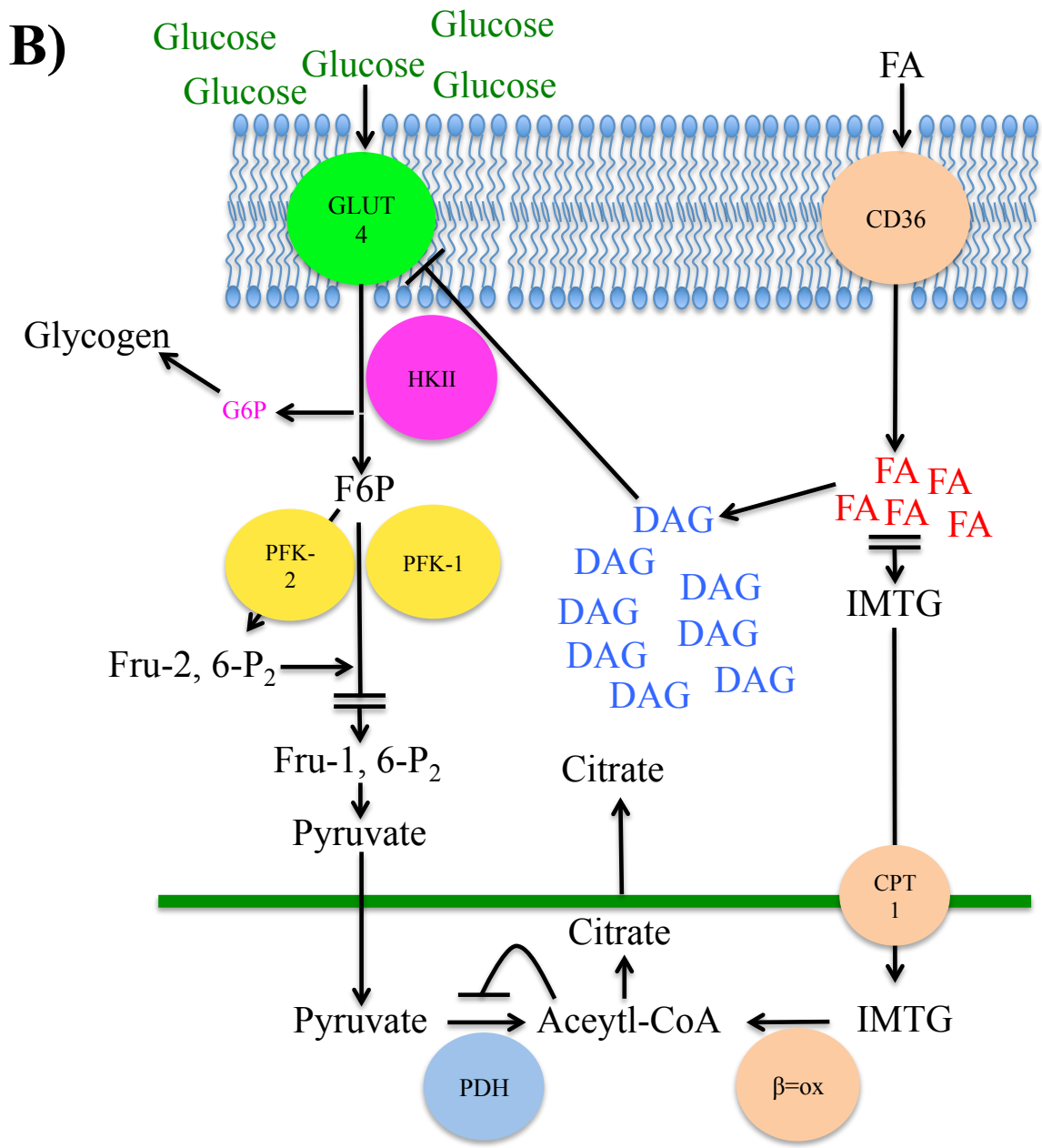

Figure 4: Schematic representation of (A) Randle theory for the development of insulin resistance and (B) Schematic representation of DAG mediated insulin resistance. (A) Displaying the Randle cycle's approach to the development of diet-induced insulin resistance: Glucose is usually entering the cell and subject to oxidation or is stored as glycogen. However, when there is an abundance of fat in the diet Fatty acids (FA) are actively entering the myocyte via cluster of differentiation 36 (CD36). Once inside the myocyte FAs are converted into intramuscular triglycerides (IMTGs), these triglycerides enter the mitochondria via carnitine palmitoyltransferase I (CPT1) thus β-oxidation (β=ox) rates are increased to help combat this influx of LCFA. This results in a significantly higher production of acetyl-CoA, which inhibits pyruvate dehydrogenase (PDH) activity and increases citrate concentrations in the mitochondria. The accumulation of citrate in the mitochondria causes leakage into the cytoplasm. The accretion

of citrate in the cytoplasm not only creates malonyl-CoA but also inhibits hexokinase II (HKII) and phosphofructokinase (PFK). The inhibition of these enzymes prevents glucose oxidation from taking place and causes an accumulation of G6P in the cell. However, more recent work has lead to an alternative hypothesis. (**B**), This hypothesis states that increased fat intake would cause the accumulation of lipid intermediates in the cytoplasm. Primarily diacylglycerol (DAG), this lipid will indirectly interrupt the insulin-signaling cascade and lead to reduced activity of GLUT4 amongst other things. The result is that glucose remains in the circulation without being stored or oxidized.

2.6 Exercise and Insulin Resistance

A common and well-documented approach to the reversal and prevention of the effects of diet-induced insulin resistance is exercise[110-111]. Exercise is considered a more powerful means of increasing insulin sensitivity than drug interventions. Studies have shown that exercise increases insulin sensitivity significantly more than Metformin[112] or Troglitazone[113] in humans, with the additional improvements in cardiovascular and respiratory performance[114]. In general, physical activity levels are lower in those with insulin resistance and pre-diabetes than healthy individuals[115]. The Diabetes Prevention Program showed that exercise reduced the incidence of T2D by 58% in individuals who were at significant risk for the development of the disease[116]. Based on the data from healthy subjects, an acute bout of aerobic/endurance exercise of at least 60% VO_2 max for 60-90 minutes is required to stimulate significant improvements in insulin sensitivity[117]. Aerobic training is not the only means by which metabolic profile can be improved; resistance training is a valid alternative platform[118]. Resistance training improves GLUT4 protein content and causes hypertrophy of both type I and type II fibers[120-121]. Yet, the overall consensus seems to favor aerobic exercise as the primary form of physical activity. This in part may be due to its ability to produce a more significant anti-inflammatory effect as oppose to resistance training[121].

There is significant evidence that moderate to high-intensity aerobic training can improve muscle insulin sensitivity[122]. Chibalin et al. (1999) have shown the mechanistic benefits of

exercise by assessing the activity of GLUT 4 and key upstream proteins involved in the insulin-signaling cascade[123]. In Chibalin's study, Wistar rats were exercised for one day and five days, each day for six hours[123]. Sixteen hours after the last exercise bout, the epitrochlearis muscle was isolated and GLUT4 content and signaling proteins were assessed[123]. Exercise increased GLUT4 content 2-fold after a one day bout and 4-fold after a five day bout of exercise[123]. Insulin-stimulated tyrosine phosphorylation of IRS-1 and PI-3K activity were markedly increased after five days[123]. IRS-2 expression and IRS-2 associated PI-3K activity increased after one day of exercise[123]. Finally, insulin-stimulated serine/threonine phosphorylation of AKT increased 2.3-fold after five days of exercise[123]. Furthermore, in a different study by Jensen et al. (2012) exercise was shown to stimulate downstream targets of AKT[124]. Jensen et al. performed a study on lean, obese and T2D human subjects undergoing an acute bout of endurance exercise at 70% VO_2 max[124]. It was found that GS serine residues were dephosphorylated regardless of inactivation of the AKT downstream target GSK-3[124]. Additionally, irrespective of whether the subject was lean, obese or type 2 diabetic, exercise caused an increase of the affinity of GS for UDP-glucose[124].

Exercise not only improves glucose metabolism, but also stimulates glucose uptake. Exercise-mediated glucose uptake is independent of insulin and is activated via muscle contractions[37]. When muscle contractions occur, adenosine 5'-triphosphate (ATP) is broken down into adenosine diphosphate (ADP)[37]. ADP is then further metabolized giving rise to adenosine monophosphate (AMP). The latter binds to the catalytic site of 5' adenosine monophosphate-activated protein kinase (AMPK)[37] causing it to undergo a conformational change and activation[37]. Activated AMPK will promote the phosphorylation of Akt substrate of 160 kDa (AS160) a known mediator of GLUT4 translocation[125]. Once phosphorylated AS160,

indirectly promotes GLUT4 translocation thus increasing glucose uptake[37]. Increased glucose uptake stimulates HKII activity, which increases G6P content. The augmented concentrations of G6P can stimulate allosteric activation of the terminal enzyme in glycogen synthesis, GS.

The effects of exercise go beyond the insulin-signaling cascade and even affect mitochondrial content and functioning[126]. Physical training improves oxidative capacity *in vivo* this is mostly likely due to increased mitochondrial content and/or increased functionality per mitochondrion[126]. Increased oxidative capacity and mitochondrial function would also provide a reason as to why in the context of lipid-mediated insulin resistance exercise leads to a decrease in intramyocellular DAG content and improves insulin sensitivity[127]. The reduction of intracellular DAG concentration has been linked to less PKC-θ activation, which shifts back to normal tyrosine phosphorylation of IRS-1 protein, allowing for proper insulin signaling to occur[127].

Exercise and inflammatory cytokines

IL-6

Much like DAG, IL-6 is considered a harmful agent in the context of diet-induced insulin resistance. This was initially hypothesized due to TNF-α stimulating the production of IL-6[128]. However, in a more recent study in which hyperinsulinaemic–euglycaemic clamp was performed in T2D and control patients, it was demonstrated that no relationship existed between insulin sensitivity and IL-6[129]. Part of the controversy surrounding the effects IL-6 results from its increased presence during exercise[130]. In fact, plasma IL-6 levels can increase 100-fold during exercise[131]. Additionally, muscle contractions can cause the increased production of IL-6 independent from the production of TNF- α[132]. Highlighting that muscular IL-6 has a role to play in metabolism rather than just inflammation[132]. It was first thought that the severe increase in IL-6 was a result of an immune response from the muscle in an attempt to address any local damage

developed over the course of exercise[133]. More recently, it has been shown that during exercise IL-6 has more of a metabolic than inflammatory role[149-151]. This notion is supported by enhancement of intramuscular IL-6 mRNA expression[134] and protein release[135] when muscle glycogen stores are low[136]. Further evidence supporting this hypothesis is provided by a study demonstrating glucose infusion during exercise reduced plasma IL-6 levels[131].

TNF-alpha

When IL-6 concentrations increase as a result of exercise, it has been shown that this increase helps down-regulate TNF-α concentrations[137]. TNF-α concentrations can be normalized in mice that overexpress the TNF-α gene through a single bout of exercise[138]. Additionally, Balducci et al. (2009) determined that subjects undergoing a bi-weekly endurance-training program consisting of 60 min sessions at 70-80% of VO_2 max for 12 months exhibited a significant decrease in circulating TNF-α levels and improvement in insulin sensitivity[139].

ROS

Hey-Mogensen et al. (2010) have shown that 10 weeks of exercise training program that consisted of stationary cycling for 20-35min, 4-5 times per week at 65% VO_2 was able to cause significantly less skeletal muscle ROS production in obese control subjects compared to obese T2D subjects[126]. On the other hand, The generation of ROS from non-mitochondrial sources has proven to be important in relation to healthy insulin signaling[140]. The enigmatic role of ROS is linked to the degree and duration of the ROS that is produced[83]. In other words, the transient increases in ROS concentrations in the myocyte can help improve insulin sensitivity, but sustained concentrations as seen in hyperlipidemia will cause harmful effects[126].

Glucocorticoids

The effect of exercise upon elevated glucocorticoids within an animal model is still undergoing research. The most recent work by Beaudry et al. (2015) has shown that exercised animals (voluntary exercise) with exogenously elevated glucocorticoids still present with hyperglycemia under fasted conditions. However, exercised animals glycemic values were significantly lower in comparison to the sedentary animals with elevated glucocorticoids[141]. It should be noted that in both of these groups, a high fat diet was administered. Therefore, high fat fed exercised animals with elevated glucocorticoids exhibited an improved, but not normalized metabolic profile compared to their sedentary counterparts[141].

Despite the uncertainty surrounding the precise effect of exercise upon certain mechanistic factors of diet-induced obesity, exercise has shown to be a very effective tool in reversing the detrimental effects of HF-diet-induced insulin resistance.

2.7 Underlying questions of skeletal muscle insulin resistance

What is the unifying theory in HF induced skeletal muscle insulin resistance?

Almost all the theories that attempt to explain the development of HF induced skeletal muscle insulin resistance (except glucocorticoids) share a similar premise, chronic HF feeding can negatively affect the mitochondria (Figure 5A). It is hypothesized that the mitochondria are becoming overwhelmed by the excessive lipid uptake. This can result in the production of excess $O_2 \cdot^-$, and inadequate removal of $O_2 \cdot^-$ stimulates the activation of inflammatory transcription factors, that leads to the production of TNF-α and IL-6[8]. The mitochondria are also central to the Randle cycle theory, as it is suggested that chronic HF feeding causes an increase in citrate output from the mitochondria which prevents glucose utilization in the muscle[142]. Finally, there is the most popular theory describing the pathogenesis of skeletal muscle insulin resistance[143]. The theory, which involves lipid uptake surpassing mitochondria oxidation rates leading to toxic

lipid intermediate build up[143]. This theory is currently considered the predominating cause of skeletal muscle insulin resistance, that is why the focus of our study will be on this pathway[144]. With all these different pathways in mind it is clear that mitochondria content must be taken into consideration when discussing skeletal muscle insulin resistance.

With respect to the muscle, the amount of mitochondria is related to the muscle fiber type composition in the muscle. Of the two major muscle fiber types in skeletal muscle, type I fibers contain the most mitochondria. As a result these fibers are able to oxidize fats more easily, while type II fibers contain less mitochondria, thus the oxidation of fats is not as efficient. This crucial difference between muscle fibers is not normally considered with studies concerning lipid induced skeletal muscle insulin resistance research. We agree with comments by Dr. ZengKui Guo, who suggests that when a study is conducted on muscle of mixed fiber type, extrapolating the findings of a study to apply to all muscle fiber types may not be the most accurate approach[145]. To gather an even deeper understanding of the pathogenesis of skeletal muscle insulin resistance, the discussion must be broken down into fiber type specific manner (figure 5B). As it is clear from previous work that type I fibers are significantly more insulin sensitive than type II fibers. Type II fibers are more heavily expressed in T2D patients than type I fibers. This is all that is in known about fiber type specific insulin resistance thus in our study we would like to focus upon one of the most well researched pathways that lead to skeletal muscle insulin resistance but observe its pathogenesis between a number of muscles expressing predominantly one muscle fiber type (figure 7). Additionally, we want to include an exercise component to our study that allows us to observe how chronic endurance exercise affected fiber type specific insulin resistance (figure 7).

Therefore, the main hypothesis of this study was that muscles rich in mitochondria would less susceptible to suffering from toxic lipid intermediate build up when compared to muscles with lower amounts of mitochondria (figure 6). The rationale behind this hypothesis was that fiber types with more mitochondria would be less likely to be overwhelmed with lipids due to a greater capacity to oxidize lipids. In order to test this hypothesis, we used an animal model exposed to lipid oversupply (high-fat diet) either under sedentary or chronically endurance-trained conditions.

A

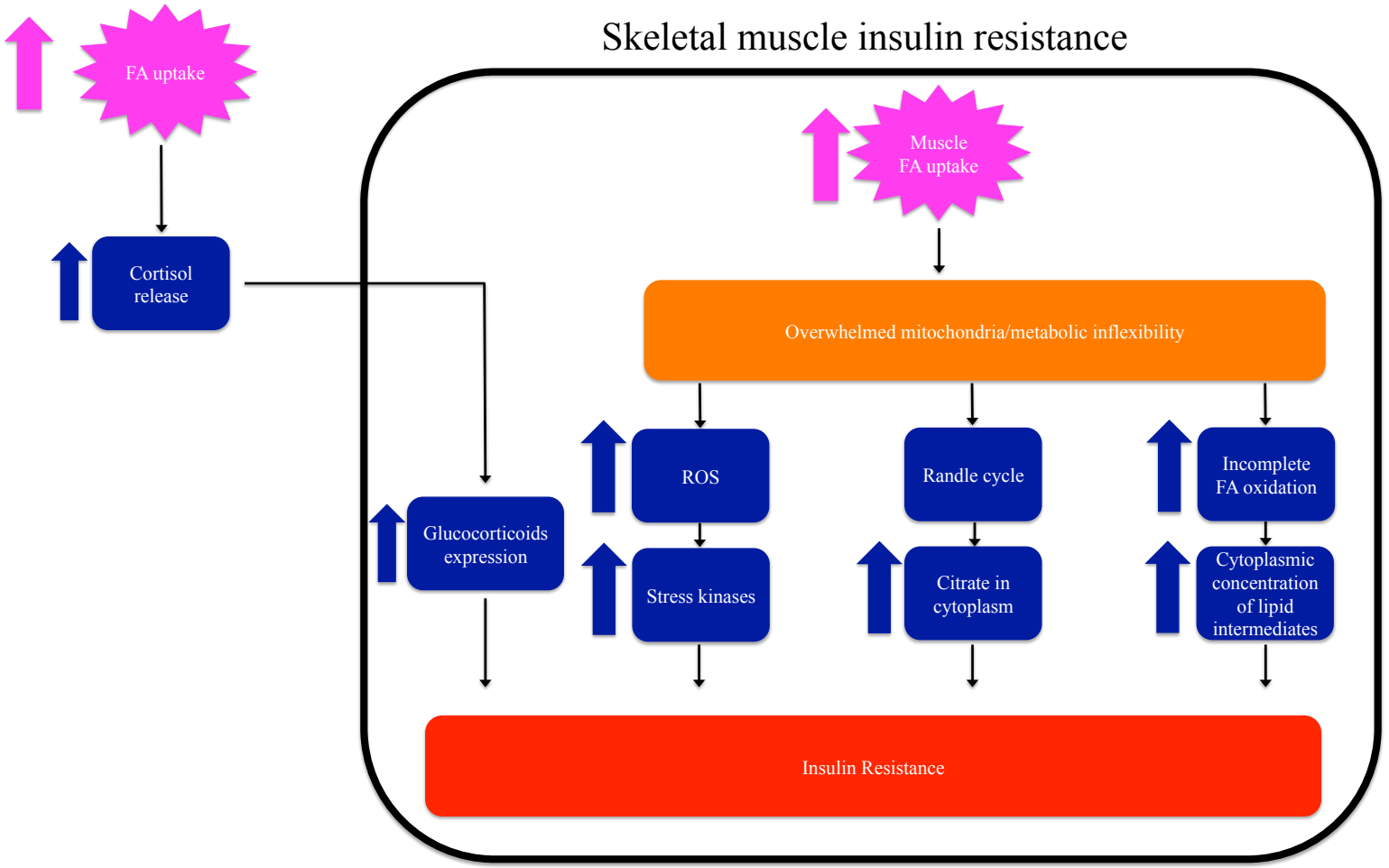
Skeletal muscle insulin resistance
FA uptake
Cortisol release
Muscle FA uptake
Overwhelmed mitochondria/metabolic inflexibility
Glucocorticoids expression
ROS
Stress kinases
Randle cycle
Citrate in cytoplasm
Incomplete FA oxidation
Cytoplasmic concentration of lipid intermediates
Insulin Resistance

B

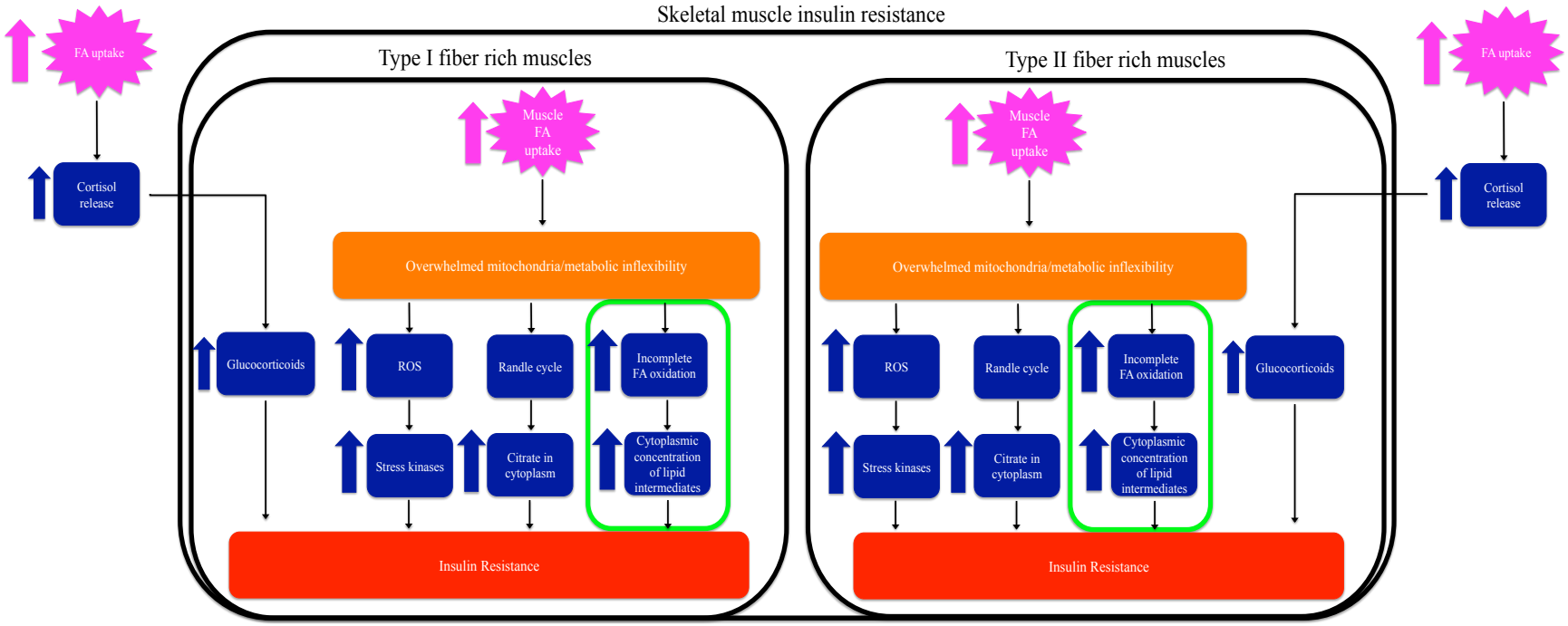

Figure 5: (A) A schematic briefly highlighting the key research topics concerning the pathogenesis of skeletal muscle insulin resistance and how they are normally researched. (B) A similar schematic of key insulin resistance research topics but adjusted to address topics in a fiber type specific manner, the focus of our study is highlighted in green.

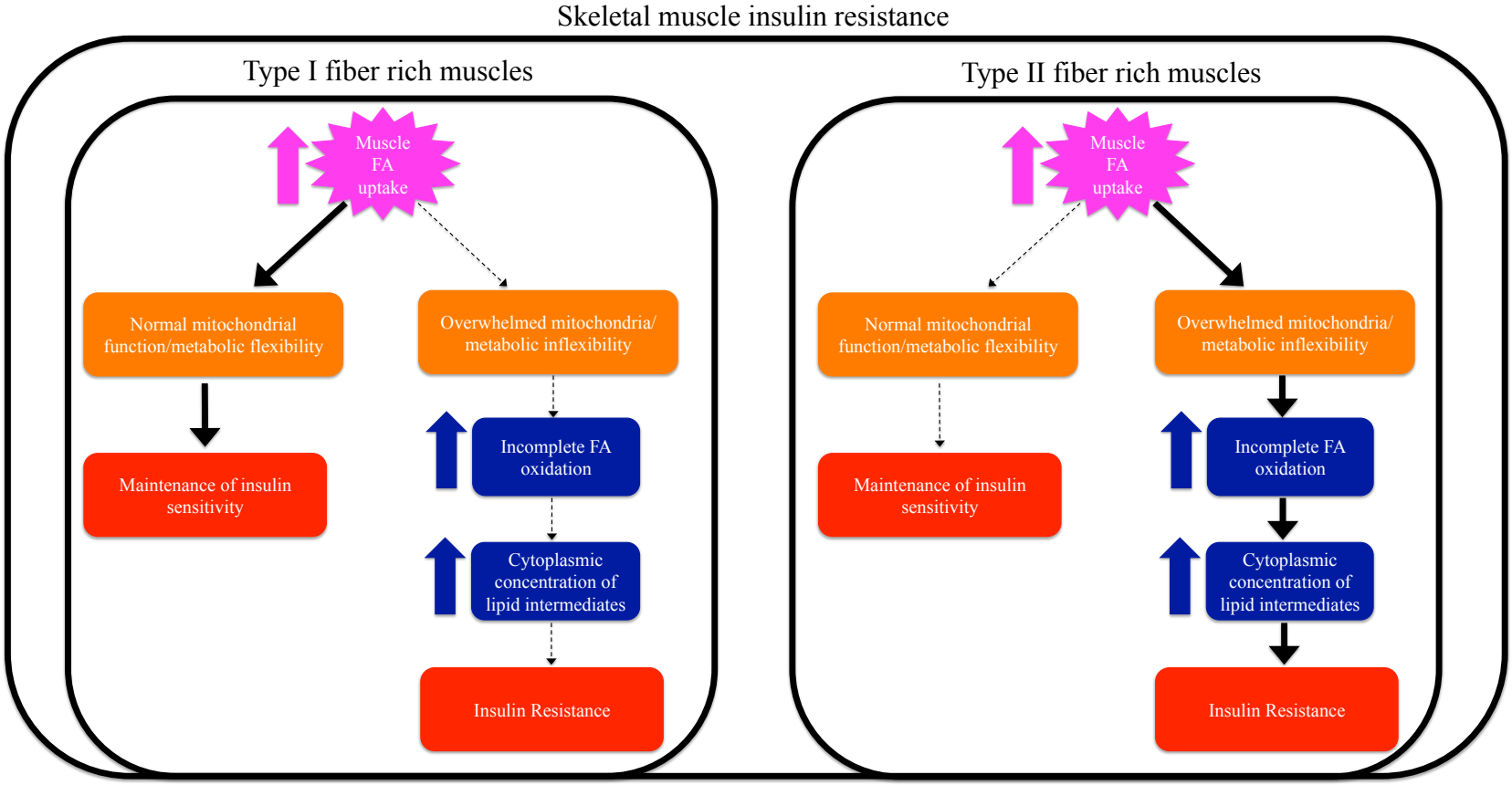

Figure 6: A schematic illustrating the approach to our study, we will be discussing insulin resistance in a more fiber type specific way rather than generalizing findings to all muscle fiber types. Our hypothesis is also highlighted in this schematic: type I fibers are more likely in maintaining their insulin sensitivity due to their abundance of mitochondria, while type II fibers will be more susceptible to mitochondrial dysfunction and metabolic inflexibility due to a significantly lower amount of mitochondria thus leading to insulin resistance.

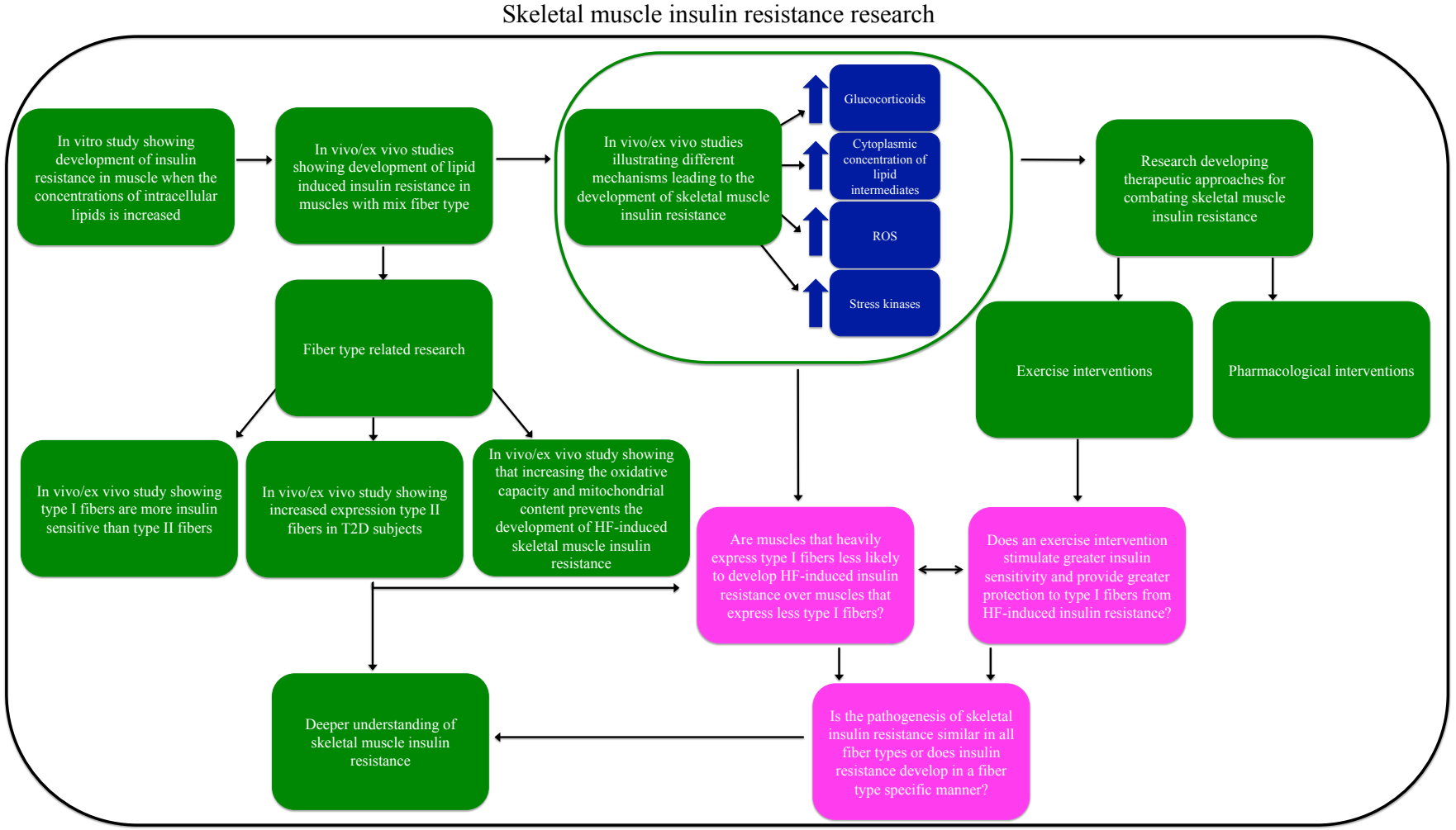

Figure 7: A schematic displaying the rich body of research present in the field of skeletal muscle insulin resistance. Our work (highlighted in purple) is critical in better understanding how the pathogenesis of skeletal muscle insulin resistance maybe different in different muscle fiber types.

3. Objectives and Hypotheses

The hypotheses that this study tested were:

a) That highly oxidative muscles are less prone to developing insulin resistance under conditions of lipid oversupply than highly glycolytic ones.

b) Endurance exercise will stimulate greater insulin sensitivity in oxidative muscles and consequently provide greater protection from the build-up of toxic lipid intermediates.

These hypotheses were tested through the following objectives:

1. Using an animal model to observe how chronic high-fat feeding along with physical inactivity or activity affects insulin sensitivity. This model will separate rodents into 4 conditions: Sedentary SC (SED SC), sedentary high fat (SED HF), exercise SC (EX SC) and exercise HF (EX HF).
2. Measuring fasted circulating glucose and insulin levels to determine if our model was successful in developing systemic insulin resistance.
3. Harvesting muscles that favor specific muscle fiber types after the 8 weeks to assess glycogen synthesis rates and glycogen content to comprehend if the ability of the glycolytic muscles to synthesize and store glycogen was more severely affected than oxidative muscles.
4. Western blots analysis probing for key mechanistic proteins involved in the insulin-signaling cascade, to observe whether oxidative fibers are less affected by the disruptions in the insulin-signaling cascade caused by chronic HF feeding.
5. Assessing G6P content between muscle fiber types in each condition, which will help determine if any of the three muscles G6P production was differently affected than others.

Studies have shown that training induced GLUT 4 content increase mainly in type I fibers[146], thus more G6P content should be expected in trained oxidative fibers.

6. Measuring intramuscular palmitate oxidation to establish the oxidative capacities of each muscle. Additionally, we will observe how chronic HF feeding affects the fatty acid oxidation rates in muscles of varying oxidative capacities.

4. Materials and Methods

4.1 Reagents

Rat Triacylglycerol quantification kit and glucose 6 phosphate assay kit was purchased from Abcam (Toronto, Canada). Specific antibodies against Akt, P-Akt (Thr 308 and Ser 473), GSK-3β, P-GSK-3α/β (Ser 21 of GSK-3α and Ser 9 of GSK-3β), GS, P-GS (Ser 641, site 3a) were from Massachusetts, USA. [1-^{14}C]palmitic acid and D-[U-^{14}C]glucose was obtained from GE Healthcare Radiochemicals (Quebec, Canada). Human insulin (Humulin R) was purchased from Eli Lilly Inc. (Toronto, Ontario, Canada).

4.2 Animals

Male albino rats Wistar strain (Charles River Laboratories, Montreal, Quebec, Canada) weighing 45-55 g were maintained in a 12-hour light (07:00-19:00) and 12-hour dark cycle (19:00-07:00) at 22°C with *ad libitum* access to water and standard chow (SC) diet. The rats were allowed to acclimatize for 1 week upon their arrival and then they were fed a SC diet until they achieved a body mass of ~250g. Animals were individually housed so that body weight (BW) and food intake could be monitored on a daily basis. Subsequently, the diet and/or exercise interventions begun and BW and food intake were continuously measured on a daily basis throughout the study. Animals were randomly assigned to one of the following groups: Sedentary SC (SED SC), sedentary high fat (SED HF), exercise SC (EX SC) and exercise HF (EX HF). The SC diet consisted of 60.0 % carbohydrate, 13.0 % fat, and 27.0 % protein (3.43 kcal/g). The HF diet consisted of 20.0% carbohydrate, 60.0% fat, and 20.0% protein (5.24 kcal/g). The York University Animal Care Ethics Committee has approved all experimental procedures.

4.3 Exercise Selection

Following acclimatization, the rats underwent an exercise selection protocol to identify animals that are not willing to run. This selection protocol was done on three separate occasions. It began with a 5 min warm up at a speed of 10 m/min with 5% inclination on the treadmill. The speed was then increased by 2 m/min every 2 min for 30 min. Animals that were capable of running beyond 20 m/min for 20 min on all three occasions were placed in an exercise group. Those that were unable to fulfill these criteria were placed in the sedentary group.

Figure 8.0: Exercise selection protocol

Stage	Speed (m/min)	Incline (%)	Duration
Warm up	10	0	5
1	12	5	2
2	14	10	2
3	16	10	2
4	18	10	2
5	20	10	2
6	22	10	2
7	24	10	2
8	26	10	2
9	28	10	2
10	30	10	5

4.4 Peak VO2 tests

Peak VO_2 tests were conducted at weeks 0, 2, 4, and 6 of the study in order to adjust the intensity of exercise as the endurance capacity of the animals improved. Peak VO_2 tests in rats were conducted using the Comprehensive Laboratory Animal Monitoring System (CLAMS) through an exercise protocol of incremental workloads. Prior to initiating the peak VO_2 tests, resting VO_2 was measured. Subsequently, a 5 min warm-up period consisting of running at 10 m/min with no inclination began. Once the warm-up period was over, the inclination and speed

of the treadmill were increased to 12 m/min and 5%, respectively, for the next 2 min. Subsequently, the treadmill inclination was raised to 10% and maintained at that level throughout the test, while the speed was increased by 2 m/min every 2 min. The animals were required to run until exhaustion, which was characterized by the animals remaining on the shocking pad for 5 consecutive seconds, by reaching a plateau in VO_2 despite increased speed, and/or by reaching a RER value of 1 or greater.

4.5 Endurance Training protocol

Rats in the endurance training groups were exposed to treadmill running at 70 – 85% of peak VO_2, 1h/day, 5 days/week for 8 weeks. The intensity range of 70-85% of peak VO_2 was chosen based on the recommendations by the American College of Sports Medicine (ACSM) to improve cardiovascular fitness and promote health benefits in humans[147]. Peak VO_2 tests were conducted bi-weekly in order to adjust the exercise intensity as the animals improved their aerobic capacity with training. Additionally, to maintain equal conditions among all groups, the SED animals were placed on the treadmill for 1h/day at a speed of 2 m/min.

4.6 Glucose Tolerance Test (GTT)

After acclimatizing, at week 0 a GTT was done to gather baseline measurements of glycemic control. After 8 weeks of diet and exercise interventions, the animals were fasted overnight and baseline (time 0) blood glucose measurements were taken by saphenous vein bleeding. Subsequently, each animal received an intraperitoneal (IP) injection of glucose (2g/kg of BW) prepared in a 30% glucose solution in physiological saline. Plasma glucose was determined after 15, 30, 60, 90, and 120 min by the glucose oxidase method using the OneTouch UltraMini blood glucose monitoring system from LifeScan Canada Ltd (BC, Canada). Blood was

also collected after 15, 30, 60, 90, and 120 min for the determination of serum insulin concentrations. After collection, blood was centrifuged for 10 min at 13,000 rpm (4°C) and plasma was then extracted and stored at -80°C.

4.7 Circulating Insulin

After a 14-hr fast, blood samples were collected from the saphenous vein at week 0, 3, & 6 for analysis of circulating insulin concentrations. Samples were immediately centrifuged @ 13,000 rpm for 10 min (4°C). Plasma was extracted and stored at - 80°C. Plasma was assayed using a commercially available ELISA from EMD Millipore (Cat # EZRMI-13K).

4.8 Muscle isolation and incubation

If animals were exercised, 24 hours of rest was given before they were anesthetized with a single i.p. injection of ketamine/xylazine (90 mg and 10 mg/100g B.W., respectively). Subsequently, the soleus (Sol), extensor digitorium longus (EDL), and epitrochlearis (Epit) muscles were quickly extracted. These muscles were chosen because of their wide range of reported fiber-type distributions with distinct mitochondrial contents and oxidative capacities. The percentages of type I, type IIa and type IIb in Sol, EDL and Epit muscles are 84/16/0, 3/57/40, and 15/20/65, respectively[148-149]. Three sets of muscle strips (18 – 22 mg) were prepared from each muscle and mounted onto thin stainless steel wire clips in order to maintain optimal resting length. The muscle strips were immediately placed in plastic scintillation vials containing 2 ml of pre-gassed [30 min with O_2:CO_2-95:5% (vol/vol)] Krebs-Ringer bicarbonate (KRB) buffer with added 4% fat-free BSA and 6 mM glucose. These vials were sealed with rubber stoppers and gasification was continued for the entire one hour pre-incubation period. Following the pre-incubation period, one set of muscles was transferred to vials containing 2 ml of the same

KRB buffer plus D-[U-^{14}C] glucose (0.2 μCi/ml) and incubated under continuous gasification for one additional hour either in the absence (basal) or presence of insulin (100 nM) for glycogen synthesis determination. Another set of muscles were transferred to vials containing 2 ml of the KRB buffer and incubated under continuous gasification for one additional hour either in the absence or presence of insulin (100nM) for the purposes of assessing insulin signaling.

4.9 Assays

After muscle isolation and extraction, tissues were immediately snap-frozen in liquid nitrogen and stored in -80^{o}C until subsequent analysis. 100mg of Sol, EDL and Epit basal tissue were weighed and homogenized, triacylglycerol and G6P content of homogenates were determined using their commercially available assay kits from Abcam.

4.10 Measurement of glycogen synthesis and content in isolated muscles

Glycogen synthesis was assessed by measuring the incorporation of D-[U-^{14}C]glucose into glycogen as previously described.[150] Briefly, immediately after incubation, muscle strips were quickly washed in ice-cold PBS, blotted on filter paper, frozen (N_2), and digested in 0.5 ml of 1mol/l KOH at 70°C for 1 hour. Of the digested muscle solution, aliquots were taken for the determination of glycogen content (100ul) and glycogen synthesis (400ul). To each of the glycogen synthesis aliquots, 100ul of carrier glycogen, 80ul of saturated Na_2SO_4 and 1.2 ml of Ethanol was added. Solutions were vortexed and left to precipitate overnight at -20°C. The tubes were then centrifuged and the remaining pellets re-suspended in 0.5 ml of water and its radioactivity determined using a scintillation counter.

Glycogen content was measured using 100 μl of the KOH digested sample. 10% (v/v) of acetic acid 17M, 500 μl of acetate buffer (4.8 pH) with amyloglucosidase (0.5 mg/ml) was added

and the resulting solution was left to incubate at room temperature overnight. On the following day, the solution was neutralized with 1/16 (v/v) of NaOH (5N). Then, 1 ml of ATP-TRA buffer was added to each sample and then vortexed. Finally, 1 ml of the solution was placed in a cuvette and counted on the spectrophotometer at 340 nm.

4.11 Measurement of palmitate oxidation in isolated muscles

Palmitate oxidation was measured by assessing the production of $^{14}CO_2$ from [1-^{14}C] palmitic acid. The flasks where muscle strips were incubated and contained 2 ml of KRB buffer and 0.2 mM of cold palmitic acid previously complexed with fatty acid-free BSA and [1-^{14}C] palmitic acid (0.2 μCi/ml). The muscles were incubated under continuous gasification for one hour in vials in which a centered isolated well held a loosely folded piece of filter paper moistened with 0.2 ml of 2-phenylethylamine/methanol (1:1, vol/vol). Following the one hour incubation period, the muscles were rapidly removed and the media acidified with 0.2 ml of H_2SO_4 (5N). The flasks were immediately re-sealed and incubated for an additional one hour to collect the $^{14}CO_2$ released. Subsequently, the filter papers were carefully removed and transferred to scintillation vials containing 10 ml of scintillation fluid for radioactivity counting.

4.12 Western blotting analysis of content and phosphorylation of Akt, GSK3, and GS

Incubated muscle strips were homogenized in a buffer containing 25 mmol/l Tris-HCl and 25 mmol/l NaCl (pH 7.4), 1 mmol/l $MgCl_2$, 2.7 mmol/l KCl, 1% Triton-X, and protease and phosphatase inhibitors (0.5 mmol/l Na_3VO_4, 1 mmol/l NaF, 1 mmol/l leupeptin, 1 mmol/l pepstatin, and 20 mmol/l PMSF). Muscle homogenates were centrifuged and the supernatant was collected. An aliquot was used to measure protein content by the Bradford method. Samples were diluted 1:1 (vol/vol) with 2 x Laemmli sample buffer, heated to 95° C for 5 min, and

subjected to SDS-PAGE. All primary antibodies were used in a dilution of 1:1,000. GAPDH and β-actin were used as loading controls. Samples were run with antibodies for Total AKT, P-AKT (473 and 308), Total GSK3, P-GSK3α and β, GS, and P-GS. The blots were scanned and density was quantified using ImageJ software from National Institutes of Health (Maryland, USA).

4.13 Statistical analysis

All data was analyzed using a two-way ANOVA with Bonferroni multiple comparisons post-hoc tests indicated in the figure legends. The level of significance was set at $p< 0.05$. All statistical analysis was done using Graph Pad Prism 5. We evaluated the fold changes from basal glycogen synthesis rates to insulin-stimulated glycogen synthesis rates. These calculations of glycogen synthesis rates fold changes between the basal and insulin-stimulated condition were performed to provide insight on how insulin sensitive the muscles were. To evaluate this sensitivity we divided a rat's insulin-stimulated glycogen synthesis rate by the same rat's basal glycogen synthesis rate. We did this for all of our rats and then tabulated their means, standard deviations and SEMs. Means were then analyzed using a two-way ANOVA with Bonferroni multiple comparisons post-hoc tests and the level of significance was set at $p< 0.05$.

5. Results

5.1 Glucose tolerance test (GTT)

With the exception of time 0, glycemia of the SED HF animals was greater than all other conditions at all time points (figure 6**A**). In fact, glycemia was (which was expressed as area under the curve (AUC)) of SED HF rats was 1.29-, 1.61- and 1.19-fold higher than SED SC, EX SC, and EX HF groups, respectively (figure 6**B**). Exercise attenuated this effect, as glycemia of the EX HF group was significantly lower than SED HF rats. Additionally, EX HF rats GTT response was similar to SED SC condition. SC EX showed the lowest levels of glycemia, eliciting values for glycemia that were 1.26-, 1.63- and 1.35-fold lower than SED SC, SED HF, and EX HF, respectively. These results indicate exercise can prevent HF-diet-induced insulin resistance.

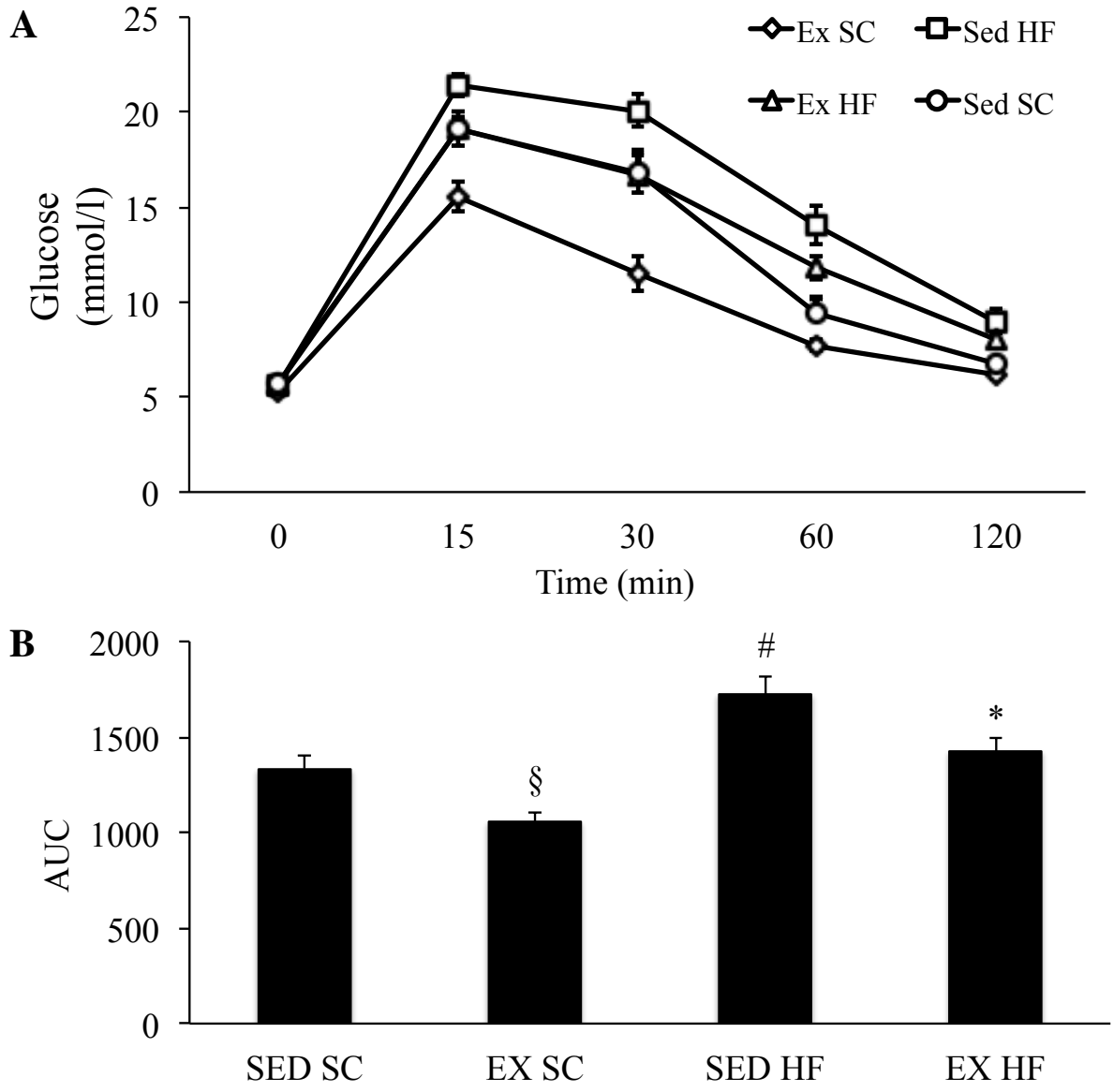

Figure 9: Time-course of plasma glucose during a GTT after an overnight fast. AUC = Area under the curve, was calculated for each condition followed by a two-way ANOVA followed by a Bonferroni post-hoc test. n=14. (B): *p< 0.001 vs. EX SC and p< 0.01 vs. SED HF. § p< 0.05 vs. SED SC and p< 0.001 vs. EX HF vs. SED HF and # p< 0.001 vs SED SC

5.2 Effects of HF diet and exercise on systemic insulin concentrations

Fasting plasma insulin concentrations were not different among any of the four conditions at week 0. However, by week 3 SED HF insulin concentrations were 1.79-, 2.87- and 1.96-fold greater than SED SC, EX SC, and EX HF, respectively. This significant difference continued during week 6, as SED HF insulin concentrations were 1.96-, 2.46- and 2.03-fold greater than SED SC, EX SC, and EX HF, respectively. Intriguingly, EX prevented high concentrations of insulin in the EX HF group at both weeks 3 and 6.

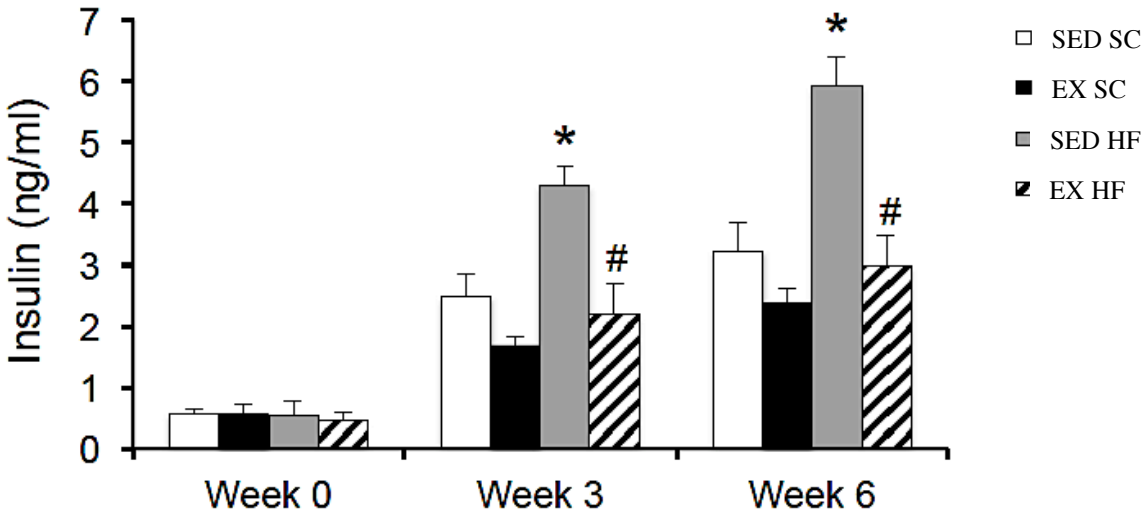

Figure 10: Measurements of fasting plasma insulin. Blood samples were taken from overnight fasted rats to quantify circulating insulin concentrations in SED SC, EX SC, SED HF, & EX HF rats. Data are presented as mean ± SEM. Two-way ANOVA followed by a Bonferroni post-test. n=6. *p< 0.05 vs. Sed SC; #p< 0.05 vs. Sed HF.

5.3 Glycogen synthesis in oxidative and glycolytic muscles

Sol (figure 8**A**), EDL (figure 8**B**) and Epit (figure 8**C**) muscles from SED SC rats elicited 3.39-, 1.75- and 1.97-fold increases in glycogen synthesis in response to insulin, respectively. No significant changes were present under basal conditions between SED SC and SED HF conditions.

Under basal conditions EX SC muscles exhibit a 4.81-, 2.72- and 5.49-fold increase in glycogen synthesis in comparison to the SED SC muscles of Sol (figure 8**A**), EDL (figure 8**B**) and Epit (figure 8**C**), respectively. Similarly, under basal conditions EX HF muscles showed a 4.98-, 2.66- and 3.97-fold increase in basal glycogen synthesis rates in Sol (figure 8**A**), EDL (figure 8**B**) and Epit muscles (figure 8**C**), when compared to the SED SC condition. Similar differences were observed between both EX conditions and the SED HF conditions. Sol (figure 8**A**), EDL (figure 8**B**) and Epit (figure 8**C**) of EX SC rats, presented a 4.33-, 5.02- and 5.86-fold increase in basal glycogen synthesis rates in comparison to SED HF muscles, respectively. Finally, muscle from EX HF rats showed a 4.20-, 4.86- and 4.72-fold increase in basal glycogen synthesis rates of Sol (figure 8**A**), EDL (figure 8**B**) and Epit (figure 8**C**) in comparison to SED HF muscles, respectively.

Insulin stimulation of EX muscles caused significant increases in glycogen synthesis rates, as EX SC insulin-stimulated glycogen synthesis rates increased by 1.68-, 1.82- and 1.35-fold in Sol (figure 8**A**), EDL (figure 8**B**) and Epit (figure 8**C**), respectively when compared to basal EX SC condition. Furthermore, similar increases in glycogen synthesis rates are were found in insulin stimulated EX HF muscles, the Sol (figure 8**A**), EDL (figure 8**B**) and Epit (figure 8**C**) respectively, showed a 2.18-, 1.31- and 1.60-fold increase, respectively, when compared to basal EX HF condition.

Differences in fold changes from basal glycogen synthesis rates to insulin-stimulated glycogen synthesis of each muscle were measured (Figure 8.1). SED SC Sol fold changes were significantly greater than all other conditions ($p < 0.001$). Additionally, EX HF Sol muscle exhibited greater fold changes than SED HF Sol, SED HF EDL, SED HF Epit, EX HF EDL and EX SC Epit ($p < 0.001$). To conclude, it seems that the Sol muscle is the most profoundly affected muscle in HF induced insulin resistance, as the decrease in the fold changes of glycogen synthesis from the SED SC Sol muscle to the SED HF Sol muscle is the largest. EX HF Sol muscle EX seems to prevent insulin sensitivity from declining to similar levels as the SED HF group.

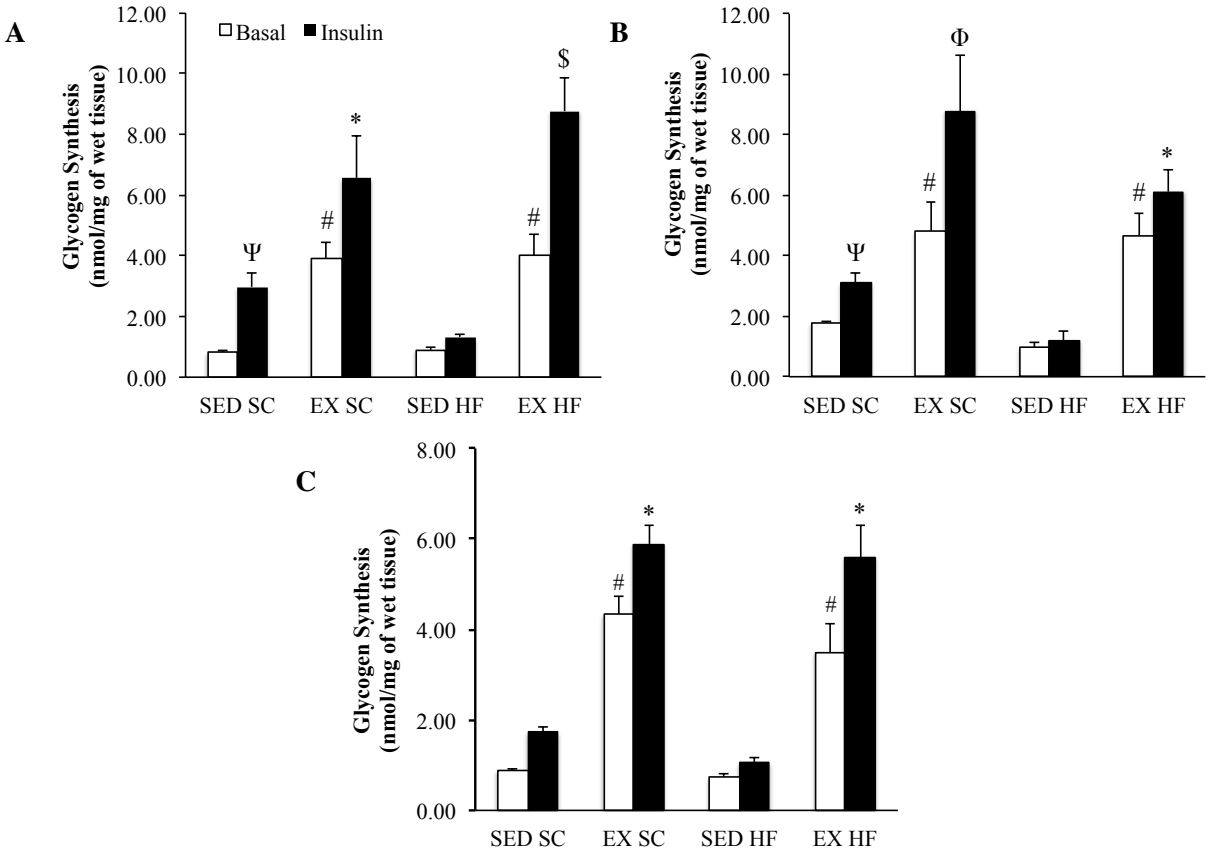

Figure 11: Glycogen synthesis rates in Sol (A), EDL (B) and Epit (C) of SED SC), EX SC, SED HF and EX HF rats. Data are presented as mean ± SEM. Two-way ANOVA followed by a Bonferroni post-test. n=3-6.

$ $p < 0.05$ vs. all other conditions.

* $p < 0.001$ vs. SED SC basal and insulin, vs. SED HF basal and insulin. $p < 0.05$ vs. EX SC basal and vs. EX HF basal.

# $p < 0.01$ vs. SED SC basal, vs. SED HF basal and insulin.

Ψ $p < 0.001$ vs. SED HF basal $p < 0.01$ vs. SED SC basal, vs. SED HF basal and insulin.

Φ $p < 0.05$ vs. all other conditions.

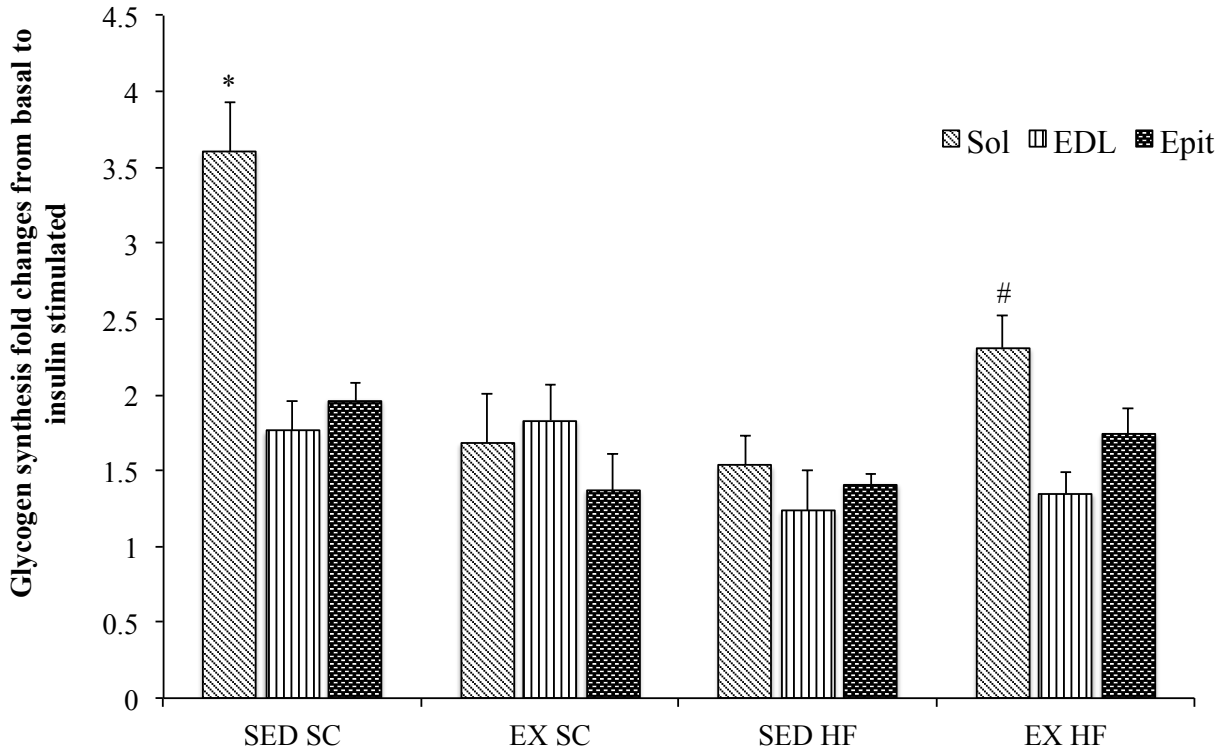

Figure 11.2: **Glycogen synthesis fold change differences among oxidative and glycolytic muscles.** Data are presented as mean ± SEM. Two-way ANOVA followed by a Bonferroni post-test. n=3-8. * $p< 0.001$ vs all other conditions. # $p< 0.001$ vs SED HF Sol, SED HF EDL, SED HF Epit, EX HF EDL and EX SC Epit.

5.4 Western blotting analysis of content and phosphorylation of Akt, GSK3, and GS:
Sedentary animals:

AKT phosphorylation was undetected under basal conditions. However, phosphorylation of AKT at serine 473 and threonine 308 was significantly higher in insulin-stimulated Sol, EDL and Epit muscles of the SC animals in comparison to HF animals (Figure 9 **A**-**C**). AKT phosphorylation was significantly reduced in the Sol, EDL and Epit (Figure 9 **A**-**C**) muscles of HF rats when compared to SC counterparts. Sol, EDL and Epit muscle from SC animals displayed a robust phosphorylation of GSK-3 in both alpha (α) and beta (β) isoforms, upon exposure to insulin in SC animals. In contrast, insulin-stimulated phosphorylation of GSK-3 α and β in all three muscles from HF-fed rats was almost undetected (Figure 9 **D**-**F**). Finally, insulin caused a marked dephosphorylation of GS in Sol, EDL and Epit muscles from SC rats (Figure 9.1 **A**-**C**). Muscles from HF rats displayed blunted dephosphorylation of GS (Figure 9.1 **A**, **B** & **C**). These findings clearly show that insulin signaling is defective in skeletal muscles of rats fed a HF diet, which is consistent with the reduction in insulin-stimulated glycogen synthesis in oxidative and glycolytic muscles of these animals.

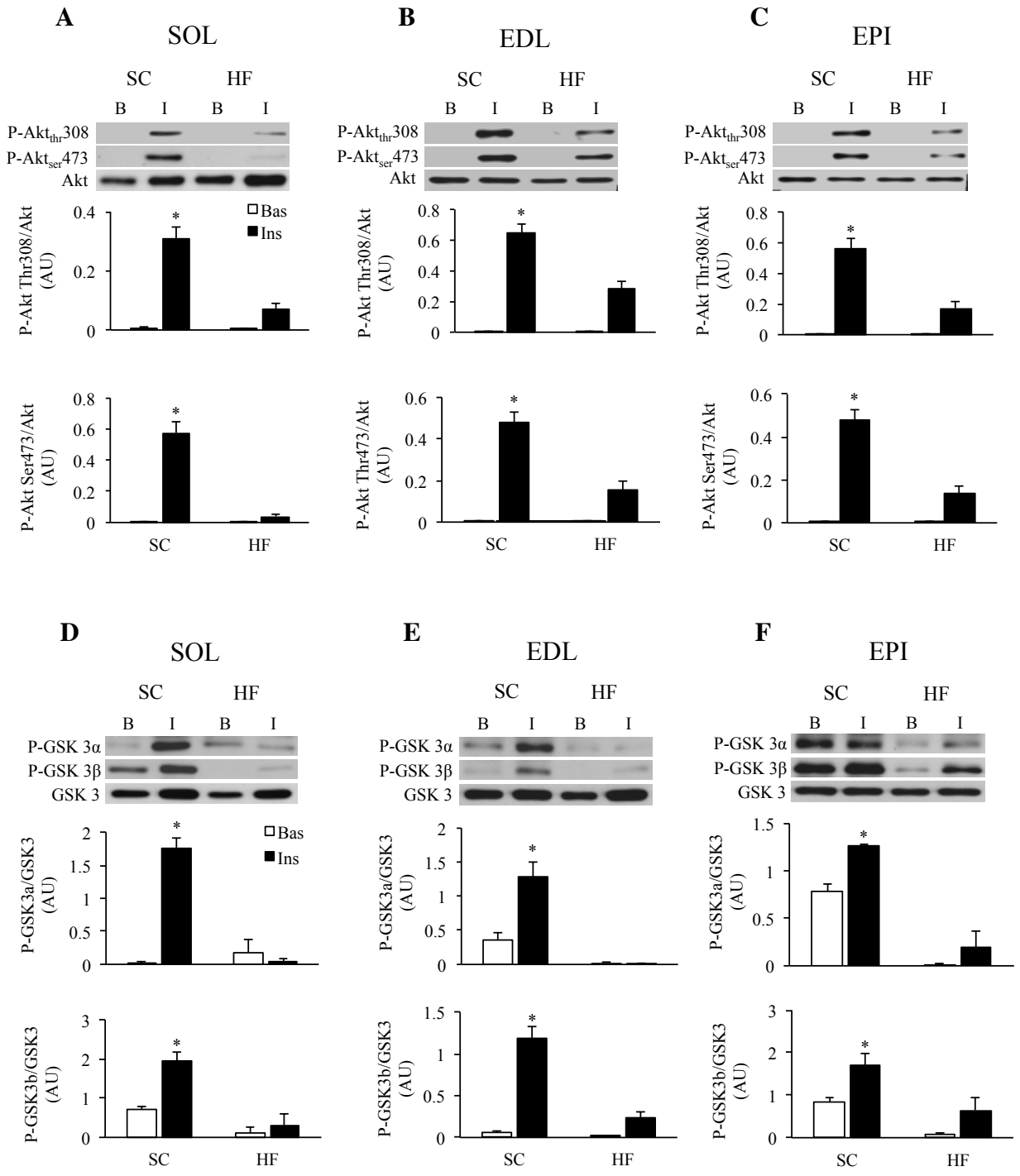

Figure 12.0: **Densitometry and Western Blot - HF feeding inhibits insulin-mediated phosphorylation of AKT and GSK3 in skeletal muscles.** Representative blots for P-AKT Thr308, P-AKT Ser473, P-GSK-3α, and P-GSK-3β under basal (Bas) and insulin-stimulated (Ins) conditions in the Sol (A and D), EDL (B and E), and Epit (C and F) muscles. Two-way ANOVA followed by a Bonferroni post-hoc test. n=4. Data are presented as mean ± SEM.* p< 0.05 vs. all other conditions.

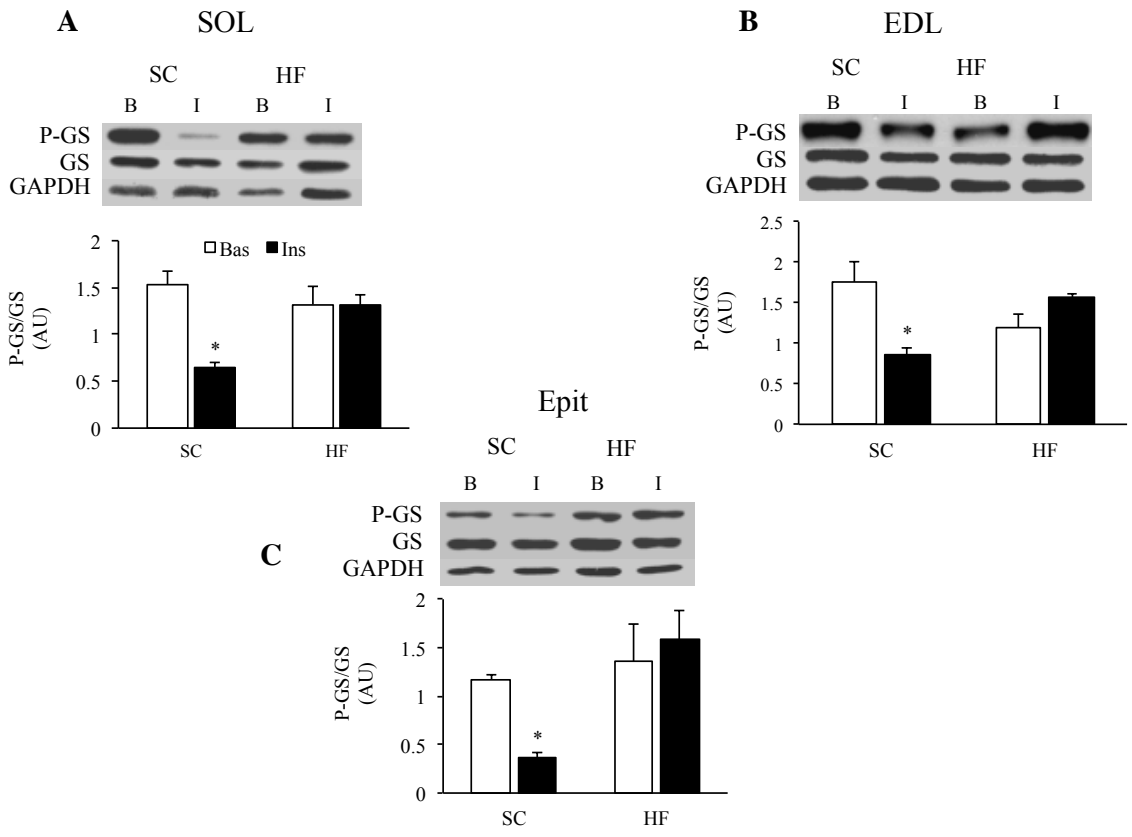

Figure 12.1: Densitometry and Western Blot - HF feeding inhibits insulin-mediated dephosphorylation of GS in skeletal muscles. Representative blots for P-GS under basal (Bas) and insulin (Ins)-stimulated conditions in the Sol, (A), EDL (B), and Epit (C) muscles. Two-way ANOVA followed by a Bonferroni post-hoc test. n=4. Data are presented as mean ± SEM. * p< 0.05 vs. all other conditions,

5.5 Glucose-6-phosphate content in glycolytic and oxidative muscles

Significantly lower levels of intracellular G6P were observed in the EDL of both SED SC and SED HF groups in comparison to the EX SC and EX HF conditions (figure 10B). The EDL of EX SC presented a 4.79-fold increase of intramuscular G6P in comparison to SED SC conditions (figure 10B). Additionally, EX SC showed a 12.6-fold increase of intramuscular G6P content in comparison to the SED HF group (figure 10B). The EX HF muscles showed a 4.55- and 12.4-fold increase of intramuscular G6P content in comparison to the SED SC and SED HF conditions, respectively (figure 10B). An analogous trend is present in the Epit data, as EX SC animals demonstrated a 2.77- and 7.07-fold increase in comparison to the SED SC and SED HF groups, respectively (figure 10C). Additionally, EX HF Epit muscles presented a 2.09- and 5.30-fold increase in G6P content compared to the SED SC and SED HF rats, respectively (figure 10C). Lower concentrations were found in the Sol of both SED SC and SED HF rats but the differences compared to the EX condition were not statistically significant (figure 10A).

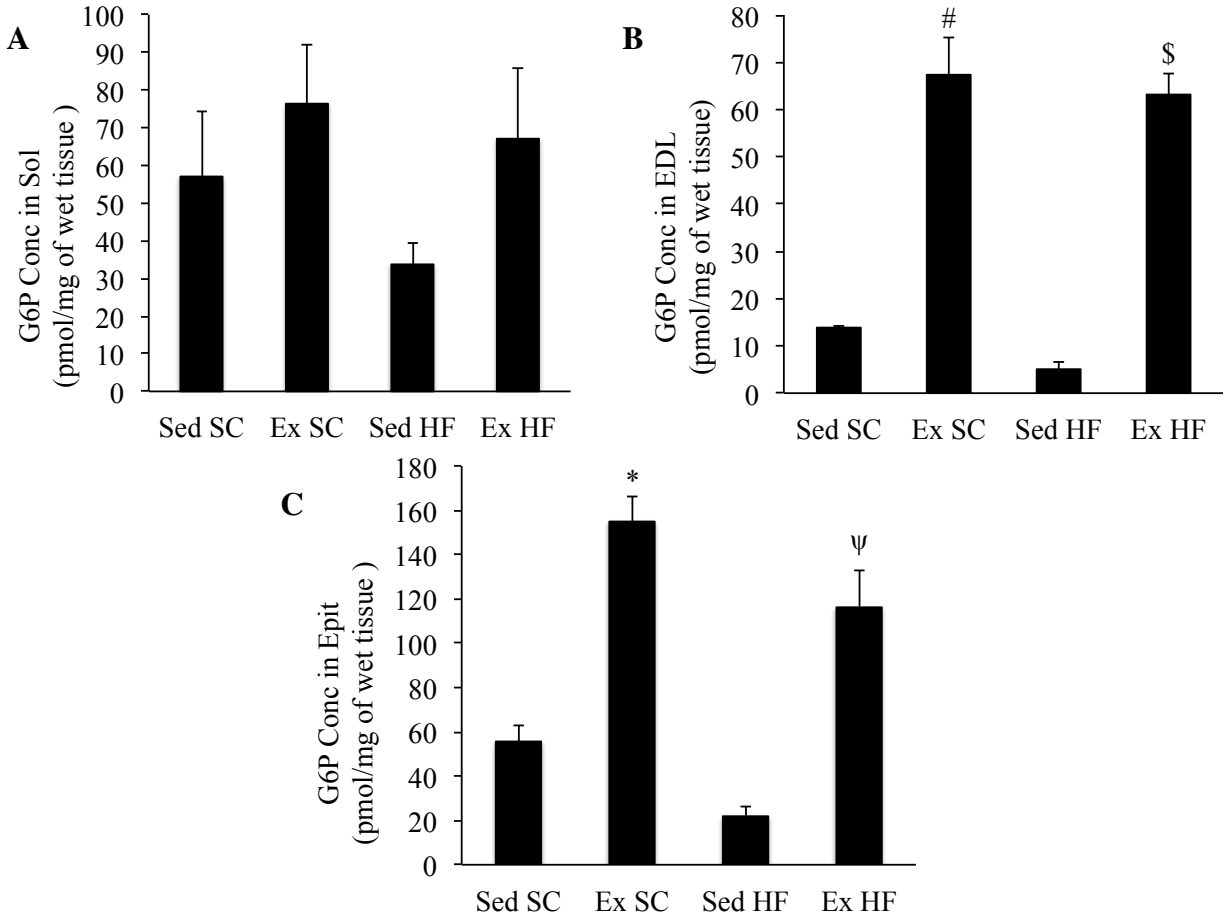

Figure 13: Concentration of G6P in the Sol (A**), EDL (**B**) and Epit (**C**) after the 8-week protocol.** All tissues are expressed as nmol of G6P per milligram of wet tissue (mg of wet tissue). Data are presented as mean ± SEM. Two-way ANOVA followed by a Bonferroni post-hoc test. n=3-5. # $p< 0.001$ vs. SED HF and SED SC. $ $p< 0.001$ vs. SED HF and SED SC. Ψ $p< 0.05$ vs. SED HF. * $p< 0.05$ vs. SED SC, and $p< 0.01$ vs. SED HF

5.6 Palmitate oxidation in glycolytic and oxidative muscles

As expected, HF-feeding increased the rates of palmitate oxidation by 1.58-, 1.75- and 1.6-fold in Sol, EDL, and Epit muscles, respectively, when compared to SC rats (figure 11). However, the rate of palmitate oxidation was highest in Sol, the most oxidative muscle, followed by EDL, and Epit tissues from SC-fed rats (figure 11). SED HF muscles have the greatest rates of palmitate oxidation (figure 11.1 **A**) among all the conditions tested. In the Sol SED HF muscles show a 2.41-, 1.90- and 2.03-fold increase in oxidation rates in comparison to SED SC, EX SC, and EX HF, respectively. Similarly, in the EDL (figure 11.1 **B)**, SED HF muscles exhibit increases of 2.42-, 2.3- and 1.78-fold of oxidation rats in comparison to SED SC, EX SC and EX HF, respectively. Finally, SED HF Epit (figure 11.1 **C)** fatty acid oxidation rates were 1.79-, 1.53- and 1.38-fold higher than SED SC, EX SC, and EX HF conditions, respectively.

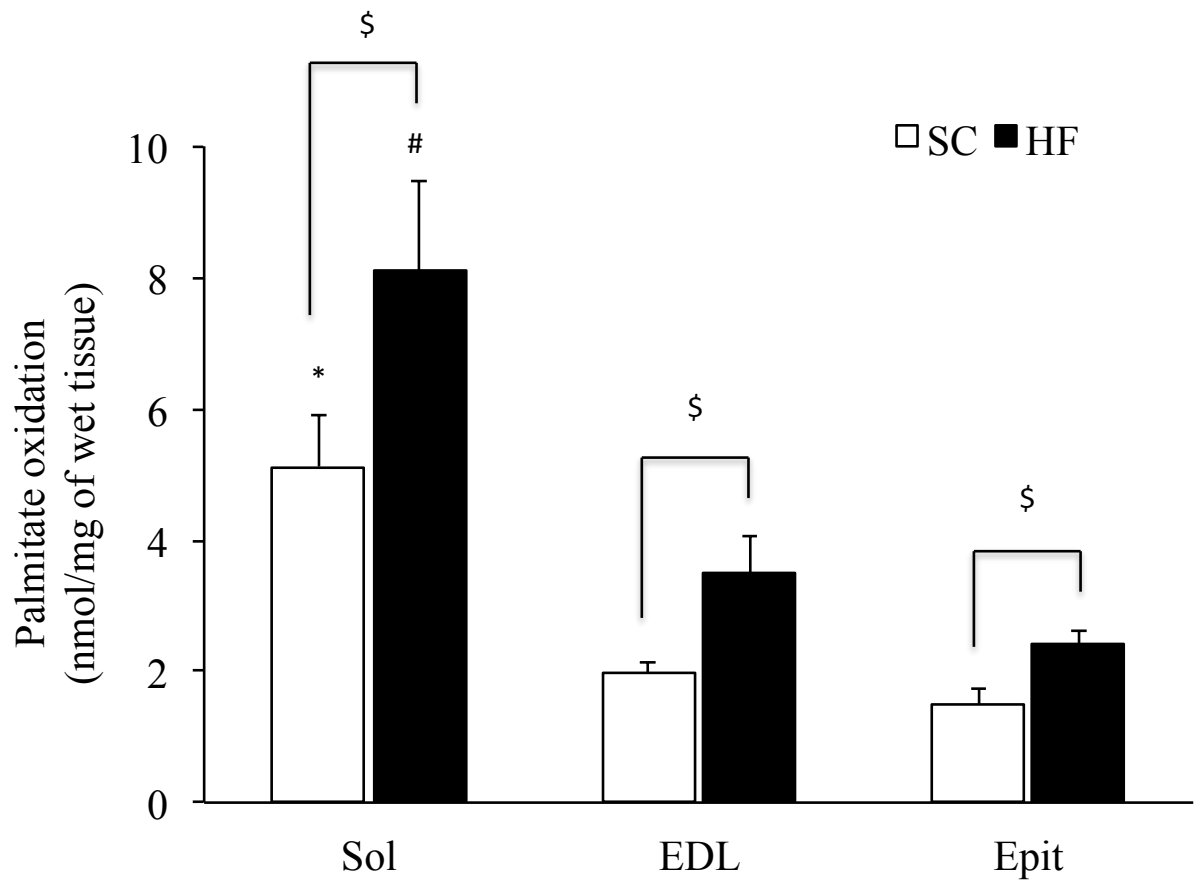

Figure 14: The effects of high-fat (HF) diet on palmitate oxidation in oxidative and glycolytic muscles. Strips of Sol, EDL, and Epit muscles from SC and HF-fed rats were assayed for $^{14}CO_2$ production from ^{14}C-palmitic acid at week 8 of the study. Data are presented as mean ± SEM. Two-way ANOVA followed by a Bonferroni post-test. n=6 * $p < 0.05$ vs. EDL and Epit SC; # $p < 0.05$ vs. Sol SC; $ $p < 0.05$ vs. SC.

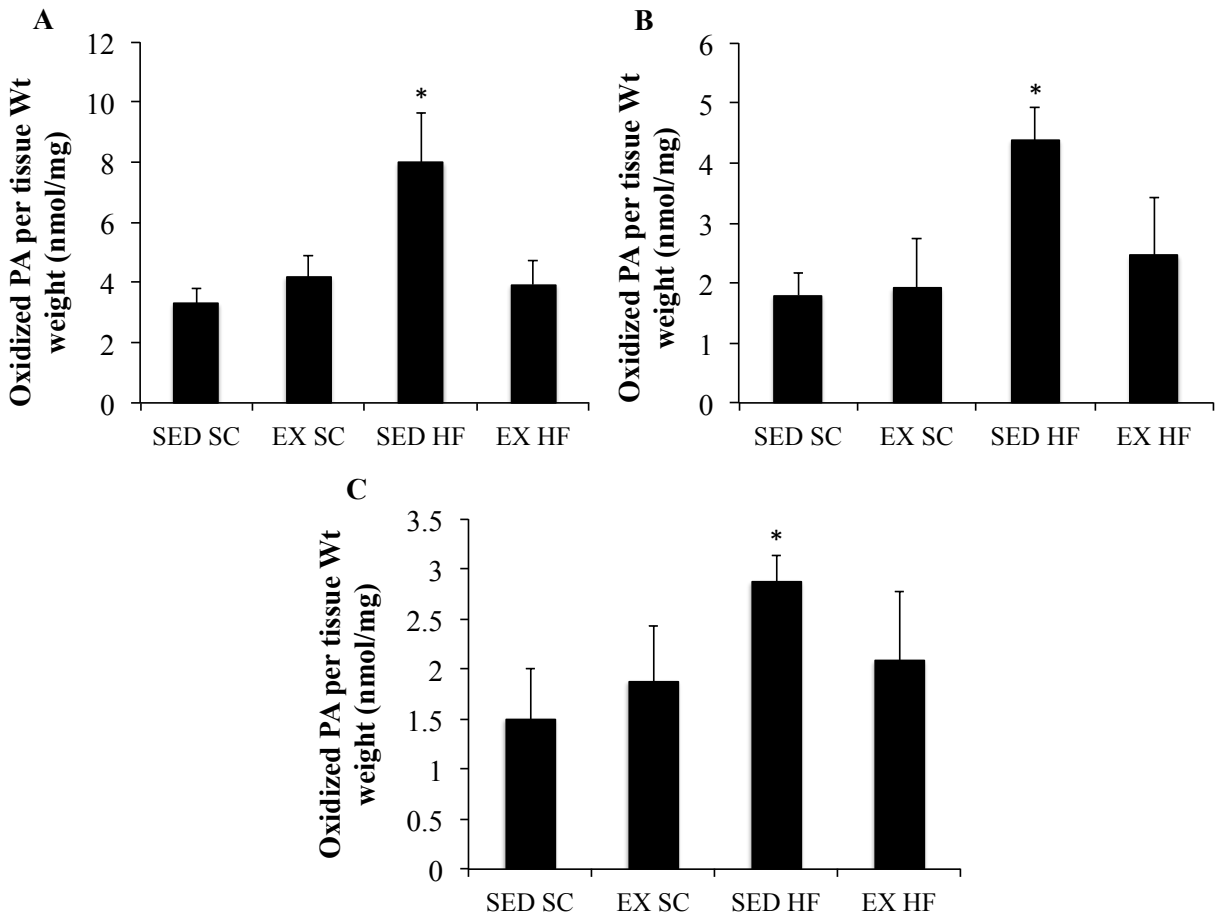

Figure 14.1: Measurement of Palmitate Oxidation of Sol (A), EDL (B) and Epit (C) muscle SED SC, EX SC, SED HF and EX HF rats. Data are presented as mean ± SEM. Two-way ANOVA followed by a Bonferroni post-test. n=5-7. (A) * $p < 0.001$ vs SED SC and EX HF, $p < 0.01$ vs EX SC. (B) * $p < 0.001$ vs all other conditions. (C) * $p < 0.01$ vs SED SC and EX SC.

6.0 Discussion

In this study we provide novel evidence that, Sol, EDL, and Epit muscles of SED HF rats develop insulin resistance despite major differences in oxidative capacities of each muscle. All three muscles displayed decreased G6P content; reduction in the activity of key mechanistic proteins involved in insulin signaling and finally decreased rates of glycogen synthesis. Furthermore, our study is the first study to suggest that type I fibers may be more profoundly affected by HF-induced skeletal muscle insulin resistance than type II fibers.

Successful development of systemic insulin resistance

In our study we showed that SED HF rats displayed a significantly higher concentration of both circulating blood glucose and insulin. This provides proof that our model was successful in developing diet induced insulin resistance. As the muscle plays one of the largest roles in insulin-stimulated glucose disposal, we attribute the hyperglycemia and hyperinsulinemia in these rats to the impairment of muscle glucose uptake[18].

Exercise can prevent the development of impaired glucose tolerance

GTT data showed that the EX HF muscles displayed similar glycemic control to SED SC muscles. Similarly, fasting insulin data revealed that insulin concentrations were alike between the SED SC and EX HF conditions at week 3 and 6. The similar blood glucose and insulin concentrations of these two groups are noteworthy as even though a HF diet was fed to the EX HF group, this condition still maintained its' insulin sensitivity and glucose tolerance to the same degree as the control group. The ability of the EX HF group to do this can be accredited to the adaptive characteristics of exercise[37]. Characteristics such as exercise-mediated glucose uptake and the ability of chronic endurance training to cause a shift in fiber type expression in the muscle[37,151]. Suggesting that exercise simulated increased expression of insulin sensitive type I

fibers in the EX muscles, along with exercise-mediated glucose uptake promoting glucose uptake and preventing the development of hyperinsulinemia[152]. The shift to the more insulin sensitive type I fibers and the increased glucose uptake in the exercise condition would also explain why EX SC condition displayed the lowest levels of blood glucose at all time points.

HF feeding decreases G6P content in all SED HF muscles

Exercise-mediated glucose uptake and shift in muscle fiber type could also rationalize why greater G6P content was found in the EDL and Epit EX conditions in comparison to their SED counterparts. Conversely, we found no significant differences in the measurement of G6P concentrations among any of the conditions of the Sol muscle. However, when the significant increases of G6P in the EX EDL and EX Epit are considered then it was unusual for there to be an absence of an increase of G6P content in EX Sol tissue. We concluded that the reason why a similar pattern was not found in this muscle is that there was an experimental issue during the G6P assay for this muscle.

The higher concentrations of G6P in the EX EDL and Epit could be a result exercise stimulating the increase of GLUT4 translocation[37]. It is reported that GLUT4 translocation is the rate limiting step in non-oxidative glucose disposal, thus increased glucose uptake due to exercise will stimulate HKII activity which readily converts glucose to G6P[45]. Our conclusions concerning the increased G6P content in EX muscles is in agreement with other studies, which have shown that chronic endurance exercise will increase GLUT4 translocation[153]. Interestingly, the EX SC Epit muscle presented with the highest levels of G6P content, this is a finding that is in contrast to other research which indicates, that exercise mediated increases in GLUT 4 content are greater in type I fibers than type II[146]. Furthermore, other work has shown that a greater

percentage of HK II is present in type I fibers than type II, thus it is unclear why the muscle with the highest type II fiber percentage had the highest levels of G6P content[154].

All muscles, regardless of fiber type, had key mechanistic proteins of insulin signaling affected

A potential argument for the decrease of intramuscular G6P and the development of insulin resistance in all of the SED HF muscles is that HF-feeding diminished GLUT4 protein content[155]. However, insulin resistant subjects have shown to have equal amounts of GLUT4 content as controls[153]. A more apt explanation for the lower amounts of G6P in the SED HF condition is that SED HF muscles were unable to stimulate glucose uptake. This could have been due to the lipid-rich diet causing indirect disruptions to the insulin-signaling cascade, which would prevent the translocation of GLUT4. In fact, our Western blot analysis showed that Sol, EDL, and Epit muscles from SED-HF rats presented with reduced insulin-stimulated phosphorylation of Akt and phosphorylation/deactivation of GSK-3α/β. Moreover, insulin-induced dephosphorylation/activation of GS was clearly impaired in all three muscles from SED HF rats. Although many studies have shown the importance of maintaining the phosphorylation of AKT and GSK isoforms and the dephosphorylation of GS, the phosphorylation of the tyrosine residue of IRS-1 is one of the initial steps and without its' phosphorylation the signal is arrested[50,12]. Many studies describing the mechanistic effects of lipid-induced insulin resistance indicate that the tyrosine residue of IRS-1 is not phosphorylated, but it is rather the serine residue of IRS-1 that undergoes phosphorylation which prevents any further downstream signaling[15,156]. It is plausible that serine phosphorylation took place in our SED HF muscles because we observed the blunted activity of the downstream targets of IRS-1.

In contrast to our SED western blot data; our EX western blot data was not as well defined. Our initial data (not included in this paper) had shown almost no differences in the

phosphorylation of Akt, GSK and dephosphorylation of GS between the basal and insulin-stimulated exercise muscles. There are numerous studies reporting the maintenance and increased activity of the insulin signaling cascade with exercise[157,158]. However, we could not observe the anticipated increases in the phosphorylation of Akt, GSK and dephosphorylation of GS with insulin stimulation and other studies have reported a similar discrepancy[159]. The reason for this discrepancy could be due to a negative feedback loop from increased glycogen in the EX muscle[160]. Increased glycogen content would inhibit stimulation of insulin signaling thus preventing phosphorylation of Akt, GSK and dephosphorylation of GS. Manabe et al. (2013) revealed that voluntary exercise training decreased the phosphorylation and deactivation of GSK-3α/β in muscle[159]. Regardless of the reduction in GSK-3α/β phosphorylation GS activity was still increased in these trained muscles, which is probably due to the allosteric activation of GS through increased intramyocellular G6P concentrations in exercise muscles[159]. Considering the conclusions from previous work, the increased G6P content found in our results and the robust glycogen synthesis rates found in our basal and insulin stimulated exercise muscles we suggest the insulin signalling cascade in the EX condition was by-passed due to exercise training causing increased GS expression and allosteric activation of GS[159].

Chronic HF feeding severely reduces glycogen synthesis rates of all muscles, but exercise can protect HF fed muscles from blunted glycogen synthesis rates

With regards to glycogen synthesis, we have shown previously that G6P content is greater in EX muscles than in SED muscles. This would likely cause allosteric activation of GS, leading to higher rates of basal glycogen synthesis rates in both EX SC and EX HF muscles. Additionally, this increase could be a result of the chronic exercise training causing an up-regulation of the active form of GS which would lead to increases of basal glycogen synthesis rates[159].

Underlining the protective effect of exercise from HF-induced insulin resistance, as the HF diet did not cause the EX HF group to exhibit lesser insulin stimulated glycogen synthesis rates than the EX SC condition. We also found that insulin-stimulated glycogen synthesis rates in Sol, EDL, and Epit muscles of SED HF rats were blunted. Considering the severely reduced activity of the key mechanistic enzymes in the insulin signaling cascade and the decreased G6P content already reported in SED HF rats, it was clear why glycogen synthesis rates were significantly lower than all other groups. Our work shows that muscles with greater oxidative capacity do not have a protective affect over diet induced insulin resistance.

Is the Sol the most severely affected muscle?

In fact based on our results, we hypothesized that perhaps the Sol (the muscle with the greatest oxidative capacity) was the most profoundly affected muscle with regards to insulin resistance. Our results indicate that the SED SC Sol provides significantly higher fold changes of insulin stimulated glycogen synthesis compared to all other conditions. However, in the SED HF condition Sol muscle produced fold changes that were significantly smaller than the SED SC and EX HF conditions. Highlighting the physiological toll that physical inactivity and the HF diet had on the Sol muscle. The highest fold changes in glycogen synthesis rates are found in the Sols because it contains the most insulin-sensitive type I fibers than the other muscles[23]. This is compatible with the fact that type 1 fibers display a greater degree of insulin binding and receptor kinase phosphorylation than type II fibers[24]. With these properties in mind, the disappearance of the Sol's significant fold change in the HF condition was mostly likely due to the Sol's more insulin sensitive properties succumbing to the deleterious effects of a lipid-rich diet.

Our concerns with respect to the Sol being the most affected muscle are supported by Gaster et al (2001) who found that GLUT4 density of type I fibers was significantly lower than type II fibers in T2D subjects[161]. If in fact the there is less GLUT4 in type I fibers of T2D subjects then this could provide a possible explanation for the disappearance of the glycogen synthesis fold changes in the Sol. Moreover, triglyceride content data (appendix) showed the highest concentrations of triglycerides were found in the Sol of SED HF rats. These results also suggest the Sol SED HF muscle could have been the most affected muscle. Research has found that triglycerides content more closely correlates with insulin resistance than BMI or total adiposity[143]. However, most researchers agree that the triglycerides themselves do not directly cause insulin resistance rather they act as surrogates for increased fatty acid metabolites which have a direct link to the pathogenesis of the insulin signaling cascade[143,164].

Furthermore, our finding of EX HF Sol muscle exhibiting significantly greater fold changes than the SED HF was a positive and yet peculiar finding, as exercise is clearly protecting the EX HF Sol from any harmful effects of the HF diet, possibly due to the increase mitochondria biogenesis that occurs in EX muscle along with exercise training stimulating a greater increase in GLUT 4 content in type I fibers[146,151]. As the Sol is the most insulin sensitive and contains the greatest amount of mitochondria between all the muscles then increasing the oxidative capacity through exercise would only serve to better the glycogen synthesis ability of this muscle. However, it was unusual that the EX SC Sol muscle did not exhibit similar if not greater fold changes to the EX HF Sol when we consider that exercise training should increase the GLUT 4 content of this type I fiber rich muscle.

Skeletal muscle insulin resistance is most likely a result of both the Randle cycle and an overwhelmed mitochondria

Lastly, our study demonstrates that chronic HF-feeding increases oxidation rates. Interestingly, this finding falls in line with an argument against the involvement of mitochondria in skeletal muscle insulin resistance. In 2013 Dr. Holloszy proposed that mitochondrial deficiency has little influence on insulin resistance, for the following reasons: a) studies have shown that rodents who are fed a high fat diet display an increase in mitochondrial content while developing insulin resistance, b) mitochondrial deficiency severe enough to impair fat oxidation will lead to an increase in insulin action not an decrease and c) similar to the results in our study, studies have shown that insulin resistant subjects have higher fat oxidation rates than insulin sensitive subjects[165]. However, more recent work has supported the theory of mitochondria involved in skeletal muscle insulin resistance. A study by Henstridge et al. (2014) showed increasing heat shock protein 72 expression in mice causes increased oxidative capacity and mitochondrial number[166]. These mice are protected from HF-induced skeletal muscle insulin resistance[166]. This work clearly indicates the influence of mitochondria on the development of skeletal muscle insulin resistance. Thus, we believe that insulin resistance comes about in the SED HF muscles due to mitochondrial dysfunction. Although it is true, that as Dr. Holloszy proposes, HF-feeding increases mitochondrial activity and content, as our study demonstrates the highest rates of oxidation were present in SED HF muscles. These high rates were present due to the consumption of a HF diet providing FAs beyond the oxidation means of the myocyte, leading to the overwhelmed mitochondria in the muscle. Our findings are compatible with the theory purposed by Muoio et al (2006) who proposed a modified version of the Randle cycle whereby high fat feeding increased fatty acid oxidation rates, which leads to the acceleration of incomplete fatty acid oxidation[143]. This acceleration, as seen in our palmitate oxidation results,

most likely resulted from a mismatch between the rates of β-oxidation and TCA cycle causing mitochondrial stress[143]. This stress is characterized by disruptions in the redox status and depletion of the CoA and carnitine levels[143]. With the depletion of CoA and carnitine the flow of fatty acid transport to the mitochondria is interrupted causing for incomplete oxidation[143]. The incomplete oxidation would enrich the myocyte with toxic lipid metabolites, which would lead to lipid mediated insulin resistance.

Our conclusion and Muoio's theory is supported by the work of Keung et al. (2013) who reported that inhibiting CPT-1 in mice increased pyruvate dehydrogenase activity, increased membrane GLUT4 content, and insulin-stimulated Akt phosphorylation[167]. In addition, these mice's intramyocellular DAG content was decreased[167]. Meaning that decreased fatty acid uptake and utilization lead to increased carbohydrate usage. Moreover, inhibition of CPT-1 in these mice caused increased insulin sensitivity. However, research that shows increasing fatty acid oxidation improves insulin signaling in muscle is at odds with our conclusion. Bruce et al. (2009) reported that increasing muscle CPT1 expression in HF fed rats allows for even more long chain fatty acids to enter the mitochondria and undergo more oxidation than under normal conditions[168]. This prevented the build up of harmful lipid intermediates which would otherwise affect the insulin signaling by increasing the amount of fatty acids that can enter the mitochondria[168]. However, this could suggest that the amount CPT-1 content is the variable that can differentiate a HF-induced insulin resistant myocyte from an insulin sensitive myocyte. Suggesting that the mitochondria in the wild type rodent has the capacity to deal with abundance of lipids from a HF-diet but as it does not have enough CPT-1 to cope with the abundance of cytosolic fatty acids, this would then lead to the build up of toxic lipid intermediates.

Discussing the pathogenesis of high-fat induced skeletal muscle insulin resistance in a fiber type specific manner

Finally, recent work has shown that knockout pyruvate dehydrogenase kinase 2 and 4 mice (which leads to constitutively activated pyruvate dehydrogenase) are not protected from HF-induced insulin resistance[169]. The study indicated that genetically removing glucose oxidation inhibitors causes substrate usage to be shifted to glucose and although this shift increases glucose oxidation, it does not prevent a severe decrease in insulin-stimulated muscle glucose uptake[169]. Furthermore, HF-feeding in this study led to decreases in fatty acid oxidation. These results conflict with our and other researchers views on the pathogenesis of insulin resistance and they highlight that the original Randle does retain some accuracy in describing insulin resistance and the interplay between glucose-fatty acid usage in a state of lipid oversupply. However, this study used the quadriceps, which is a muscle with mostly glycolytic fibers. As our study has shown muscles with type II fibers undergo less oxidation, thus the required increase in fatty acid oxidation, which produces citrate concentrations, which would inhibit PDH are less likely to occur in this fiber type. As oppose to the type I fibers, which are rich in mitochondria and can produce citrate concentrations that would inhibit PDH. In conclusion, it seems that a more thorough approach to the discussion of skeletal muscle insulin resistance is required. Findings need to be limited to specific muscle fiber type rather than studying muscles that contain different muscle fibers and extrapolating results to apply to all muscle fiber types. With this outlook we believe that type I and II fibers are both affected by DAG mediated insulin resistance. However, in the case of Type I fibers we believe they could be affected by the proposed modified Randle cycle, while it seems that type II fibers are affected by a build of toxic lipid intermediates as a result the lower oxidative capacity.

Conclusion

However each muscle fiber type may be affected, it is clear that all SED HF muscles displayed blunted glycogen synthesis rates and insulin-signaling. In addition, these muscles also display low levels of G6P content and higher concentrations of circulating blood glucose and insulin. Indicating that our study was successful in showing that HF diet and lack of physical activity will lead to skeletal muscle insulin resistance in all muscle fiber types, while our work also showed that a higher oxidative capacity does not provide a protective effect from insulin resistance. Additionally, while most studies generalize their findings concerning skeletal muscle insulin resistance to all muscle fiber types, this study discusses skeletal muscle insulin resistance in a fiber type specific manner. Our work suggests that perhaps oxidative fibers are affected more severely by insulin resistance than glycolytic ones. The higher concentrations of triglycerides in Sol muscle and the disappearance of the significant glycogen synthesis fold change in the SED HF condition support our theory. Moreover, if our conclusion concerning the development of mitochondrial dysfunction is accurate, then it would stand to reason that the mitochondria rich type I fibers in the Sol would be more severely affected by this than the type II fibers found in the EDL and Epit. Lastly, if our work was to consider the other pathways in the pathogenesis of insulin resistance then it would stand to reason that the mitochondrial rich type I fibers would be more affected by the increases in ROS production.

However, our study does possess limitations in that it lacks evidence, which underlines the direct involvement of DAG. This was not presented due to attempts at measuring intramuscular DAG content being unsuccessful, thus in the next phase of our study we would like to continue our pursuit for the measurements of intracellular concentrations of DAG.

Finally, the importance of exercise as a major therapeutic tool in dealing with insulin resistance must be stated. In our work it is clear through the significantly increased glycogen synthesis rates, normal concentrations of circulating insulin, the appropriate regulation glycemia after glucose infusion and increased G6P content that chronic endurance exercise did seem to exert somewhat of a protective effect against high fat diet-induced insulin resistance in oxidative and glycolytic muscles. This protective effect of exercise is likely due to the shift of fiber type expression to more insulin sensitive type I fibers. The development of these characteristics would also explain why insulin resistance was prevented in the trained oxidative muscle, and why higher glycogen synthesis fold changes were observed in EX HF Sol muscle.

6.2 Future Directions

Previous work done in our lab has suggested that oxidative muscles develop insulin resistance as a result of substrate competition while insulin resistance in glycolytic muscles is due to accretion of lipid intermediates. We want to clarify that insulin resistance in all muscles is indeed a result of toxic lipid build up by measuring DAG content in all the muscles. We were previously extracting lipids from muscle homogenates then using DAG kinase we would label DAG molecules with radioactive P-32 creating phosphatidic acid, then isolating labeled phosphatidic molecules using TLC and finally superimposing the silica gel plate on a phosphorimaging screen to be quantified using densitometry. In the future, we would like to use mass spectrometry as it has been shown to be the most effective way of measuring DAG in muscle tissue[171]. In conjunction with the DAG assays, we would like conduct western blot analysis on SED HF muscles probing for the 307-serine residue of the IRS-1 protein[172]. We predict that higher levels of DAG content should correlate with more 307-serine residue

phosphorylation. These results will also help establish if DAG mediated insulin resistance is developed in type II fibers or if this fiber type is differently affected.

Finally, to provide support to the Muoio hypothesis, we would like to test the remaining blood samples for acyl-carnitine esters. If in fact the mitochondria are dysfunctioning then excess acetyl-CoA and other acetyl-CoA intermediates are converted back into acyl-carnitine via CPT 2[143]. The acyl-carnitine esters that are formed can exit the matrix of the mitochondria through carnitine acylcarnitine translocase, then once inside the cytoplasm, they can enter the blood stream[143]. Thus, there will be an increase in the concentrations of acyl-carnitine esters in the blood.

References:

1. Kelly T, Yang W, Chen C-S, Reynolds K, He J. Global burden of obesity in 2005 and projections to 2030. *Int J Obes (Lond)*. 2008;32(9):1431-1437. doi:10.1038/ijo.2008.102.
2. Haslam DW, James WPT. Obesity. *Lancet*. 2005;366(9492):1197-1209. doi:10.1016/S0140-6736(05)67483-1.
3. Wild S, Roglic G, Green A, Sicree R, King H. Global prevalence of diabetes: estimates for the year 2000 and projections for 2030. *Diabetes Care*. 2004;27(5):1047-1053.
4. Diabetes DOF. Diagnosis and classification of diabetes mellitus. *Diabetes Care*. 2010;33(SUPPL. 1). doi:10.2337/dc10-S062.
5. Kahn SE, Hull RL, Utzschneider KM. Mechanisms linking obesity to insulin resistance and type 2 diabetes. *Nature*. 2006;444(7121):840-846. doi:10.1038/nature05482.
6. Ye J. Role of insulin in the pathogenesis of free fatty acid-induced insulin resistance in skeletal muscle. *Endocr Metab Immune Disord Drug Targets*. 2007;7:65-74.
7. Shulman GI. On diabetes : insulin resistance Cellular mechanisms of insulin resistance. 2000;106(2):171-176. doi:10.1172/JCI10583.On.
8. Fridlyand LE, Philipson LH. Reactive species and early manifestation of insulin resistance in type 2 diabetes. *Diabetes Obes Metab*. 2006;8:136-145. doi:10.1111/j.1463.
9. Björntorp P, Sjöström L. Carbohydrate storage in man: speculations and some quantitative considerations. *Metabolism*. 1978;27(12 Suppl 2):1853-1865. doi:10.1016/S0026-0495(78)80004-3.
10. Wallberg-Henriksson H, Constable SH, Young D a, Holloszy JO. Glucose transport into rat skeletal muscle: interaction between exercise and insulin. *J Appl Physiol*. 1988;65(19):909-913.
11. Banks E a, Brozinick JT, Yaspelkis BB, Kang HY, Ivy JL. Muscle glucose transport, GLUT-4 content, and degree of exercise training in obese Zucker rats. *Am J Physiol*. 1992;263:E1010-E1015.
12. Taniguchi CM, Emanuelli B, Kahn CR. Critical nodes in signalling pathways: insights into insulin action. *Nat Rev Mol Cell Biol*. 2006;7(February):85-96. doi:10.1038/nrm1837.
13. Xu H, Barnes GT, Yang Q, et al. Chronic inflammation in fat plays a crucial role in the development of obesity-related insulin resistance. *J Clin Invest*. 2003;112(12):1821-1830. doi:10.1172/JCI19451.tivity.
14. Erion DM, Shulman GI. Diacylglycerol-mediated insulin resistance. *Nat Med*. 2010;16(4):400-402. doi:10.1038/nm0410-400.
15. Miguel Bronfman, M. Nelly Morales AO. Diacylglycerol activation of protein kinase C is modulated by long-chain acyl-CoA. 1988;152(3):987-992.
16. Rizza RA, Gerich JE, Haymond MW, et al. Control of Blood Sugar in Insulin-Dependent Diabetes: Comparison of an Artificial Endocrine Pancreas, Continuous Subcutaneous Insulin Infusion, and Intensified Conventional Insulin Therapy. *N Engl J Med*. 1980;303(23):1313-1318. doi:10.1056/NEJM198012043032301.
17. Gerich JE. *Control of Glycaemia.*; 1993. doi:10.1016/S0950-351X(05)80207-1.
18. Poretsky L. Principles of diabetes mellitus. *Princ Diabetes Mellit*. 2010:1-887. doi:10.1007/978-0-387-09841-8.
19. Schiaffino S, Reggiani C. Fiber Types in Mammalian Skeletal Muscles. *Physiol Rev*. 2011;91(4):1447-1531. doi:10.1152/physrev.00031.2010.
20. Essen B, Jansson E, Henriksson J, Taylor AW, Saltin B. Metabolic characteristics of fibre

types in human skeletal muscle. *Acta Physiol Scand*. 1975;95(2):153-165. doi:10.1111/j.1748-1716.1975.tb10038.x.
21. James DE, Zorzano A, Boni-Schnetzler M, et al. Intrinsic differences of insulin receptor kinase activity in red and white muscle. *J Biol Chem*. 1986;261(32):14939-14944.
22. Bonen A, Tan MH, Watson-Wright WM. Insulin binding and glucose uptake differences in rodent skeletal muscles. *Diabetes*. 1981;30(8):702-704.
23. Wang YX, Zhang CL, Yu RT, et al. Regulation of muscle fiber type and running endurance by PPAR?? *PLoS Biol*. 2004;2(10). doi:10.1371/journal.pbio.0020294.
24. Kern M, Wells J a, Stephens JM, et al. Insulin responsiveness in skeletal muscle is determined by glucose transporter (Glut4) protein level. *Biochem J*. 1990;270(2):397-400.
25. James DE, Jenkins a B, Kraegen EW. Heterogeneity of insulin action in individual muscles in vivo: euglycemic clamp studies in rats. *Am J Physiol*. 1985;248(5 Pt 1):E567-E574.
26. Andersen JL, Gravholt CH, Kaal A, et al. Evidence of an increased number of type IIb muscle fibers in insulin-resistant first-degree relatives of patients with NIDDM. 1997;46(11):1822+. http://go.galegroup.com.ezproxy.library.yorku.ca/ps/i.do?id=GALE%7CA20060337&v=2.1&u=yorku_main&it=r&p=EAIM&sw=w&asid=c1c49e0ec920cfdbf967c0502a06d207.
27. Hickey MS, Carey JO, Azevedo JL, et al. Skeletal muscle fiber composition is related to adiposity and in vitro glucose transport rate in humans. *Am J Physiol*. 1995;268(3 Pt 1):E453-E457.
28. Stuart C a., McCurry MP, Marino A, et al. Slow-twitch fiber proportion in skeletal muscle correlates with insulin responsiveness. *J Clin Endocrinol Metab*. 2013;98(5):2027-2036. doi:10.1210/jc.2012-3876.
29. Gaster M, Staehr P, Beck-Nielsen H, Schrøder HD, Handberg a. GLUT4 is reduced in slow muscle fibers of type 2 diabetic patients: is insulin resistance in type 2 diabetes a slow, type 1 fiber disease? *Diabetes*. 2001;50(6):1324-1329. doi:10.2337/diabetes.50.6.1324.
30. Charron MJ, Brosius FC, Alper SL, Lodish HF. A glucose transport protein expressed predominately in insulin-responsive tissues. *Proc Natl Acad Sci U S A*. 1989;86(8):2535-2539. doi:10.1073/pnas.86.8.2535.
31. Olson a L, Pessin JE. Structure, function, and regulation of the mammalian facilitative glucose transporter gene family. *Annu Rev Nutr*. 1996;16:235-256. doi:10.1146/annurev.nu.16.070196.001315.
32. Zeigerer A, Lampson MA, Karylowski O, et al. GLUT4 Retention in Adipocytes Requires Two Intracellular Insulin-regulated Transport Steps. Lippincott-Schwartz J, ed. *Mol Biol Cell*. 2002;13(7):2421-2435. doi:10.1091/mbc.E02-02-0071.
33. Wilson CM, Cushman SW. Insulin stimulation of glucose transport activity in rat skeletal muscle: increase in cell surface GLUT4 as assessed by photolabelling. *Biochem J*. 1994;299 (Pt 3(1 994):755-759.
34. Kelley DE, Reilly JP, Veneman T, Mandarino LJ. Effects of insulin on skeletal muscle glucose storage, oxidation, and glycolysis in humans. *Am J Physiol*. 1990;258(6 Pt 1):E923-E929.
35. DeFronzo RA, Jacot E, Jequier E, Maeder E, Wahren J, Felber JP. The Effect of Insulin on the Disposal of Intravenous Glucose: Results from Indirect Calorimetry and Hepatic and Femoral Venous Catheterization. *Diabetes* . 1981;30(12):1000-1007.

doi:10.2337/diab.30.12.1000.
36. Kong X, Manchester J, Salmons S, Lawrence JCJ. Glucose transporters in single skeletal muscle fibers. Relationship to hexokinase and regulation by contractile activity. *J Biol Chem*. 1994;269(17):12963-12967.
37. Rose AJ, Richter EA. Skeletal muscle glucose uptake during exercise: how is it regulated? *Physiology (Bethesda)*. 2005;20:260-270. doi:10.1152/physiol.00012.2005.
38. Bokhari S, Emerson P, Israelian Z, Gupta A, Meyer C. Metabolic fate of plasma glucose during hyperglycemia in impaired glucose tolerance: evidence for further early defects in the pathogenesis of type 2 diabetes. *Am J Physiol Endocrinol Metab*. 2009;296(3):E440-4. doi:10.1152/ajpendo.90505.2008.
39. Felber JP, Golay A, Felley C, Jequier E. Regulation of glucose storage in obesity and diabetes: metabolic aspects. *Diabetes Metab Rev*. 1988;4(7):691-700.
40. Thiebaud D, Jacot E, DeFronzo RA, Maeder E, Jequier E, Felber JP. The effect of graded doses of insulin on total glucose uptake, glucose oxidation, and glucose storage in man. *Diabetes*. 1982;31(11):957-963.
41. Shulman GI, Rothman DL, Jue T, Stein P, DeFronzo RA, Shulman RG. Quantitation of muscle glycogen synthesis in normal subjects and subjects with non-insulin-dependent diabetes by 13C nuclear magnetic resonance spectroscopy. *N Engl J Med*. 1990;322(4):223-228. doi:10.1056/NEJM199001253220403.
42. Braithwaite SS, Colca JE, Edwards III CW, Hofmann C, Palazuk BBT-D. Reduced expression of hexokinase II in insulin-resistant diabetes. 1995;44(1):43+. http://go.galegroup.com.ezproxy.library.yorku.ca/ps/i.do?id=GALE%7CA16285233&v=2.1&u=yorku_main&it=r&p=AONE&sw=w&asid=5eadc19462499f1524a1af73bcc6ca17.
43. Thorburn AW, Gumbiner B, Bulacan F, Brechtel G, Henry RR. Multiple defects in muscle glycogen synthase activity contribute to reduced glycogen synthesis in non-insulin dependent diabetes mellitus. *J Clin Invest*. 1991;87(2):489-495. doi:10.1172/JCI115022.
44. Lawrence Jr. JC, Roach PJ. New insights into the role and mechanism of gycogen synthase activation by insulin. *Diabetes*. 1997;46(4):541-547.
45. Dresner a, Laurent D, Marcucci M, et al. Effects of free fatty acids on glucose transport and IRS-1- associated phosphatidylinositol 3-kinase activity U. *J Clin Invest*. 1999;103(2):253-259. doi:10.1172/JCI5001.
46. Cline GW, Petersen KF, Krssak M, Shen J, Hundal RS, Trajanoski Z, Inzucchi S, Dresner A RD& SG. Impaired glucose transport as a cause of decreased insulin-stimulated muscle glycogen synthesis in type 2 diabetes. *N Engl J Med*. 1999.
47. Patti ME, Kahn CR. The insulin receptor--a critical link in glucose homeostasis and insulin action. *J Basic Clin Physiol Pharmacol*. 1998;9(2-4):89-109.
48. Zierath JR, Krook a, Wallberg-Henriksson H. Insulin action and insulin resistance in human skeletal muscle. *Diabetologia*. 2000;43:821-835. doi:10.1007/s001250051457.
49. Gual P, Le Marchand-Brustel Y, Tanti J-F. Positive and negative regulation of insulin signaling through IRS-1 phosphorylation. *Biochimie*. 2005;87(1):99-109. doi:10.1016/j.biochi.2004.10.019.
50. White MF. The IRS-signalling system: A network of docking proteins that mediate insulin action. *Mol Cell Biochem*. 1998;182(1-2):3-11. doi:10.1023/A:1006806722619.
51. Y K, Dj B, D W. Tissue-specific insulin resistance in mice with mutations in the insulin receptor, IRS- 1. *IRS-2 J Clin*. 2000;105(2):199-205. doi:10.1172/JCI7917.
52. Brozinick JT, Roberts BR, Dohm GL. Defective Signaling Through Akt-2 and -3 But Not

Akt-1 in Insulin-Resistant Human Skeletal Muscle. :935-941.
53. White MF. The IRS-signalling system: a network of docking proteins that mediate insulin action. *Mol Cell Biochem*. 1998;182(1-2):3-11.
54. Shepherd PR, Withers DJ, Siddle K. Phosphoinositide 3-kinase: the key switch mechanism in insulin signalling. *Biochem J*. 1998;333 (Pt 3:471-490.
55. Vanhaesebroeck B, Leevers SJ, Timms J, et al. Synthesis and Function of 3-Phosphorylated I Nositol L Ipids. *Annu Rev Biochem*. 2001:535-602.
56. Alessi DR, James SR, Downes CP, et al. Characterization of a 3-phosphoinositide-dependent protein kinase which phosphorylates and activates protein kinase Balpha. *Curr Biol*. 1997;7(4):261-269. doi:10.1016/S0960-9822(06)00122-9.
57. Stokoe D, Stephens LR, Copeland T, et al. Dual role of phosphatidylinositol-3,4,5-trisphosphate in the activation of protein kinase B. *Science*. 1997;277(5325):567-570. doi:10.1126/science.277.5325.567.
58. Eldar-Finkelman H. Glycogen synthase kinase 3: an emerging therapeutic target. *Trends Mol Med*. 2002;8(3):126-132. doi:Pii s1471-4914(01)02266-3\n10.1016/s1471-4914(01)02266-3.
59. Jope RS, Johnson GVW. The glamour and gloom of glycogen synthase kinase-3. *Trends Biochem Sci*. 2004;29(2):95-102. doi:10.1016/j.tibs.2003.12.004.
60. Printen J a, Brady MJ, Saltiel a R. PTG, a protein phosphatase 1-binding protein with a role in glycogen metabolism. *Science*. 1997;275(5305):1475-1478. doi:10.1126/science.275.5305.1475.
61. Parker PJ, Caudwell FB, Cohen P. Glycogen synthase from rabbit skeletal muscle; effect of insulin on the state of phosphorylation of the seven phosphoserine residues in vivo. *Eur J Biochem*. 1983;130(1):227-234.
62. Leloir, L F Olavarria, JM Goldemberg SC. Biosynthesis of glycogen from uridine diphosphate glucose. *Arch Biochem Biophys*. 1959;81(2):508-520.
63. Roach PJ. Control of glycogen synthase by heiarachial protein phosphorylation.pdf. *Fed Am Soc Exp Biol*. 1990;4.
64. DePaoli-Roach AA, Ahmad Z, Camici M, Lawrence JCJ, Roach PJ. Multiple phosphorylation of rabbit skeletal muscle glycogen synthase. Evidence for interactions among phosphorylation sites and the resolution of electrophoretically distinct forms of the subunit. *J Biol Chem*. 1983;258(17):10702-10709.
65. Bouskila M, Hunter RW, Ibrahim AFM, et al. Allosteric regulation of glycogen synthase controls glycogen synthesis in muscle. *Cell Metab*. 2010;12(5):456-466. doi:10.1016/j.cmet.2010.10.006.
66. Azpiazu I, Manchester J, Skurat a V, Roach PJ, Lawrence JC. Control of glycogen synthesis is shared between glucose transport and glycogen synthase in skeletal muscle fibers. *Am J Physiol Endocrinol Metab*. 2000;278(2):E234-E243.
67. Villar-Palasi C. Substrate specific activation by glucose 6-phosphate of the dephosphorylation of muscle glycogen synthase. *Biochim Biophys Acta*. 1991;1095(3):261-267.
68. Villar-Palasí C, Guinovart JJ. The role of glucose 6-phosphate in the control of glycogen synthase. *Faseb J*. 1997;11(7):544-558. http://www.ncbi.nlm.nih.gov/pubmed/9212078.
69. Kahn CR, Flier JS, Bar RS, et al. The Syndromes of Insulin Resistance and Acanthosis Nigricans. *N Engl J Med*. 1976;294(14):739-745. doi:10.1056/NEJM197604012941401.
70. Wei Y, Chen K, Whaley-Connell a. T, Stump CS, Ibdah J a., Sowers JR. Skeletal muscle

insulin resistance: role of inflammatory cytokines and reactive oxygen species. *AJP Regul Integr Comp Physiol*. 2008;294(82):R673-R680. doi:10.1152/ajpregu.00561.2007.
71. Boden G. Fatty acid-induced inflammation and insulin resistance in skeletal muscle and liver. *Curr Diab Rep*. 2006;6:177-181. doi:10.1007/s11892-006-0031-x.
72. Ruzzin J, Wagman a. S, Jensen J. Glucocorticoid-induced insulin resistance in skeletal muscles: Defects in insulin signalling and the effects of a selective glycogen synthase kinase-3 inhibitor. *Diabetologia*. 2005;48(10):2119-2130. doi:10.1007/s00125-005-1886-0.
73. Itani SI, Ruderman NB, Schmieder F, Boden G. Lipid-induced insulin resistance in human muscle is associated with changes in diacylglycerol, protein kinase C, and IkappaB-alpha. *Diabetes*. 2002;51(17):2005-2011. doi:10.2337/diabetes.51.7.2005.
74. Kershaw EE, Flier JS. Adipose Tissue as an Endocrine Organ. *J Clin Endocrinol Metab*. 2004;89(6):2548-2556. doi:10.1210/jc.2004-0395.
75. Henry WL. Does an Adipokine-Induced Activation of the Immune System Mediate the Effect of Overnutrition on Type 2 Diabetes? *J Natl Med Assoc*. 1962;54:476-478. doi:10.2337/diabetes.52.1.1.
76. Boden G. Perspectives in Diabetes Role of Fatty Acids in the Pathogenesis of Insulin Resistance and NIDDM. *Diabetes*. 1997;46(JANUARY):3-10. doi:10.2337/diabetes.46.1.3.
77. Pedersen BK, Steensberg A, Schjerling P. Topical Review Muscle-derived interleukin-6 : possible biological effects. 2001;6:329-337.
78. del Aguila LF, Claffey KP, Kirwan JP. TNF-alpha impairs insulin signaling and insulin stimulation of glucose uptake in C2C12 muscle cells. *Am J Physiol*. 1999;276(5 Pt 1):E849-E855.
79. Hotamisligil G, Shargill N, Spiegelman B. Adipose Expression of Tumor Necrosis Factor α : Direct Role in Obesity-Linked Insulin Resistance. *Science (80-)*. 1993;259(5091):87-91. http://www.sciencemag.org/content/259/5091/87.short.
80. Nieto-Vazquez I, Fernández-Veledo S, Krämer DK, Vila-Bedmar R, Garcia-Guerra L, Lorenzo M. Insulin resistance associated to obesity: the link TNF-alpha. *Arch Physiol Biochem*. 2008;114(April):183-194. doi:10.1080/13813450802181047.
81. Carey AL, Steinberg GR, Macaulay SL, et al. Interleukin-6 increases insulin-stimulated glucose disposal in humans and glucose uptake and fatty acid oxidation in vitro via AMP-activated protein kinase. *Diabetes*. 2006;55(10):2688-2697. doi:10.2337/db05-1404.
82. Kim HJ, Higashimori T, Park SY, et al. Differential effects of interleukin-6 and-10 on skeletal muscle and liver insulin action in vivo. *Diabetes*. 2004;53(4):1060-1067. doi:10.2337/diabetes.53.4.1060.
83. Barazzoni R, Zanetti M, Gortan Cappellari G, et al. Fatty acids acutely enhance insulin-induced oxidative stress and cause insulin resistance by increasing mitochondrial reactive oxygen species (ROS) generation and nuclear factor-kappaB inhibitor (IkappaB)-nuclear factor-kappaB (NFkappaB) activation in rat. *Diabetologia*. 2012;55(3):773-782. doi:10.1007/s00125-011-2396-x.
84. Taniyama Y, Griendling KK. Reactive Oxygen Species in the Vasculature: Molecular and Cellular Mechanisms. *Hypertension*. 2003;42(6):1075-1081. doi:10.1161/01.HYP.0000100443.09293.4F.
85. Hoeks J, Schrauwen P. Muscle mitochondria and insulin resistance: a human perspective. *Trends Endocrinol Metab*. 2012;23(9):444-450. doi:10.1016/j.tem.2012.05.007.

86. Halliwell B. Antioxidant characterization. Methodology and mechanism. *Biochem Pharmacol*. 1995;49(10):1341-1348. doi:10.1016/0006-2952(95)00088-H.
87. Kang L, Lustig ME, Bonner JS, et al. Mitochondrial antioxidative capacity regulates muscle glucose uptake in the conscious mouse: effect of exercise and diet. *J Appl Physiol*. 2012;113(8):1173-1183. doi:10.1152/japplphysiol.01344.2011.
88. Evans JL, Goldfine ID, Maddux BA, Grodsky GM. Oxidative stress and stress-activated signaling pathways: A unifying hypothesis of type 2 diabetes. *Endocr Rev*. 2002;23(5):599-622. doi:10.1210/er.2001-0039.
89. Lark DS, Kang L, Lustig ME, et al. Enhanced Mitochondrial Superoxide Scavenging Does Not Improve Muscle Insulin Action in the High Fat-Fed Mouse. Moro C, ed. *PLoS One*. 2015;10(5):e0126732. doi:10.1371/journal.pone.0126732.
90. Wei Y, Sowers JR, Nistala R, et al. Angiotensin II-induced NADPH oxidase activation impairs insulin signaling in skeletal muscle cells. *J Biol Chem*. 2006;281(46):35137-35146. doi:10.1074/jbc.M601320200.
91. Blendea MC, Jacobs D, Stump CS, et al. Abrogation of oxidative stress improves insulin sensitivity in the Ren-2 rat model of tissue angiotensin II overexpression. *Am J Physiol Endocrinol Metab*. 2005;288(2):E353-E359. doi:10.1152/ajpendo.00402.2004.
92. Nourooz-Zadeh J, Rahimi a., Tajaddini-Sarmadi J, et al. Relationships between plasma measures of oxidative stress and metabolic control in NIDDM. *Diabetologia*. 1997;40(6):647-653. doi:10.1007/s001250050729.
93. Dimitriadis G, Leighton B, Parry-Billings M, et al. Effects of glucocorticoid excess on the sensitivity of glucose transport and metabolism to insulin in rat skeletal muscle. *Biochem J*. 1997;321 (Pt 3:707-712.
94. Qi D, Rodrigues B, Dulin-keita A, et al. Glucocorticoids produce whole body insulin resistance with changes in cardiac metabolism. 2010;3(October 2006):654-667. doi:10.1152/ajpendo.00453.2006.
95. Van Raalte DH, Ouwens DM, Diamant M. Novel insights into glucocorticoid-mediated diabetogenic effects: Towards expansion of therapeutic options? *Eur J Clin Invest*. 2009;39(2):81-93. doi:10.1111/j.1365-2362.2008.02067.x.
96. Whorwood CB, Donovan SJ, Wood PJ, Phillips DI. Regulation of glucocorticoid receptor alpha and beta isoforms and type I 11beta-hydroxysteroid dehydrogenase expression in human skeletal muscle cells: a key role in the pathogenesis of insulin resistance? *J Clin Endocrinol Metab*. 2001;86(5):2296-2308. doi:10.1210/jcem.86.5.7503.
97. Giorgino F, Almahfouz A, Goodyear LJ, Smith RJ. Glucocorticoid regulation of insulin receptor and substrate IRS-1 tyrosine phosphorylation in rat skeletal muscle in vivo. *J Clin Invest*. 91(5):2020-2030. doi:10.1172/JCI116424.
98. Morgan SA, Sherlock M, Gathercole LL, et al. 11b-Hydroxysteroid Dehydrogenase Type 1 Regulates Glucocorticoid-Induced Insulin Resistance in Skeletal Muscle. *Diabetes*. 2009;58(November):2506-25015. doi:10.2337/db09-0525.
99. Morton NM, Holmes MC, Fievet C, et al. Improved lipid and lipoprotein profile, hepatic insulin sensitivity, and glucose tolerance in 11beta-hydroxysteroid dehydrogenase type 1 null mice. *J Biol Chem*. 2001;276(44):41293-41300. doi:10.1074/jbc.M103676200.
100. Santomauro AT, Boden G, Silva ME, et al. Overnight lowering of free fatty acids with Acipimox improves insulin resistance and glucose tolerance in obese diabetic and nondiabetic subjects. *Diabetes*. 1999;48(9):1836-1841.
101. Hue L, Taegtmeyer H. The Randle cycle revisited: a new head for an old hat. *Am J*

Physiol Endocrinol Metab. 2009;297:E578-E591. doi:10.1152/ajpendo.00093.2009.
102. Randle PJ, Newsholme E a, Garland PB. Regulation of glucose uptake by muscle. Effects of fatty acids, ketone bodies and pyruvate, and of alloxan-diabetes and starvation, on the uptake and metabolic fate of glucose in rat heart and diaphragm muscles. *Biochem J*. 1964;93(3):652-665.
103. Roden M, Price TB, Perseghin G, et al. Mechanism of free fatty acid-induced insulin resistance in humans. *J Clin Invest*. 1996;97(12):2859-2865. doi:10.1172/JCI118742.
104. Krebs M, Krssak M, Bernroider E, et al. Mechanism of amino acid-induced skeletal muscle insulin resistance in humans. *Diabetes*. 2002;51(3):599-605.
105. Morino K, Petersen KF, Shulman GI. Molecular mechanisms of insulin resistance in humans and their potential links with mitochondrial dysfunction. *Diabetes*. 2006;55 Suppl 2:S9-S15. doi:10.2337/diabetes.
106. Samuel VT, Shulman GI. The pathogenesis of insulin resistance: integrating signaling pathways and substrate flux. *J Clin Invest*. 2016;126(1):12.
107. Ritov VB, Menshikova E V, He J, Ferrell RE, Goodpaster BH, Kelley DE. Deficiency of subsarcolemmal mitochondria in obesity and type 2 diabetes. *Diabetes*. 2005;54(1):8-14.
108. Morino K, Petersen KF, Dufour S, et al. Reduced mitochondrial density and increased IRS-1 serine phosphorylation in muscle of insulin-resistant offspring of type 2 diabetic parents. *J Clin Invest*. 2005;115(12):3587-3593. doi:10.1172/JCI25151.
109. Carrasco S, Mérida I. Diacylglycerol, when simplicity becomes complex. *Trends Biochem Sci*. 2007;32(1):27-36. doi:10.1016/j.tibs.2006.11.004.
110. Hayashi T, Goodyear LJ. Exercise regulation of glucose transport in skeletal muscle. *Am J Physiol*. 1997;(5):1039-1051. doi:10.1152/ajpregu.00109.2011.
111. Borghouts LB, Keizer H a. Exercise and insulin sensitivity: A review. *Int J Sports Med*. 2000;21(1):1-12. doi:10.1055/s-2000-8847.
112. Widen EI, Eriksson JG, Groop LC. Metformin normalizes nonoxidative glucose metabolism in insulin-resistant normoglycemic first-degree relatives of patients with NIDDM. *Diabetes*. 1992;41(3):354-358.
113. Nolan JJ, Ludvik B, Beerdsen P, Joyce M, Olefsky J. Improvement in glucose tolerance and insulin resistance in obese subjects treated with troglitazone. *N Engl J Med*. 1994;331(18):1188-1193. doi:10.1056/NEJM199411033311803.
114. Perseghin G, Price TB, Petersen KF, et al. Increased Glucose Transport–Phosphorylation and Muscle Glycogen Synthesis after Exercise Training in Insulin-Resistant Subjects. *N Engl J Med*. 1996;335(18):1357-1362. doi:10.1056/NEJM199610313351804.
115. Sisson SB, Camhi SM, Church TS, et al. Leisure time sedentary behavior, occupational/domestic physical activity, and metabolic syndrome in U.S. men and women. *Metab Syndr Relat Disord*. 2009;7(6):529-536. doi:10.1089/met.2009.0023.
116. Group DPPR. Reductin in the incidence of type 2 diabetes with lifestyle intervention or metformin. *N Engl J Med*. 2002;29(6):393-403. doi:10.1016/j.biotechadv.2011.08.021.Secreted.
117. Magkos F, Tsekouras Y, Kavouras SA, Mittendorfer B, Sidossis LS. Improved insulin sensitivity after a single bout of exercise is curvilinearly related to exercise energy expenditure. *Clin Sci (Lond)*. 2008;114(1):59-64. doi:10.1042/CS20070134.
118. Stiegler P, Cunliffe A. The role of diet and exercise for the maintenance of fat-free mass and resting metabolic rate during weight loss. *Sports Med*. 2006;36(3):239-262.
119. Brooks N, Layne JE, Gordon PL, Roubenoff R, Nelson ME, Castaneda-Sceppa C.

Strength training improves muscle quality and insulin sensitivity in Hispanic older adults with type 2 diabetes. *Int J Med Sci*. 2007;4(1):19-27.
120. Tabata I, Suzuki Y, Fukunaga T, Yokozeki T, Akima H, Funato K. Resistance training affects GLUT-4 content in skeletal muscle of humans after 19 days of head-down bed rest. *J Appl Physiol*. 1999;86(3):909-914.
121. Bruunsgaard H, Bjerregaard E, Schroll M, Pedersen BK. Muscle strength after resistance training is inversely correlated with baseline levels of soluble tumor necrosis factor receptors in the oldest old. *J Am Geriatr Soc*. 2004;52(2):237-241.
122. Ivy JL. Role of exercise training in the prevention and treatment of insulin resistance and non-insulin-dependent diabetes mellitus. *Sports Med*. 1997;24(5):321-336.
123. Song XM, Ryder JW, Kawano Y, Chibalin a V, Krook a, Zierath JR. Muscle fiber type specificity in insulin signal transduction. *Am J Physiol*. 1999;277(6 Pt 2):R1690-R1696.
124. Jensen J, Tantiwong P, Stuenæs JT, et al. Effect of acute exercise on glycogen synthase in muscle from obese and diabetic subjects. *Am J Physiol - Endocrinol Metab*. 2012;303(1):E82-E89. doi:10.1152/ajpendo.00658.2011.
125. Cartee GD, Wojtaszewski JFP. Role of Akt substrate of 160 kDa in insulin-stimulated and contraction-stimulated glucose transport. *Appl Physiol Nutr Metab*. 2007;32(3):557-566. doi:10.1139/H07-026.
126. Hey-Mogensen M, H??jlund K, Vind BF, et al. Effect of physical training on mitochondrial respiration and reactive oxygen species release in skeletal muscle in patients with obesity and type 2 diabetes. *Diabetologia*. 2010;53(9):1976-1985. doi:10.1007/s00125-010-1813-x.
127. Dubé JJ, Amati F, Toledo FGS, et al. Effects of weight loss and exercise on insulin resistance, and intramyocellular triacylglycerol, diacylglycerol and ceramide. *Diabetologia*. 2011;54(5):1147-1156. doi:10.1007/s00125-011-2065-0.
128. Neta R, Sayers TJ, Oppenheim JJ. Relationship of TNF to interleukins. *Immunol Ser*. 1992;56:499-566.
129. Carey AL, Bruce CR, Sacchetti M, et al. Interleukin-6 and tumor necrosis factor-alpha are not increased in patients with Type 2 diabetes: evidence that plasma interleukin-6 is related to fat mass and not insulin responsiveness. *Diabetologia*. 2004;47(6):1029-1037. doi:10.1007/s00125-004-1403-x.
130. Fischer CP. Interleukin-6 in acute exercise and training: what is the biological relevance? *Exerc Immunol Rev*. 2006;12:6-33.
131. Pedersen BK, Febbraio MA. Muscle as an endocrine organ: focus on muscle-derived interleukin-6. *Physiol Rev*. 2008;88(4):1379-1406. doi:10.1152/physrev.90100.2007.
132. Pedersen BK, Febbraio M a. Muscles, exercise and obesity: skeletal muscle as a secretory organ. *Nat Rev Endocrinol*. 2012;8(8):457-465. doi:10.1038/nrendo.2012.49.
133. Nieman DC, Nehlsen-Cannarella SL, Fagoaga OR, et al. Influence of mode and carbohydrate on the cytokine response to heavy exertion. *Med Sci Sports Exerc*. 1998;30(5):671-678.
134. Keller C, Steensberg A, Hansen AK, Fischer CP, Plomgaard P, Pedersen BK. Effect of exercise, training, and glycogen availability on IL-6 receptor expression in human skeletal muscle. *J Appl Physiol*. 2005;99(6):2075-2079. doi:10.1152/japplphysiol.00590.2005.
135. Steensberg A, Febbraio MA, Osada T, et al. Interleukin-6 production in contracting human skeletal muscle is influenced by pre-exercise muscle glycogen content. *J Physiol*. 2001;537(Pt 2):633-639.

136. Pedersen BK. Muscular interleukin-6 and its role as an energy sensor. *Med Sci Sports Exerc*. 2012;44(3):392-396. doi:10.1249/MSS.0b013e31822f94ac.
137. Starkie R, Ostrowski SR, Jauffred S, Febbraio M, Pedersen BK. Exercise and IL-6 infusion inhibit endotoxin-induced TNF-alpha production in humans. *FASEB J*. 2003;17(8):884-886. doi:10.1096/fj.02-0670fje.
138. Keller C, Keller P, Giralt M, Hidalgo J, Pedersen BK. Exercise normalises overexpression of TNF-α in knockout mice. *Biochem Biophys Res Commun*. 2004;321(1):179-182. doi:http://dx.doi.org/10.1016/j.bbrc.2004.06.129.
139. Balducci S, Zanuso S, Nicolucci a, et al. Anti-inflammatory effect of exercise training in subjects with type 2 diabetes and the metabolic syndrome is dependent on exercise modalities and independent of weight loss. *NutrMetab Cardiovasc*.
140. Espinosa A, Garcia A, Hartel S, Hidalgo C, Jaimovich E. NADPH oxidase and hydrogen peroxide mediate insulin-induced calcium increase in skeletal muscle cells. *J Biol Chem*. 2009;284(4):2568-2575. doi:10.1074/jbc.M804249200.
141. Beaudry JL, Dunford EC, Leclair E, et al. Voluntary exercise improves metabolic profile in high-fat fed glucocorticoid-treated rats. *J Appl Physiol*. 2015;118(11):1331-1343. doi:10.1152/japplphysiol.00467.2014.
142. Randle PJ. Regulatory interactions between lipids and carbohydrates: The glucose fatty acid cycle after 35 years. *Diabetes Metab Rev*. 1998;14(June):263-283. doi:10.1002/(SICI)1099-0895(199812)14:4<263::AID-DMR233>3.0.CO;2-C.
143. Muoio DM, Newgard CB. Obesity-related derangements in metabolic regulation. *Annu Rev Biochem*. 2006;75:367-401. doi:10.1146/annurev.biochem.75.103004.142512.
144. Szendroedi J, Yoshimura T, Phielix E, et al. Role of diacylglycerol activation of PKCθ in lipid-induced muscle insulin resistance in humans. *Proc Natl Acad Sci* . 2014;111(26):9597-9602. doi:10.1073/pnas.1409229111.
145. Guo Z. Pyruvate dehydrogenase, Randle cycle, and skeletal muscle insulin resistance. *Proc Natl Acad Sci U S A*. 2015;112(22):E2854-E2854. doi:10.1073/pnas.1505398112.
146. Daugaard JR, Nielsen JN, Kristiansen S, Andersen JL, Hargreaves M, Richter EA. Fiber type-specific expression of GLUT4 in human skeletal muscle: influence of exercise training. *Diabetes*. 2000;49(7):1092-1095.
147. Association AD. Standards of medical care in diabetes—2015. *J Clin Appl Res Educ*. 2015;38(January). doi:10.2337/dc15-S005.
148. Ariano M a, Armstrong RB, Edgerton VR. Hindlimb muscle fiber populations of five mammals. *J Histochem Cytochem*. 1973;21:51-55. doi:10.1177/21.1.51.
149. Nesher R, Karl IE, Kaiser KE, Kipnis DM. Epitrochlearis muscle. I. Mechanical performance, energetics, and fiber composition. *Am J Physiol*. 1980;239:E454-E460.
150. Ceddia RB, William WN, Curi R. Comparing effects of leptin and insulin on glucose metabolism in skeletal muscle: evidence for an effect of leptin on glucose uptake and decarboxylation. *Int J Obes Relat Metab Disord*. 1999;23:75-82.
151. Yan Z, Okutsu M, Akhtar YN, Lira V a. Regulation of exercise-induced fiber type transformation, mitochondrial biogenesis, and angiogenesis in skeletal muscle. *J Appl Physiol*. 2011;110(October 2010):264-274. doi:10.1152/japplphysiol.00993.2010.
152. Henriksen EJ. Invited Review: Effects of acute exercise and exercise training on insulin resistance. *J Appl Physiol*. 2002;93(2):788-796. http://jap.physiology.org/content/93/2/788.abstract.
153. Lund S, Vestergaard H, Andersen PH, Schmitz O, Gotzsche LB, Pedersen O. GLUT-4

content in plasma membrane of muscle from patients with non- insulin-dependent diabetes mellitus. *Am J Physiol*. 1993;265(6 Pt 1):E889-97. Insulin Resistance\8279544.pdf\nhttp://www.ncbi.nlm.nih.gov/htbin-post/Entrez/query?db=m&form=6&dopt=r&uid=8279544.
154. Jensen TE, Leutert R, Rasmussen ST, et al. EMG-normalised kinase activation during exercise is higher in human gastrocnemius compared to soleus muscle. *PLoS One*. 2012;7(2):e31054. doi:10.1371/journal.pone.0031054.
155. Friedman JE, Dohm GL, Leggett-Frazier N, et al. Restoration of insulin responsiveness in skeletal muscle of morbidly obese patients after weight loss. Effect on muscle glucose transport and glucose transporter GLUT4. *J Clin Invest*. 1992;89(2):701-705. http://www.ncbi.nlm.nih.gov/pmc/articles/PMC442905/.
156. Sesti G. Pathophysiology of insulin resistance. *Best Pract Res Clin Endocrinol Metab*. 2006;20(4):665-679. doi:10.1016/j.beem.2006.09.007.
157. Thorell A, Hirshman MF, Nygren J, et al. Exercise and insulin cause GLUT-4 translocation in human skeletal muscle. *Am J Physiol*. 1999;277(4 Pt 1):E733-41.
158. Wojtaszewski JF, Hansen BF, Gade, et al. Insulin signaling and insulin sensitivity after exercise in human skeletal muscle. *Diabetes*. 2000;49(22):325-331.
159. Manabe Y, Gollisch KSC, Holton L, et al. Exercise training-induced adaptations associated with increases in skeletal muscle glycogen content. *FEBS J*. 2013;280(3):916-926. doi:10.1111/febs.12085.
160. Nielsen JN, Richter EA. Regulation of glycogen synthase in skeletal muscle during exercise. *Acta Physiol Scand*. 2003;178(4):309-319. doi:10.1046/j.1365-201X.2003.01165.x.
161. Gaster M, Staehr P, Beck-Nielsen H, Schroder HD, Handberg A. GLUT4 is reduced in slow muscle fibers of type 2 diabetic patients: is insulin resistance in type 2 diabetes a slow, type 1 fiber disease? *Diabetes*. 2001;50(6):1324-1329.
162. Goodpaster BH, Thaete FL, Simoneau JA, Kelley DE. Subcutaneous abdominal fat and thigh muscle composition predict insulin sensitivity independently of visceral fat. *Diabetes*. 1997;46(10):1579-1585.
163. Pan DA, Lillioja S, Kriketos AD, et al. Skeletal muscle triglyceride levels are inversely related to insulin action. *Diabetes*. 1997;46(6):983-988.
164. Bruce CR, Anderson MJ, Carey AL, et al. Muscle oxidative capacity is a better predictor of insulin sensitivity than lipid status. *J Clin Endocrinol Metab*. 2003;88(11):5444-5451. doi:10.1210/jc.2003-030791.
165. Holloszy JO. "Deficiency" of mitochondria in muscle does not cause insulin resistance. *Diabetes*. 2013;62(4):1036-1040. doi:10.2337/db12-1107.
166. Henstridge DC, Bruce CR, Drew BG, et al. Activating HSP72 in rodent skeletal muscle increases mitochondrial number and oxidative capacity and decreases insulin resistance. *Diabetes*. 2014;63(6):1881-1894. doi:10.2337/db13-0967.
167. Keung W, Ussher JR, Jaswal JS, et al. Inhibition of carnitine palmitoyltransferase-1 activity alleviates insulin resistance in diet-induced obese mice. *Diabetes*. 2013;62(3):711-720. doi:10.2337/db12-0259.
168. Bruce CR, Hoy AJ, Turner N, et al. Overexpression of carnitine palmitoyltransferase-1 in skeletal muscle is sufficient to enhance fatty acid oxidation and improve high-fat diet-induced insulin resistance. *Diabetes*. 2009;58(3):550-558. doi:10.2337/db08-1078.
169. Rahimi Y, Camporez J-PG, Petersen MC, et al. Genetic activation of pyruvate

dehydrogenase alters oxidative substrate selection to induce skeletal muscle insulin resistance. *Proc Natl Acad Sci U S A*. 2014;111(46):16508-16513. doi:10.1073/pnas.1419104111.

170. Wright DC, Geiger PC, Rheinheimer MJ, Han DH, Holloszy JO. Phorbol esters affect skeletal muscle glucose transport in a fiber type-specific manner. *Am J Physiol Endocrinol Metab*. 2004;287(2):E305-9. doi:10.1152/ajpendo.00082.2004.
171. Lee S-Y, Kim JR, Ha M-Y, Shim S-M, Park T-S. Measurements of diacylglycerols in skeletal muscle by atmospheric pressure chemical ionization mass spectrometry. *Lipids*. 2013;48(3):287-296. doi:10.1007/s11745-013-3766-6.
172. Aguirre V, Werner ED, Giraud J, Lee YH, Shoelson SE, White MF. Phosphorylation of Ser307 in insulin receptor substrate-1 blocks interactions with the insulin receptor and inhibits insulin action. *J Biol Chem*. 2002;277(2):1531-1537. doi:10.1074/jbc.M101521200.

Appendix A:

Intramuscular triglyceride content

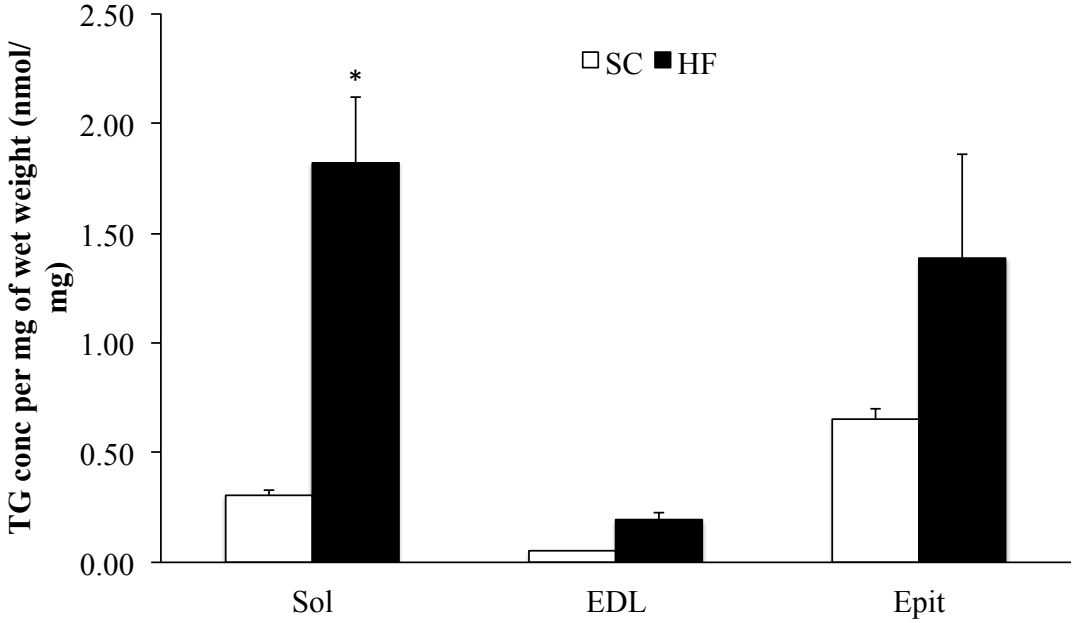

Intramuscular triglyceride measurements of Sol, EDL and Epit muscle of SED SC (SC) and SED HF (HF) groups. Data are presented as mean ± SEM. Two-way ANOVA followed by a Bonferonni post-test. N=1-4. * $p < 0.01$ vs. EDL SC and EDL HF

Intramuscular glycogen content

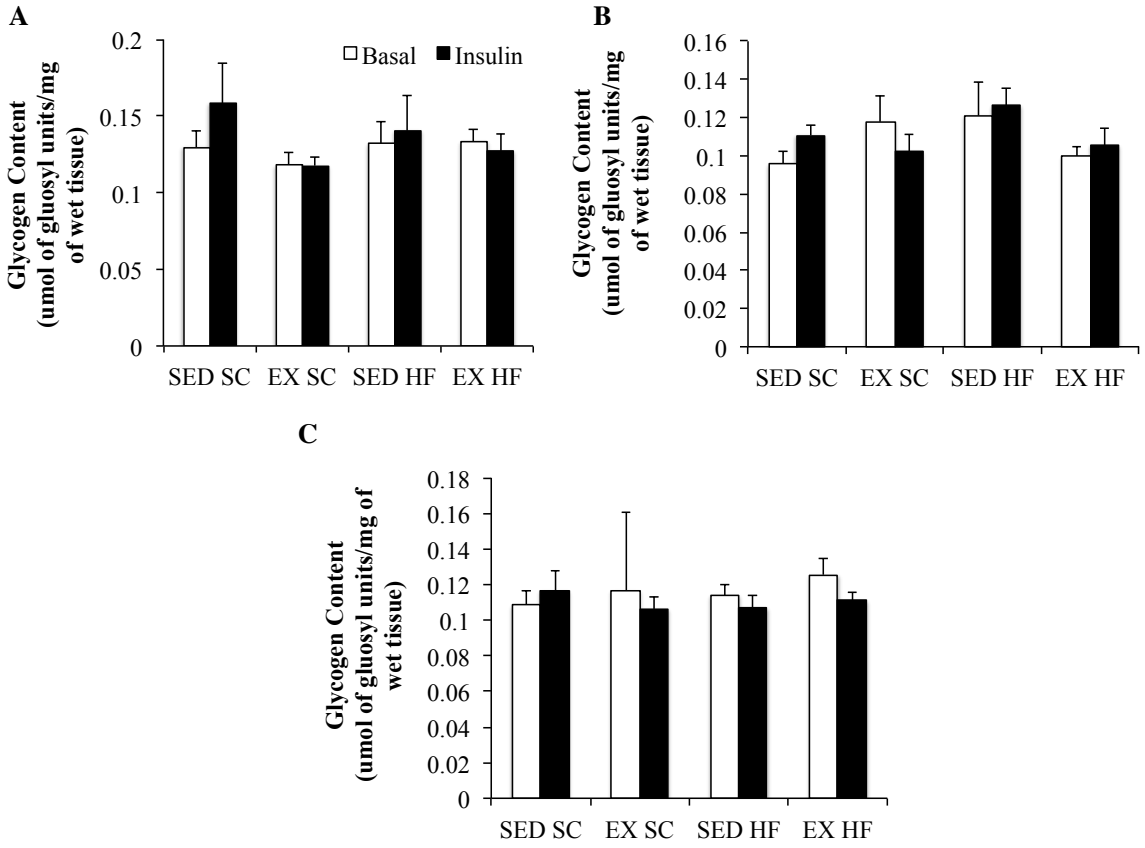

Intramuscular glycogen content measurements of Sol (A), EDL (B) and Epit (C) muscle of SED SC, EX SC, SED HF and EX HF groups. Data are presented as mean ± SEM. Two-way ANOVA followed by a Bonferonni post-test.

7.0 Detailed experimental methods

7.1 Glucose-6-phosphate assay kit

In this assay, glucose-6-phosphate was oxidized which generated a product that is used to convert a colorless probe into a colored product with an absorbance of 450 nm. This kit can identify glucose-6-phosphate from 1 to 30 nmol, with a detection sensitivity of ~10uM.
Store kit in -20 freezer, away from light. Warm the Glucose 6 Phosphate Assay Buffer to room temperature before use. Centrifuge all vials before use.
Kit components:

Glucose 6 Phosphate Assay Buffer	25ml
Glucose 6 Phosphate Enzyme Mix (lyophilized)	1 vial
Glucose 6 Phosphate Substrate Mix (lyophilized)	1 vial
Glucose 6 Phosphate Standard (10umol; lyophilized)	1 vial

GLUCOSE 6 PHOSPHATE STANDARD:
Dissolve in 100 µl in dH_20 producing 100 nmol/µl Glucose 6 Phosphate Standard solution. Keep on ice while in use.

GLUCOSE 6 PHOSPHATE ENZYME MIX:
Dissolve with 220 µL dH_2O. Pipette up and down to dissolve. Aliquot and store at -20°C. Avoid repeated freeze/thaw cycles. Keep on ice while in use. Avoid repeated freeze/thaw cycles. Use within two months.

GLUCOSE 6 PHOSPHATE SUBSTRATE MIX: Dissolve in 220 µL of Glucose 6 Phosphate Assay Buffer. Pipette up and down to dissolve. Keep on ice while in use. Stable for 2 months at +4°C.

Addition items required:
Clear bottom 96-well plate
Colorimetric plate reader
Centrifuge
Orbital shaker
Pipette and pipette tips

1) Sample preparation:
   A) For muscle tissue, ~100mg was homogenized in ice cold PBS (ph 6.5-8.0). Homogenized tissue was then centrifuged at top speed for 10 minutes.
   B) Enzymes in samples may interfere with the assay; as a result samples were deproteinzed using a 10kDa molecular weight cut off spin column.
   C) Each sample was centrifuged for 1 hour at max speed whilst inside a 10kDa molecular weight cut spin column.
2) Standard curve preparation:

Dilute Glucose 6 Phosphate Standard to 1nmol/µl by adding 10 µl of the 100-nmol/µl standard to 990ul of dH_2O and mix well. Proceed to add 0, 2, 4, 6, 8 and 10 µl into a series of standards wells on the 96-well plate. Finally, adjust volume to 50 µl/well using the Glucose 6 Phosphate Assay Buffer to create 0, 2, 4, 6, 8 and 10 nmol/well of Glucose 6 Phosphate standard.

3) Reaction mix:
   Mix enough reaction mix for the number of samples and standards that have been prepared. Each well requires 50µl of reaction mix containing:

Item	Reaction Mix	Background
Assay Buffer	46 µl	48 µl
Enzyme Mix	2 µl	--
Substrate Mix	2 µl	2 µl

   Protect reaction mix from light and proceed to add 50 µl/well to each standard and sample well. Add 50 µl of background into allocated background wells.
4) Incubate at room temperature for 30 minutes. Place plate on shaker while incubation occurs.
5) Place plate in colorimetric plate reader and measure OD at 450 nm.

7.1 Western Blotting Buffers

10x Running Buffer (pH- 8.3)
144g Glycine
30.34g Tris base
10g SDS
Dissolve contents in 1L of ddH_20 and store at room temperature.

1x Running Buffer (pH- 8.3)
10% 10x Running buffer
90% ddH_20
Mix solutions and store at room temperature.

10x Transfer Buffer (pH- 8.3)
144g Glycine
30.3g Tris base
Dissolve contents in 1L of ddH_20 and store at room temperature.

1x Transfer Buffer (pH- 8.3)
70% ddH_20
20% Methanol
10% 10x Transfer buffer
Mix solutions and store at -20°C prior to use.

10x Wash Buffer

60.57g Tris base
87.66g Sodium Chloride (NaCl)
Dissolve contents in 1L of ddH_20, store at room temperature.

1x Wash Buffer
10% 10x Wash buffer
90% ddH_20
Add 500µl/L of Tween-20 and NP-40.
Mix solutions and store at room temperature.

Blocking Buffer
3% BSA (w/v: 1.5g/50mL)
Dissolve in 1x Wash buffer, store at 4°C.

Antibody (Ab) Buffer
1° Ab- 1part blocking buffer + 2 parts wash buffer + 0.02% NaAzide (stock in ddH_20)
2°Ab- 1part blocking buffer + 2 parts wash buffer (NO NaAzide).
Typically 1:1000-1:5000 dilution is appropriate for an Ab, may vary depending on how good the signal is.

Resolving gl Tris Buffer (1.5M) (pH-8.8)
90.86g/500mL ddH_20

Stacking gel Tris Buffer (0.5M) (pH-6.8)
30.3g/500mL ddH_20

10% APS Solution
10% (w/v) Ammoniumperoxide Sulfate in ddH_20.
Use 0.1g/mL
Store at -20°C.

10% SDS Solution
10% (w/v) Sodium dodecylsulfate in ddH_20
Use 1g/10mL
Store at room temperature.

Lysis Buffer for Protein Determination prior to Western blot

Reagent	Concentration/MW
NaCl	135mmol/L (MW=58.44)
$MgCl_2$	1mmol/L (MW=203.3)
KCl	2.7mmol/L (MW=74.55)
Tris (pH 8)	20mmol/L (MW=121.14)
Triton 1%	~500ul
Glycerol 10%	~500ul

Prepare lysis buffer stock and store at -20°C. Aliquot desired volumes and add protease (complete ULTRA Tablets) and phosphatise (PhoStop) inhibitors just prior to use.

Laemmli Sample Buffer (2x)- (Bio-Rad, Cat#161-0737)
Per 1mL: 950µl of 2x Laemmli sample buffer
50µl β-Mercaptoethanol
Store at room temperature. Dilute the sample (1 in 2) with sample buffer and boil for 5min.

Preparation of tissue lysates:

1. After extraction, tissues are snap frozen and stored at -80°C.
2. Weigh tissues (~20mg skeletal muscle) and add to 250µl lysis buffer.
3. Homogenize tissue. Keep on ice as much as possible to avoid heating up the sample.
4. Centrifuge homogenate for 5min at 13,000rpm at 4°C.
5. Remove middle aqueous protein-rich layer and place in a fresh microtube.
6. Centrifuge extracted sample for 1min at 13,000rpm at 4°C and transfer to a fresh microtube. Discard any residual cell debris.
7. Take an aliquot from each sample for protein determination by the Bradford method.
8. Dilute sample with 2x Laemmli sample buffer (1:1 v/v), vortex well and boil samples for 5min.
9. Samples can be used immediately for western blots or stored at -80°C.

7.3 Western Blotting Protocol

Preparing the Gel/Gel Recipes

Note: Use low % acrylamide gel when probing for large proteins, and a higher % acrylamide gel for smaller proteins.

Resolving Gel

RESOLVING GEL	2 gels (10%)
ddH_20	8.2 mL
30% Acrylamide (37:5:1)	6.6 mL
Tris-HCL (1.5M, pH 6.8)	5 mL
10% SDS	0.2 mL
Temed	20 µL
10% APS	100 µL

Add APS and Temed immediately prior to pouring the gel into plates. Pipette a thin layer of Isopropanol over the top of the gel to prevent resolving gel from drying out. Allow gel to set (approx. 20min).

Stacking Gel

STACKING GEL (4%)	2 gels (10mL)
ddH_20	6.1 mL
30% Acrylamide (37:5:1)	1.3 mL
Tris-HCL (0.5M, pH 6.8)	2.5 mL

10% SDS	0.1 mL
Temed	10 µL
10% APS	50 µL

Once the resolving gel is set, pour out Isopropanol and carefully blot excess with filter paper. Pour stacking gel on top of resolving gel. Put combs in place. Allow gel to set (approx. 20min).

Running the Gel

1. Take samples out of -80° freezer and place on ice.
2. Place gels into tanks, and add 1x running buffer to fill the tank.
3. Once samples have thawed, spin in centrifuge until max speed is reached.
4. Take out combs and pipette 6µL Bio-Rad protein ladder.
5. Add samples into each well accordingly.
6. Top up running buffer to make sure tank is full.
7. Match black electrodes to black and red to red.
8. Turn on the voltage for 60V for 30min, after, turn it up to 120V for approx. 1.5hours until dye runs off the gel.
9. At this point, you can prepare 1x transfer buffer. Once transfer buffer is well mixed, cover with parafilm and place in the -20°C freezer until ready for transfer.

Transferring the Gel onto a membrane

1. Fill a dish with cold transfer buffer.
2. Cut out equal sized membranes and place in methanol for 2 minutes to activate. Also cut out equal sized filter papers and prepare the appropriate number of foam pads.
3. Place membranes in transfer buffer after activation.
4. Once dye has run off the gel, remove the gels from tank and soak in transfer buffer. Carefully remove glass plates. Cut off and discard combs of the gel. Loosen gel from the glass plate with scraper. Allow for the gel to sit in transfer buffer.
5. In a dish, place the black side of the cassette on the bottom, and place two foam pads and 2 filter papers on top. Ensure there are no bubbles.
6. Carefully place gel on top of filter paper and use the roller to get any air bubbles out. Make sure gel is in the correct orientation so that the ladder will end up on the left side of the membrane when removed.

   Note: transfer runs from negative (black) to positive (red). Always ensure proteins will run from gel to the membrane.
7. Place membrane on top of the gel and roll out any bubbles.
8. Place 2 more filter papers on top and roll out any bubbles.
9. Add one more foam pad and roll out any bubbles.
10. Carefully close sandwich and place into transfer tank. Make sure black matches black and red matches red. Repeat as necessary for the number of gels used.
11. Place ice pack in tank to keep buffer cold. Attach lid by matching electrodes- black-to-black, and red-to-red. Surround transfer tank with ice to keep cold.
12. Turn on transfer at 120V for 2.5 hours or at 60V overnight.

13. Check on temperature throughout transfer time to ensure no overheating.

Probing the membrane

1. Prepare containers to hold blocking buffer for each membrane, approx. 10mL per container.
2. Once transfer has finished, open cassettes and quickly place membranes in containers with blocking buffer.
3. Allow the membranes to rinse in the blocking buffer for 1hr at room temperature.
4. Pour out blocking buffer and add primary antibody (1°Ab).
5. Incubate overnight at 4°C. Ensure containers are fully sealed to avoid evaporation.
6. The next day, remove 1°Ab and wash membranes 5x for 10min each with 10mL 1x wash buffer to rid the membrane of any unbound Ab.
7. Add secondary antibody (2° Ab) and allow membranes to rinse for 1hr at room temperature.
8. Remove 2°Ab and wash membranes 5x for 10min each with 10mL 1x wash buffer to rid the membrane of any unbound 2°Ab.
9. Membranes are ready for developing

Developing the membrane

1. For each membrane, use 2mL chemiluminescence (Millipore Immobilon Western Chemiluminescent HRP substrate) per membrane and incubate for 2 minutes.
2. Dip membranes into ddH_20 to rinse and place on transparency inside cassette.
3. In the darkroom, expose film for desired time.
4. Place film in developer for a few seconds until signal appears. Dip into water and to stop the reaction, place in fixer solution. Ensure ample fixing time.
5. Rinse with water and allow to dry.

7.4 Complexation of Palmitic Acid

1. Prepare 30mL of KRB Buffer (without glucose)
2. Add 3.75g FA-free BSA (Sigma Cat# A3803) to get a 12.5% solution
3. Heat to 50°C in water bath
4. Take 1600mg palmitic acid (Sigma Cat# P-5585) to put into a 2mL eppendorf
5. Dissolve palmitic acid with 100µl NaOH (10N) and vortex vigorously
6. Add palmitic acid into preheated medium while stirring. (note; it will precipitate)
7. Pour into falcon tube, protected from light
8. Incubate in 50°C water bath for 4+ hours while shaking at 150-200rpm
9. After the incubation period, filter solution to get chunks out using a 10mL syringe and sterile strainer
10. pH to 7.4

11. Aliquot solution and store at -20°C

7.5 Palmitate Oxidation Protocol (Incorporation of [1-14C] Palmitic acid into $14CO_2$)

1. Following extraction, weigh tissues (~20mg muscle) and place into scintillation vial containing 2mls of KRBS Ringer buffer.
2. Gasify each vial for 1 hour and incubate at 37°C
3. After 1 hour, add 200µl (1:1, vol/vol) 2-phenylethylamine/methanol onto loosely folded filter paper placed inside a 1.5ml eppendorf.
4. Gasify each scintillation vial for approx 1 hour, and incubate for 1 hour at 37°C
5. After 1 hour, add 200µl of H_2SO_4 (5N) to acidify media. Incubate for 1 hour at 37°C
6. Collect filter papers and transfer to corresponding scintillation vial containing 10mL of ECOLITE+ liquid scintillation cocktail (MP Biomedicals Cat #01882475) and place in scintillation counter for radioactivity counting

7.6 Glycogen Synthesis Protocol (Incorporation of D-[14C] glucose into Glycogen)

1. Transport the muscle slice (weighing ~ 20mg) to a 1.5ml eppendorf and add 500µl of 1M KOH.
2. Incubate the sample on the heat block for 30min @ 80-90°C.
3. 15min into the incubation period gently shake the eppendorf around once to ensure complete digestion.
4. Extract 400µl for glycogen content and place in a 2ml eppendorf.
5. Add 100µl of carrier glycogen to each sample.
6. Add 80µl of saturated Na_2SO_4 to each sample
7. Add 1.2ml of cold ethanol
8. Gently vortex each sample and incubate at -20°C overnight to allow precipitation.
9. On the following day, check for precipitation and centrifuge the samples for 20min @ 3000rpm.
10. Discard the resultant supernatant.
11. Dissolve the pellet in 500µl of ddH20.
12. Extract 400µl of sample and add to 5ml of scintillation fluid (ECOLITE+ liquid scintillation cocktail (MP Biomedicals Cat #01882475)) for counting.

Glycogen Synthesis Reagents

Note: Adjust volumes accordingly depending on number of samples.

1N KOH (pH off the scale)
5.61g KOH
Complete to 100ml using ddH_2O

Saturated Na_2SO_4
Dissolve powdered Na_2SO_4 in ddH_2O until precipitation forms. Precipitate formation is a sign of saturation.

Cold Ethanol
Place 100% Ethanol in a 50ml falcon tube and leave in -20°C freezer.

7.7 Measuring Triglyceride Content using commercially available calorimetric Kit

Note: This procedure can be done over one or two days.
Materials
• Triglyceride Quantification Kit (100 samples including 6 standards)
(Cat# ab65336)
• 5ml Tubes (1 tube/sample)
• 5% NP40
• ddH_2O

Day 1 – Sample Preparation
1. Determine the number of samples to be assayed and make an appropriate amount of 5% NP40 (diluted in water) (1ml/sample).
2. Add 100mg of tissue (muscle) to 1ml of 5% NP40 in a 5ml tube.
3. Heat the sample in the water bath for 10min @ 90°C.
4. Homogenize the sample in the 5ml tubes.
5. Heat the homogenized sample for 5min @ 90°C.
6. Remove the tubes from the water bath and let them cool down to room temperature.
7. Heat the sample once again for 5min @ 90°C.
8. Centrifuge the samples for 2 min at max speed.
9. Extract 20 µl for measuring protein content and store in an eppendorf.
10. Extract the remaining sample from the 5ml tubes and dispense into a separate eppendorf. (Be sure not to extract any insoluble material)
11. Store the samples at -80°C or continue procedure.

Day 2 – Prepare Standard Curve and Run Samples.
Note: Make room for 1 blank/condition.
1. Allow samples to thaw.
2. Vortex the samples and centrifuge them @13,200rpm for 10min.
3. While vortexing, reconstitute the enzyme mix in 220µl of assay buffer. Also, reconstitute the lipase in 220µl of assay buffer. Make aliquots and store unused portion in -20°C.
4. Dilute the stock standard (1mM) to 0.2mM by adding 100µl of the stock to 400µl of assay buffer provided in the kit.
5. Take a 96-well plate and start putting in the standards. Add 0µl, 10µl, 20µl, 30µl, 40 µl, and 50 µl of the 0.2mM standard in series.
6. Use assay buffer to top up all standards to a final volume of 50µl.
7. Dilute each of sample 10x by adding 10µl of sample to 90µl of ddH_2O. Mix well.
8. For muscle put 50 µl of the diluted sample per well.

9. Add 2ul of lipase to every well INCLUDING the standards. For blanks (1 blank/condition) add 2µl of assay buffer instead of the lipase. (This is the only difference between blanks and samples)
10. Let the well incubate for 20 min (Gently shake for 2min. Use the remaining 18min to make reaction mix).
11. Reaction mix (Light sensitive. Wrap in foil immediately. Store at room temperature)
12. Add 50µl of reaction mix to ALL wells including standards and blanks.
13. Shake the plate for 2min and incubate in a light-protected area for 1h.
14. Use the plate reader to read at 570nm.
15. Subtract your blanks from your samples.
16. Subtract absorbance of blank (standard 0) from all standards and samples.
17. Calculate concentration.

7.8 Measuring Circulating Insulin by ELISA

1. Fast the animals for 14-hr then obtain a blood sample from the saphenous vein.
2. Always keep blood on ice.
3. Centrifuge the blood at for 10min @ 13,000rpm (4°C)
4. Extract the plasma (supernatant) and place into another labeled eppendorf.
Store at -80°C until you are ready to run the ELISA.
5. When ready to assay, pre-warm all reagents of the EMD Millipore ELISA kit (Cat. # EZRMI-13K) to room temperature.
6. Dilute the provided 10X wash buffer by 10-fold.
7. Determine the number of samples to be assayed and place any extra microtiter strips in 2-8°C.
8. Place the microtiter strips that you will be using in a plate holder and wash 3 times with 300µl of diluted wash buffer.
9. Remove buffer from wells by tapping lightly onto an absorbent surface DO NOT let the wells dry completely.
10. Add 10µl of assay buffer to each blank & sample wells.
11. Add 10µl of Matrix solution to blank, standard, and control wells.
12. Add 10µl of 0.2, 0.5, 1, 2, 5 and 10 ng/mL insulin standards in ascending order.
13. Add 10µl of quality control 1 & 2 into their own wells.
14. Add 10µl of sample into the remaining wells.
15. Add 80ul of detection antibody to all wells
16. Seal the plate and incubate at room temperature for 2h on an orbital shaker
17. Remove plate sealer and tap onto an absorbent surface to empty contents.
18. Wash the plate 3 times with 300µl of wash buffer by decanting after each wash.
19. Add 100 µl of enzyme solution to each well. Seal with plate sealer and incubate for 30min at moderate speed on an orbital shaker.
20. Remove the seal and decant the contents.
21. Wash 6 times using diluted wash buffer making sure to decant contents after each wash.
22. Add 100 µl of substrate solution to each well. Cover with plate sealer and shake for 20 min on orbital shaker.
23. Add 100µl of stop solution to each well and mix well by hand. Ensure there are no bubbles and read using a plate reader at 450 and 590nm. Record absorbance.

24. Calculate insulin concentrations as outlined in the manual.

7.9 Buffers for muscle slice incubation

Stock solutions for Krebs Ringer Bicarbonate (KRB) Buffer
Note: All solutions are made with ddH_2O

Quantity Reagent/Molarity
0.9g in 100ml 0.154M NaCl (mw = 58.44)
575mg in 50ml 0.154M KCl (mw = 74.55
610mg in 50ml 0.11 $CaCl_2$ (mw = 110.99)
1.055g in 50ml 0.154M KH_2PO_4 (mw = 136.09)
927mg in 50ml 0.154M $MgSO_4$ (mw = 120.30)
650mg in 50ml 0.154M $NaHCO_3$ (mw = 84.01)
*Gasify $NaHCO_3$ with carbogen (95% O_2/5% CO_2) for 1h after assembly. Stock solutions can be stored at 0-4°C.

KRB Buffer Assembly (for 100ml)
Note: Adjust volumes accordingly depending on number of samples.
For 100ml of KRB buffer:

Quantity Reagent/Molarity
78.6ml 0.154M NaCl
3.08ml 0.154M KCl
2.32ml 0.11 $CaCl_2$
0.768ml 0.154M KH_2PO_4
0.768ml 0.154M $MgSO_4$
16.1ml 0.154M $NaHCO_3$
100mg 5.5mM Glucose
715mg 30mM Hepes

Once assembled, the KRB solution is gasified for 45min with carbogen (95% O_2/5% CO_2). pH the gasified KRB buffer to 7.4 using 10N NaOH. Finally add fatty acid free BSA (Sigma Cat# A3803) to the solution at a concentration of 4% (40mg/ml).

For glycogen synthesis and glycogen content assays, take the required amount of KRB Buffer and add radiolabelled D-[^{14}C] glucose at a concentration of 0.2 μCi/ml.

Appendix B:

Statement of Labor

All experiments conducted in this study were carried out by Arta Mohasses (AM), Diane Sepa-Kishi (DSK), Michelle Victoria Wu (MVW), George Bikopolous (GB) and Abinas Uthayakumar (AU). AM, DSK, MVW and AU were involved in the training of animals, collection of food intake and body weight data, extraction of tissues and IPGTT. AM was responsible for measuring palmitate oxidation, triglyceride content, glycogen synthesis, insulin concentrations, glycogen content and G6P content with the help of AU. George Bikopolous carried out the western blots for this study.

Dr. Rolando Ceddia is the primary investigator and supervisor of this project and this research was funded by the Natural Sciences and Engineering Research Council of Canada (NSERC) grant 311818-2011.